TECHNICAL REPORT STANDARD TITLE PAGE

1. Report No. TX - 01 1780-3	2. Government Accession No.	3. Recipient's Catalog No.
4. Title and Subtitle Determination of Nonlinear Parameters of Flexible Pavement Layers from Nondestructive Testing		5. Report Date April 2004 6. Performing Organization Code
7. Authors A. Meshkani, I. Abdallah and S. Nazarian		8. Performing Organization Report No. Research Report 1780-3
9. Performing Organization Name and Address Center for Highway Materials Research The University of Texas at El Paso El Paso, Texas 79968-0516		10. Work Unit No. 11. Contract or Grant No. Project No. 0-1780
12. Sponsoring Agency Name and Address Texas Department of Transportation Office of Research and Technology Implementation P.O. Box 5080 Austin, Texas 78763-5080		13. Type of Report and Period Covered Interim Report 9/99– 4/01 14. Sponsoring Agency Code

15. Supplementary Notes
Research Performed in Cooperation with TxDOT
Research Study Title: Design Modulus Values Using Seismic Data Collection

16. Abstract

Nondestructive testing (NDT) methods are typically used to measure the variations in the modulus of different pavement layers. Critical strains necessary for the estimation of the remaining life of a pavement system are then determined from the estimated moduli. The Falling Weight Deflectometer (FWD) and the Seismic Pavement Analyzer (SPA) are two of the NDT devices used for this purpose. The major objective of this study is to develop an algorithm for predicting the design modulus of each layer given the seismic modulus and the nonlinear parameters of each pavement layer. The feasibility of backcalculating the nonlinear parameters of the base and subgrade given the seismic modulus of each layer and the deflection basin measured at the same location are investigated in this document. An algorithm has been developed for this purpose. In the algorithm, a material model that relates the design modulus with seismic modulus was selected. A so-called equivalent linear structural model was also adopted. An optimization algorithm was developed to derive the nonlinear parameters of pavement materials from the FWD deflections and the seismic moduli.

The model was tested on four hypothetical pavement sections and three typical pavement materials. The base and subgrade were considered to exhibit load-induced nonlinear behavior. By comparing the assumed properties for the typical pavement sections with the backcalculated nonlinear parameters, the feasibility, accuracy, and the degree of uncertainty with which the nonlinear parameters can be determined are investigated.

17. Key Words	18. Distribution Statement
Falling Weight Deflectometer, Seismic Pavement Analyzer, Seismic Nondestructive Testing	No restrictions. This document is available to the public through the National Technical Information Service, 5285 Port Royal Road, Springfield, Virginia 22161

19. Security Classified (of this report)	20. Security Classified (of this page)	21. No. of Pages	22. Price
Unclassified	Unclassified	129	

Form DOT F 1700.7 (8-69)

DETERMINATION OF NONLINEAR PARAMETERS OF FLEXIBLE PAVEMENT LAYERS FROM NONDESTRUCTIVE TESTING

by

Amitis Meshkani, MSCE
Imad Abdallah, MSCE
and
Soheil Nazarian, Ph.D., P.E.

Research Project 0-1780
Design Modulus Values Using Seismic Data Collection

Conducted for
Texas Department of Transportation

Research Report TX 1780-3

The Center for Transportation Infrastructure Systems
The University of Texas at El Paso
El Paso, TX 79968-0516
April 2004

The contents of this report reflect the view of the authors, who are responsible for the facts and the accuracy of the data presented herein. The contents do not necessarily reflect the official views or policies of the Texas Department of Transportation or the Federal Highway Administration. This report does not constitute a standard, specification, or regulation.

The material contained in this report is experimental in nature and is published for informational purposes only. Any discrepancies with official views or policies of the Texas Department of Transportation or the Federal Highway Administration should be discussed with the appropriate Austin Division prior to implementation of the procedures or results.

NOT INTENDED FOR CONSTRUCTION, BIDDING, OR PERMIT PURPOSES

Amitis Meshkani, MSCE
Imad Abdallah, MSCE
Soheil Nazarian, Ph.D., P.E. (69263)

Acknowledgments

The authors would like to express their sincere appreciation to Mark McDaniel of the TxDOT Design Division, Joe Thompson of the Dallas District and John Rantz of Lubbock District for their ever-present support.

Thanks are also due to Nichols Consulting Engineers of Reno, Nevada, especially Dr. Sirous Alavi, for providing the WesTrack data.

Executive Summary

Nondestructive testing (NDT) methods are typically used to measure the variations in the modulus of different pavement layers. Critical strains necessary for the estimation of the remaining life of a pavement system are then determined from the estimated moduli. The Falling Weight Deflectometer (FWD) and the Seismic Pavement Analyzer (SPA) are two of the NDT devices used for this purpose.

The Falling Weight Deflectometer applies an impulse load to the pavement and measures the surface deflection with seven sensors. Moduli of different pavement layers can then be backcalculated from these deflections. The shortcomings of this method are the uncertainties associated with the backcalculation procedure.

The Seismic Pavement Analyzer is based on generating and detecting stress waves in a layered system. The elastic moduli of different layers are obtained from an inversion process. The SPA imparts very small external loads to the pavement; therefore, seismic moduli are linear elastic moduli. To incorporate in pavement design and analysis, seismic moduli of different layers have to be adjusted to represent moduli at strain and stress levels that are close to those applied by truck traffic. To do so, the nonlinear and viscoelastic behaviors of different layers should be accurately determined. These nonlinear parameters vary widely for different types of granular base and subgrade materials. The nonlinear parameters of each pavement layer can be preferably obtained from laboratory testing. However, adequate published information is available to be used as a first approximation.

The major objective of this study is to develop an algorithm for predicting the design modulus of each layer given the seismic modulus and the nonlinear parameters of each pavement layer. This is the third document produced as a part of this project. In the first document, the feasibility of the concept was demonstrated, and several options to be pursued further were provided.

In the second document, it was demonstrated that the design modulus could be determined reasonably accurately by combining the seismic moduli with the nonlinear parameters of the base and subgrade determined from the laboratory tests. It was also demonstrated that a simple model based either on the plasticity index (PI) or the type of the material might be used as a first approximation. That document also contained a comprehensive discussion on the most feasible method for incorporating their methodology in the day-to-day operation of the Texas Department of Transportation (TxDOT).

In this document, the work by Ke et al. (2000) is further expanded to determine the feasibility of backcalculating the nonlinear parameters of the base and subgrade given the seismic modulus of each layer and the deflection basin measured at the same location. An algorithm has been developed for this purpose. In the algorithm, a material model proposed by Ke et al. (2000) that relates the design modulus with seismic modulus was selected. A so-called equivalent linear structural model was also adopted. An equivalent linear model is based on an elasto-static layered system modified to incorporate the material model through an iterative process. An optimization algorithm was developed to derive the nonlinear parameters of pavement materials from the FWD deflections and the seismic moduli.

The model was tested on four hypothetical pavement sections and three typical pavement materials. The base and subgrade were considered to exhibit load-induced nonlinear behavior. By comparing the assumed properties for the typical pavement sections with the backcalculated nonlinear parameters, the feasibility, accuracy, and the degree of uncertainty with which the nonlinear parameters can be determined are investigated.

IMPLEMENTATION STATEMENT

With the initiation of "AASHTO 2002" program, which aims towards a mechanistic pavement design implementable by all highway agencies, this project may have significant impact. To develop a mechanistic pavement design that can contain performance-based specifications, the same engineering properties that are used to design a pavement should be used to determine the suitability of a material for construction and should be specified as criteria for accepting the material placed at the site. The only practical and available method at this time is based on seismic testing. Furthermore, it seems that with proper laboratory testing technique and proper simulation one can develop remaining life models that are more realistic.

Some of the software and protocols being developed can also be applied in pavement design with the FWD.

TABLE OF CONTENTS

CHAPTER ONE - INTRODUCTION 1
- PROBLEM STATEMENT 1
- OBJECTIVE AND APPROACHES 1
- ORGANIZATION 2

CHAPTER TWO - BACKGROUND 5
- INTRODUCTION 5
- NONDESTRUCTIVE TESTING METHODS 5
  - Falling Weight Deflectometer 5
  - Seismic Pavement Analyzer 7
- NONLINEAR MATERIAL PROPERTIES 7
  - Base and Subgrade Materials 7
  - Bituminous Materials 13
- PAVEMENT REMAINING LIFE 15

CHAPTER THREE - PAVEMENT ANALYSIS MODELS 17
- INTRODUCTION 17
- STRUCTURAL MODELS 17
  - Layered Elastic Model 17
  - Equivalent-Linear Model 17
  - Finite Element Models 18
- TYPICAL RESULTS 21

CHAPTER FOUR - PAVEMENT RESPONSE UNDER EQUIVALENT LINEAR MODEL 27
- INTRODUCTION 27
- SENSITIVITY STUDY 27
  - Sensitivity of Deflection 30
  - Sensitivity of Strains 31
  - Sensitivity of Remaining Life 40
- GENERAL OBSERVATIONS AND PRACTICAL RECOMMENDATIONS 40

CHAPTER FIVE - BACKCALCULATION OF NONLINEAR PARAMETERS 45
INTRODUCTION 45
DESCRIPTION OF ALGORITHM 45
IMPLEMENTATION OF ALGORITHM 49
VERIFICATION OF ALGORITHM 50

CHAPTER SIX - CASE STUDY 59
INTRODUCTION 59
SITE DESCRIPTION 59
FWD RESULTS 62
SPA RESULTS 71
LABORATORY RESULTS 73
ANALYSIS OF RESULTS (LINEAR ELASTIC MODELS) 74
ANALYSES OF RESULTS (EQUIVALENT LINEAR ELASTIC MODELS) 79
BACKCALCULATION OF NONLINEAR PARAMETERS 83

CHAPTER SEVEN - SUMMARY, CONCLUSIONS AND RECOMMENDATIONS 91
SUMMARY 91
CONCLUSIONS 92
RECOMMENDATIONS FOR FUTURE RESEARCH 93

REFERENCES 95

APPENDIX A - SEISMIC PAVEMENT ANALYZER 101

APPENDIX B - RELATIONSHIP BETWEEN SEISMIC AND DESIGN MODULUS 105

APPENDIX C - SENSITIVITY ANALYSIS FIGURE 109

LIST OF FIGURES

FIGURE 2.1 FALLING WEIGHT DEFLECTOMETER 6

FIGURE 2.2 SEISMIC PAVEMENT ANALYZER 8

FIGURE 2.3 INFLUENCE OF EFFECTIVE CONFINING PRESSURE ON MODULUS REDUCTION CURVE (FROM ISHIBASHI, 1992) 12

FIGURE 2.4 VARIATION IN AC MODULUS WITH FREQUENCY AND TEMPERATURE (FROM AOUAD ET AL., 1993) 13

FIGURE 2.5 FREQUENCY DEPENDENCY OF AC MODULUS (FROM DANIEL AND KIM, 1998) 14

FIGURE 2.6 IMPACT OF AIR VOID CONTENT ON AC MODULUS (FROM ROJAS, 1999) 14

FIGURE 3.1 FLOW CHART OF IMPLEMENTATION OF EQUIVALENT-LINEAR MODEL 19

FIGURE 3.2 TYPICAL PROFILE OF A PAVEMENT SECTION USED IN EQUIVALENT LINEAR MODEL 20

FIGURE 3.3 PROFILE OF PAVEMENT SECTIONS USED IN THIS STUDY 21

FIGURE 3.4 VARIATION OF MODULUS OF PAVEMENT MATERIAL UNDER TRAFFIC LOAD 24

FIGURE 4.1 VARIATION OF DEFLECTION AT SENSOR LOCATIONS (D0-D6) DUE TO VARIATION OF K_3 OF BASE FOR A HYPOTHETICAL PAVEMENT SECTION 29

FIGURE 4.2 CUMULATIVE DISTRIBUTION OF DEFLECTIONDUE TO VARIATION OF K3 OF BASE FOR A HYPOTHETICAL PAVEMENT SECTION 29

FIGURE 4.3 VARIATION OF DEFLECTION AT SENSOR LOCATIONS (D0-D6) DUE TO VARIATION OF NONLINEAR PARAMETERS FOR "PRIMARY ROAD, AVERAGE QUALITY BASE AND LOW PLASTICITY CLAY SUBGRADE" 32

FIGURE 4.4 VARIATION OF DEFLECTION AT SENSOR LOCATIONS (D0-D6) DUE TO VARIATION OF ALL NONLINEAR PARAMETERS FOR "PRIMARY ROAD, AVERAGE QUALITY BASE AND LOW PLASTICITY CLAY SUBGRADE" 33

FIGURE 4.5 CUMULATIVE DISTRIBUTION OF DEFLECTION UNDER THE LOAD FOR "PRIMARY ROAD, AVERAGE QUALITY BASE AND LOW PLASTICITY CLAY SUBGRADE" 33

FIGURE 4.6 VARIATION OF TENSILE STRAIN (ε_T), COMPRESSIVE STRAIN (ε_C), FATIGUE (N_F) AND RUTTING (N_R) REMAINING LIVES FOR "PRIMARY ROAD, AVERAGE QUALITY BASE AND LOW PLASTICITY CLAY SUBGRADE" 35

FIGURE 4.7 VARIATION OF TENSILE STRAIN (ε_T), COMPRESSIVE STRAIN (ε_C), FATIGUE (N_F), AND RUTTING (N_R) REMAINING LIVES DUE TO VARIATION OF ALL NONLINEAR PARAMETERS FOR "PRIMARY ROAD, AVERAGE QUALITY BASE AND LOW PLASTICITY CLAY SUBGRADE" 36

FIGURE 4.8 CUMULATIVE DISTRIBUTION OF CRITICAL STRAINS AND REMAINING LIVES FOR "PRIMARY ROAD, OVER AVERAGE QUALITY BASE AND LOW PLASTICITY CLAY SUBGRADE" 37

FIGURE 5.1 FLOW CHART OF IMPLEMENTATION OF BACKCALCULATION PROCESS 47

FIGURE 5.2 BACKCALCULATION ERROR FOR THE PARAMETER K_3 OF THE BASE FOR THE FOUR TYPICAL PAVEMENT SECTIONS 52

FIGURE 5.3 BACKCALCULATION ERROR FOR THE PARAMETER K_3 OF THE SUBGRADE FOR THE FOUR TYPICAL PAVEMENT SECTIONS 55

FIGURE 5.4 BACKCALCULATION ERROR FOR THE PARAMETER K_3 OF THE BASE AND SUBGRADE FOR THE FOUR TYPICAL PAVEMENT SECTIONS 57

FIGURE 6.1 FLOWCHART OF FORWARD AND BACKCALCULATION PROCESSES DEMONSTRATED USING THIS CASE STUDY 60

FIGURE 6.2 LAYOUT AND SCHEMATIC OF WESTRACK SITE 61

FIGURE 6.3 CROSS-SECTION OF TEST TRACK 62

FIGURE 6.4 WESTRACK ACTUAL PAVEMENT CROSS-SECTION AND SIMPLIFIED CROSS-SECTION USED IN THIS STUDY 63

FIGURE 6.5 COMPARISON OF EXPERIMENTAL AND THEORETICAL DISPERSION CURVES FROM SASW TESTS PERFORMED WITH SPA 72

FIGURE 6.6 TYPICAL VARIATION IN MODULUS WITH CONFINING PRESSURE AND DEVIATORIC STRESS FOR BASE USED IN WESTRACK 74

FIGURE 6.7 EFFECTS OF DEPTH TO WATER TABLE ON DEFLECTION RMS ERRORS USING LINEAR ELASTIC ANALYSIS 76

FIGURE 6.8 EFFECTS OF MODULUS OF SATURATED SUBGRADE ON DEFLECTION RMS ERRORS USING LINEAR ELASTIC ANALYSIS 77

FIGURE 6. 9 EFFECTS OF DEPTH OF RIGID LAYER (WATER TABLE/ BEDROCK) ON CRITICAL STRAINS AND REMAINING LIVES AT SECTION 12 LOCATION 35 80

FIGURE 6.10 VARIATION IN MODULI OF THE BASE AND ENGINEERING FILL UNDER STATE OF STRESS APPLIED BY A STANDARD TRUCK LOAD 82

FIGURE 6.11 VARIATIONS IN CRITICAL STRAINS ALONG SECTIONS 12 AND 25 FROM SEISMIC MODULI 84

FIGURE 6.12 VARIATIONS IN REMAINING LIFE ALONG SECTIONS 12 AND 25 FROM SEISMIC MODULI 87

FIGURE A.1 SEISMIC PAVEMENT ANALYZER 102

FIGURE B.1 STATE OF THE STRESS UNDER SEISMIC LOAD 106

FIGURE B.2 STATE OF THE STRESS UNDER TRAFFIC LOAD 106

LIST OF TABLES

TABLE 2.1 ADVANTAGES AND DISADVANTAGES OF METHODS USED TO OBTAIN MODULI 9

TABLE 2.1 PARAMETERS AFFECTING MODULUS OF GRANULAR BASE AND SUBGRADE (AFTER HARDIN AND DRNEVICH, 1972) 11

TABLE 3.1 PROPERTIES OF DIFFERENT PAVEMENT SECTIONS 22

TABLE 3.2 TYPICAL NONLINEAR VALUES OF PAVEMENT MATERIALS 23

TABLE 3.3 REMAINING LIFE OF A PRIMARY ROAD APPLYING DIFFERENT STRUCTURAL MODELS 25

TABLE 4.1 LEVELS OF SENSITIVITY BASED ON SENSITIVITY NUMBER OF EACH PARAMETER 30

TABLE 4.2 NONLINEAR PROPERTIES OF NONLINEAR LAYERS FOR "PRIMARY ROAD AVERAGE QUALITY BASE AND LOW PLASTICITY CLAY SUBGRADE" 30

TABLE 4.3 SENSITIVITY LEVEL OF DEFLECTION UNDER THE LOAD WHEN K2 AND K3 PARAMETERS ARE PERTURBED 34

TABLE 4.4 SENSITIVITY LEVEL OF CRITICAL TENSILE STRAIN WHEN K2 AND K3 PARAMETERS ARE PERTURBED 38

TABLE 4.5 SENSITIVITY LEVEL OF CRITICAL COMPRESSIVE STRAIN WHEN K2 AND K3 PARAMETERS ARE PERTURBED 39

TABLE 4.6 SENSITIVITY LEVEL OF FATIGUE REMAINING LIFE WHEN K2 AND K3 PARAMETERS ARE PERTURBED 41

TABLE 4.7 SENSITIVITY LEVEL OF FATIGUE REMAINING LIFE WHEN K2 AND K3 PARAMETERS ARE PERTURBED 42

TABLE 5.1 BACKCALCULATION OF THE PARAMETER K_3 OF THE BASE FOR THE FOUR TYPICAL PAVEMENT SECTIONS 51

TABLE 5.2 BACKCALCULATION OF THE PARAMETER K_3 OF THE SUBGRADE FOR THE FOUR TYPICAL PAVEMENT SECTIONS 54

TABLE 5.3 BACKCALCULATION OF THE PARAMETERS K3 OF THE BASE AND SUBGRADE FOR THE FOUR TYPICAL PAVEMENT SECTIONS 56

TABLE 6.1 FWD DEFLECTIONS FOR WESTRACK SITES 12 AND 25 63

TABLE 6.2 ANALYSES OF FWD DEFLECTIONS WITH PROGRAM MODULUS BASED ON A FOUR-LAYER SYSTEM WITH BEDROCK OPTION 65

TABLE 6.3 ANALYSES OF FWD DEFLECTIONS WITH PROGRAM MODULUS BASED ON A THREE-LAYER SYSTEM WITH BEDROCK OPTION 66

TABLE 6.4 ANALYSES OF FWD DEFLECTIONS WITH PROGRAM EVERCALC BASED ON A FOUR-LAYER SYSTEM WITH WATER TABLE OPTION 67

TABLE 6.5 ANALYSES OF FWD DEFLECTIONS WITH PROGRAM EVERCALC BASED ON A THREE-LAYER SYSTEM WITH WATER TABLE OPTION 68

TABLE 6.6 ANALYSES OF FWD DEFLECTIONS WITH PROGRAM EVERCALC BASED ON A FOUR-LAYER SYSTEM WITH WATER TABLE OPTION AT FIXED VALUE 69

TABLE 6.7 ANALYSES OF FWD DEFLECTIONS WITH PROGRAM EVERCALC BASED ON A THREE-LAYER SYSTEM WITH WATER TABLE OPTION AT FIXED VALUE 70

TABLE 6.8 SEISMIC MODULI AND THICKNESS FROM SPA FOR WESTRACK SITES 12 AND 25 71

TABLE 6.9 CONSTITUTIVE PARAMETERS DETERMINED FROM LABORATORY TEST RESULTS 73

TABLE 6.10 DEFLECTIONS FROM BISAR (LINEAR ELASTIC) USING SEISMIC MODULI WITH WATER TABLE AT 144 IN. (3.5 M) 78

TABLE 6.11 DEFLECTIONS FROM EQUIVALENT LINEAR PROCEDURE USING SEISMIC MODULI ALONG SECTION 12 81

TABLE 6.12 DEFLECTION RESULTS FROM EQUIVALENT LINEAR PROCEDURE USING SEISMIC MODULI ALONG SECTION 25 81

TABLE 6.13 ESTIMATED CRITICAL STRAINS AND REMAINING LIVES ALONG SECTION 12 FROM SEISMIC MODULI 85

TABLE 6.14 ESTIMATED CRITICAL STRAINS AND REMAINING LIVES ALONG SECTION 25 FROM SEISMIC MODULI 86

TABLE 6.15 BACKCALCULATED PARAMETERS K_3 OF BASE AND ENGINEERING FILL WHEN PARAMETERS K_2 ARE BASED ON LITERATURE RECOMMENDED VALUES 89

TABLE 6.16 BACKCALCULATED PARAMETERS K_3 OF BASE AND ENGINEERING FILL WHEN PARAMETERS K_2 ARE BASED ON LABORATORY RESULTS 89

CHAPTER ONE
INTRODUCTION

PROBLEM STATEMENT

Nondestructive testing (NDT) methods are typically used to measure the variations in the modulus of different pavement layers. Critical strains necessary for the estimation of the remaining life of a pavement system are then determined from the estimated moduli. The Falling Weight Deflectometer (FWD) and the Seismic Pavement Analyzer (SPA) are two of the NDT devices used for this purpose.

The Falling Weight Deflectometer applies an impulse load to the pavement and measures the surface deflection with seven sensors. Moduli of different pavement layers can then be backcalculated from these deflections. The shortcomings of this method are the uncertainties associated with the backcalculation procedure.

The Seismic Pavement Analyzer is based on generating and detecting stress waves in a layered system. The elastic moduli of different layers are obtained from an inversion process. The SPA imparts very small external loads to the pavement; therefore, seismic moduli are linear elastic moduli. To incorporate in pavement design and analysis, seismic moduli of different layers have to be adjusted to represent moduli at strain and stress levels that are close to those applied by truck traffic. To do so, the nonlinear and viscoelastic behaviors of different layers should be accurately determined.

These nonlinear parameters vary widely for different types of granular base and subgrade materials. The nonlinear parameters of each pavement layer can be preferably obtained from laboratory testing. However, adequate published information is available to be used as a first approximation.

OBJECTIVE AND APPROACHES

The major objective of this study is to develop an algorithm for predicting the design modulus of each layer given the seismic modulus and the nonlinear parameters of each pavement layer. This is the third document produced as a part of this project. In the first document, Nazarian et al. (1998a) demonstrated the feasibility of the concept and provided several options to be pursued further. They proposed the following three options to be considered for obtaining design modulus profiles:

1. Combine seismic modulus profile measured in the field with the nonlinear parameters of the base and subgrade measured in the laboratory.

2. Combine seismic modulus profile measured in the field with the material specific nonlinear parameters published in the literature.

3. Backcalculate the nonlinear parameters of the base and subgrade given the seismic modulus profile and the FWD deflection basin, and then use the estimated nonlinear parameters with the seismic modulus profile.

In the second document, Ke et al. (2000) demonstrated that the design modulus could be determined reasonably accurately by combining the seismic moduli with the nonlinear parameters of the base and subgrade determined from the laboratory tests. They also demonstrated that a simple model based either on the plasticity index (PI) or the type of the material might be used as a first approximation. Ke et al. (2000) also provided a lengthy discussion on the most feasible method for incorporating their methodology in the day-to-day operation of the Texas Department of Transportation (TxDOT). As such Ke et al. (2000) addressed the first two options.

In this document, the work by Ke et al. (2000) is further expanded to determine the feasibility of backcalculating the nonlinear parameters of the base and subgrade given the seismic modulus of each layer and the deflection basin measured at the same location. An algorithm has been developed for this purpose. In the algorithm, a material model proposed by Ke et al. (2000) that relates the design modulus with seismic modulus was selected. A so-called equivalent linear structural model was also adopted. An equivalent linear model is based on an elasto-static layered system modified to incorporate the material model through an iterative process. An optimization algorithm was developed to derive the nonlinear parameters of pavement materials from the FWD deflections and the seismic moduli.

The model was tested on four hypothetical pavement sections and three typical pavement materials. The base and subgrade were considered to exhibit load-induced nonlinear behavior. By comparing the assumed properties for the typical pavement sections with the backcalculated nonlinear parameters, the feasibility, accuracy, and the degree of uncertainty with which the nonlinear parameters can be determined are investigated.

ORGANIZATION

Chapter 2 contains a review of relevant literature regarding the FWD and SPA as well as a general description of the methods for the interpretation of data from the two devices. The two most common failure modes of the pavement and remaining life of the pavement are also described in that chapter.

Three different pavement analyses algorithms are discussed in Chapter 3. Typical pavement sections and pavement material characterizations are also introduced in this chapter. The rationale beyond selecting the algorithm recommended for this study is included there.

The degree of influence of the nonlinear pavement materials on the deflection basin, critical strains and the remaining life of the pavement sections are comprehensively analyzed in Chapter 4.

Chapter 5 contains a discussion of the algorithm for backcalculation of the nonlinear parameters of the pavement material. The strengths and limitations of the algorithm are described in that chapter.

A case study is then included to demonstrate the validity of the equivalent linear algorithm in Chapter 6. Further, the feasibility of backcalculation of nonlinear properties is discussed using the case study in that chapter.

The study is summarized and the relevant conclusions are drawn in Chapter 7. That chapter also contains recommendations for further improving this work.

CHAPTER TWO
BACKGROUND

INTRODUCTION

Resilient modulus is an important material property required for characterization of pavement layers for use in pavement design. The resilient modulus can be determined in the laboratory using various types of tests. It can also be measured from nondestructive testing. The resilient modulus is estimated from the backcalculation of the pavement surface deflections.

In this chapter, nondestructive testing devices used in this study are discussed. Nonlinear material properties and their effects on the modulus and remaining life of the pavement are also described in this chapter.

NONDESTRUCTIVE TESTING METHODS

Nondestructive testing techniques are widely used to obtain field stiffness parameters of pavement materials. Several nondestructive testing and evaluation devices are available. Two nondestructive testing (NDT) devices, Falling Weight Deflectometer and Seismic Pavement Analyzer, are utilized in this study.

Falling Weight Deflectometer

The Falling Weight Deflectometer (FWD) is the most popular NDT device. The FWD applies an impulse load to the pavement, so that the pavement deflections can be measured at seven points (see Figure 2.1). The deflections obtained from the seven sensors are input into a backcalculation program to determine the layer modulus of the pavement. The procedures used to interpret the FWD deflection data fall into three categories: empirical, mechanistic and analytical (Hicks and Monsmith, 1972). In empirical analysis, the overall stiffness of pavements relative to one another is estimated. However, material properties and pavement layer moduli are not obtained.

a) Schematic of FWD

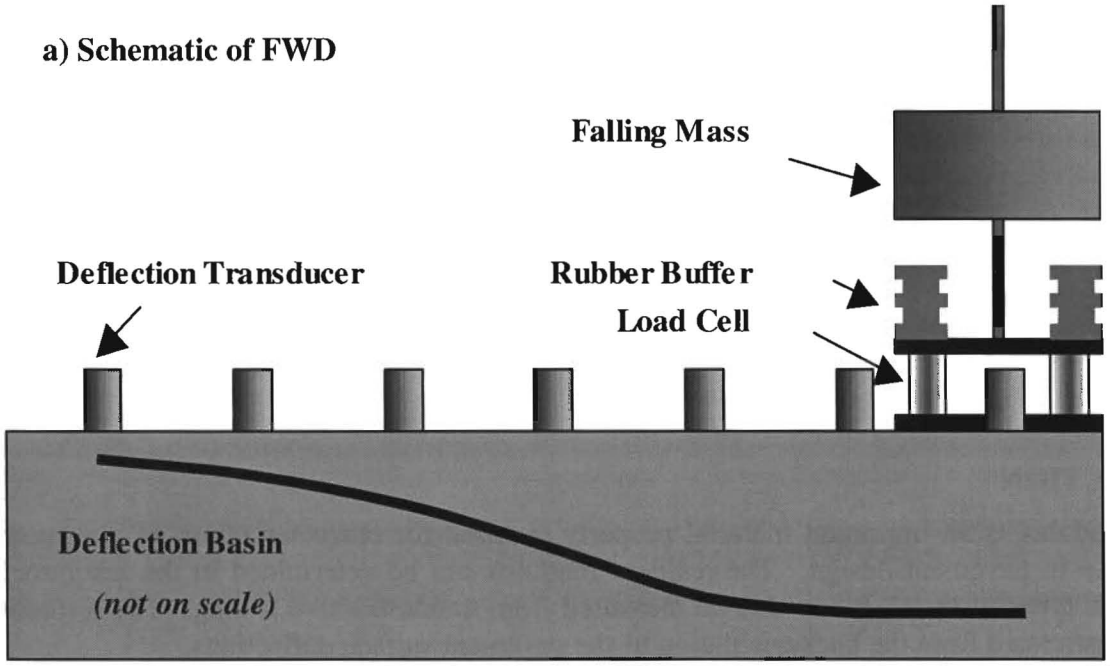

b) Picture of Actual FWD

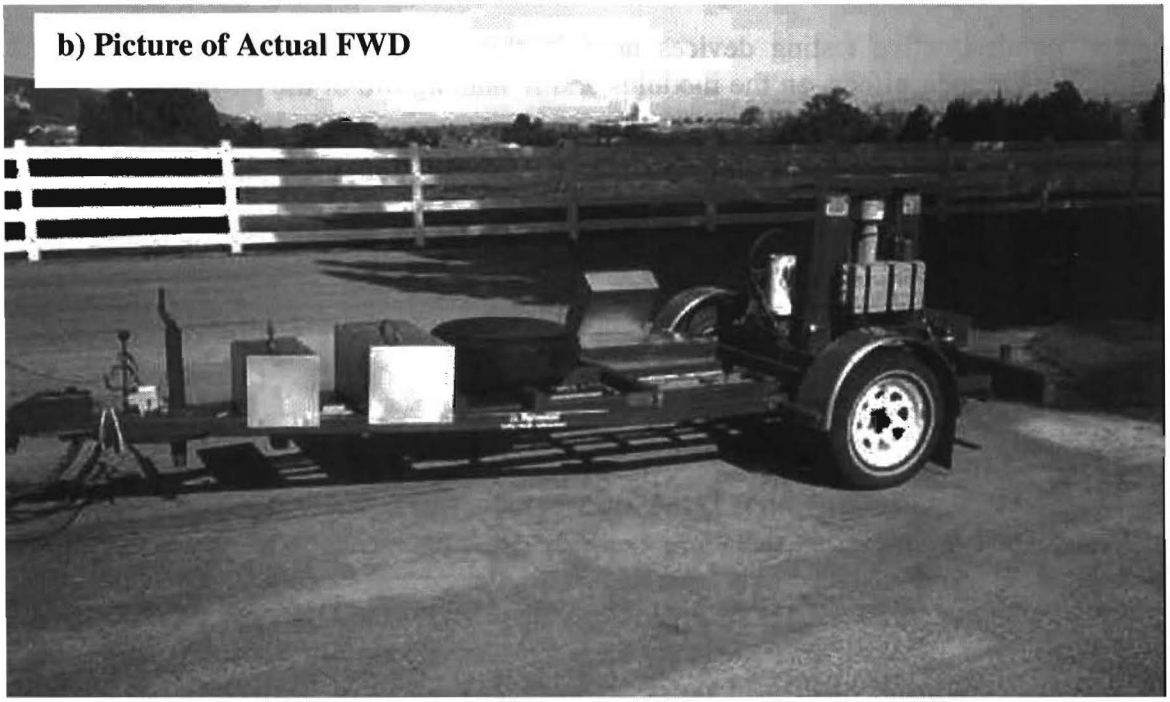

Figure 2.1 Falling Weight Deflectometer

In the mechanistic methods, deflection data from a pavement section are combined with empirical observations and mathematical equations to develop numerical correlations that quantify the condition of the pavement. These correlations are then used with only a few constraints (Hoffman and Thompson, 1982). In the analytical approaches, the determination of pavement moduli is usually done using an analytical response model in conjunction with a backcalculation algorithm. The static layer elastic model is, by far, the most widely used model (Bush, 1980; Lytton, et al., 1985; Uzan, et al. 1989). The application of layered theory for in-situ material characterization requires the estimation of only one unknown parameter, the Young's modulus, of each layer. The Poisson's ratio can be assumed from the literature. More sophisticated models can be used, as discussed later.

Seismic Pavement Analyzer

The Seismic Pavement Analyzer (SPA) is a trailer-mounted nondestructive testing device, as shown in Figure 2.2. Its operating principle is based on generating and detecting stress waves in a layered medium. The SPA uses more transducers than the FWD with higher frequencies and more sophisticated interpretation techniques. The measurement is rapid. A complete testing cycle at one point takes less than one minute (lowering sources and receivers, making measurements, and withdrawing the equipment).

In SPA several seismic testing techniques are combined. A detailed discussion on the background of the device can be found in Appendix A. Raw data collected by the SPA is then processed and interpreted using an inversion procedure. Raw data are the waveforms generated by hammer impacts and collected by the transducers. The processed data are pavement layer properties derived from the raw data through established theoretical models. Interpreted data are diagnoses of pavement distress precursors from data processed through models. Pavement properties estimated by the SPA include: Young's modulus, shear modulus, thickness, and temperature of top pavement layer; Young's modulus and thickness of base layer; and Young's modulus of subgrade.

The advantages and disadvantages of deflection-based and seismic-based methods are summarized in Table 2.1. Using a constitutive model that considers nonlinear behavior of pavement material utilizes the data collected from both FWD and SPA.

NONLINEAR MATERIAL PROPERTIES

In recent years, highway engineers have devoted considerable effort to describe nonlinear behavior of pavement materials. Resilient modulus tests have been used to explain such nonlinear behavior. During the past few decades, several constitutive models have been developed and used by pavement design engineers. The determination of the stresses or deformations is rather approximate unless correct constitutive equations that describe the actual behavior of different materials are used.

Base and Subgrade Materials

Barksdale (1972) and Witczak (1988) have shown that the resilient modulus of granular materials increases with increasing confining stress. Several relationships to describe the

a) Schematic of the SPA

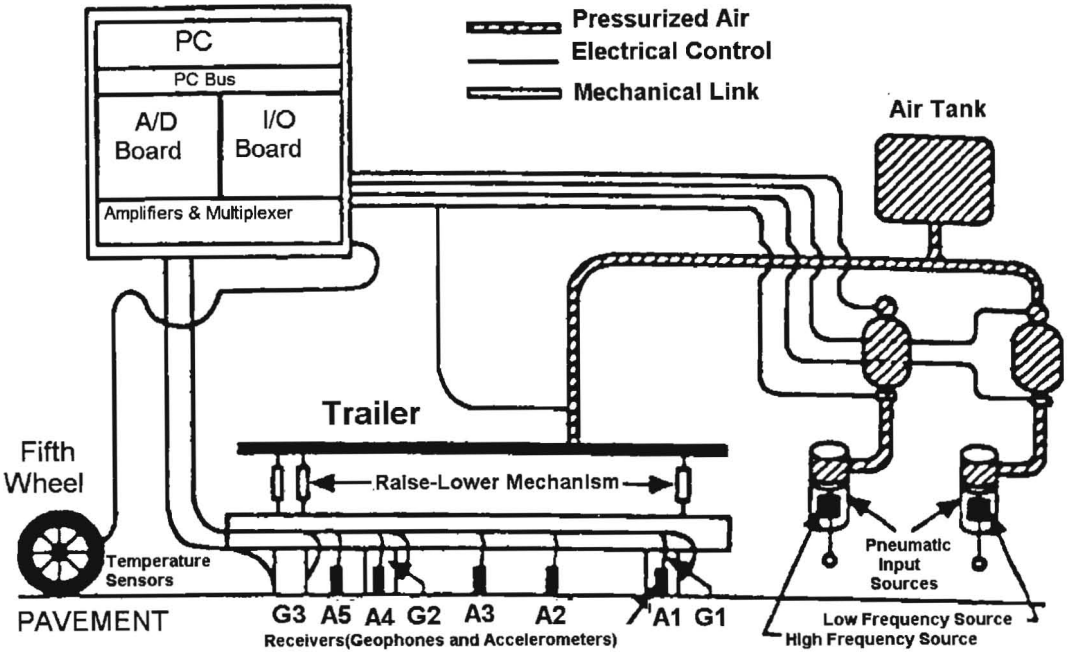

b) Picture of the Actual SPA

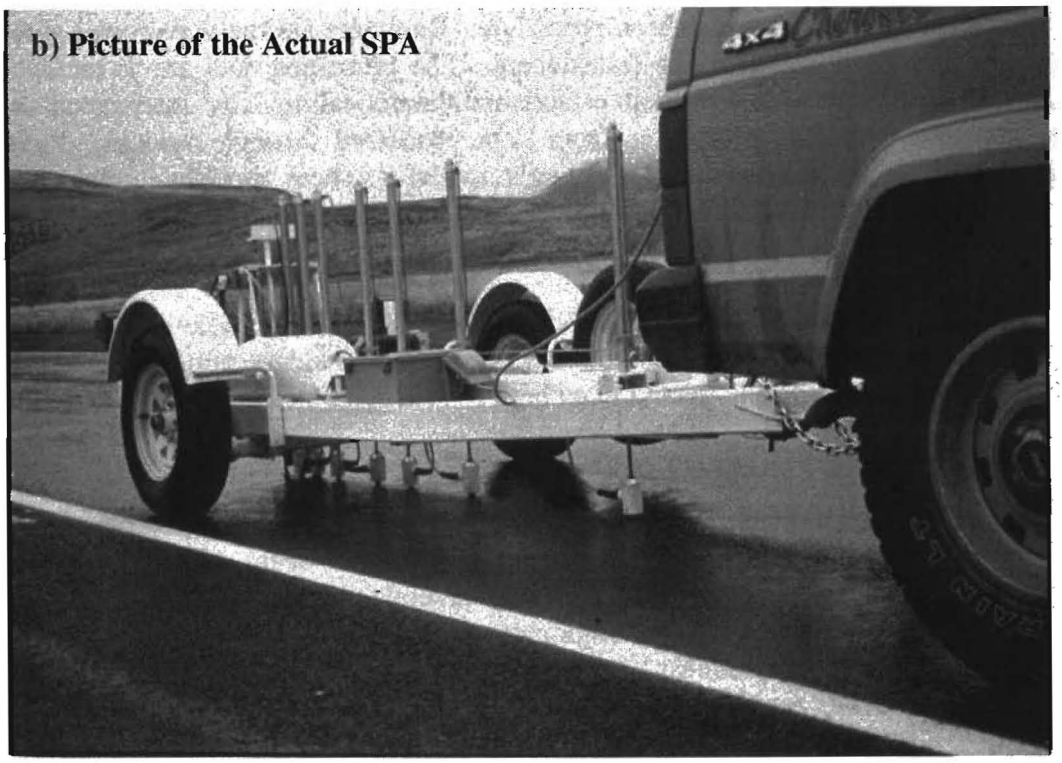

Figure 2.2 Seismic Pavement Analyzer

Table 2.1 Advantages and Disadvantages of Methods Used to Obtain Moduli

Test Method	Major Advantage	Major Weaknesses
FWD	Imposes loads that approximate wheel loads	The state-of-stress within pavement strongly depends on moduli of different layers, and hence is unknown.
SPA	Measures a fundamentally-correct parameter (i.e., linear elastic modulus)	State-of-stress during seismic tests differs from the state-of-stress under actual loads

nonlinear stress-strain characteristics of granular materials have been advocated. Most pavement design procedures use the bulk stress model, which is in the form of (Hicks, 1971)

$$M_R = k_1 P_a \left[\frac{\Theta}{P_a}\right]^{k_2} \tag{2.1}$$

In Equation 2.1, M_R is the resilient modulus, Θ is the bulk stress (summation of three normal stresses), k_1 and k_2 are material parameters, and P_a is the atmospheric pressure. May and Witczak (1981) suggested the following equation to describe the resilient modulus of pavement materials:

$$M_R = K\ k_1 \Theta^{k_2} \tag{2.2}$$

in which K is a function of pavement structure, test load, and developed shear strain, and k_1, k_2 are constants. The main disadvantage of this model is that it does not adequately consider the effects of deviatoric stress (or normal strain).

Uzan (1985) demonstrated that Equation 2.1 could not adequately describe the nonlinear behavior of pavement materials. He described the nonlinear behavior found in repeated load triaxial tests as

$$M_R = k_1 P_a \left[\frac{\Theta}{P_a}\right]^{k_2} \left[\frac{\tau_{OCT}}{P_a}\right]^{k_3} \tag{2.3}$$

The model includes the influence of bulk stress (Θ) and octahedral shear stress (τ_{oct}) on resilient modulus.

Barksdale et al. (1994) adopted the model proposed by Pezo et al. (1991). That model is in the form of

$$M_R = k_1 \sigma_c^{k_2} \sigma_d^{k_3} \tag{2.4}$$

where σ_c is the confining pressure, σ_d is the deviatoric stress, and k_2 and k_3 are material parameters. Pezo et al. indicated that Equation 2.4 is the constitutive model to use when describing the nonlinear behavior of either cohesive or granular materials. This model was adopted in this study.

Hardin and Drnevich (1972) provided a list of parameters that affect the moduli of both fine-grained and coarse-grained materials. Their observations are summarized in Table 2.2. The state of stress, void ratio, and the strain amplitude are the main parameters that affect the modulus of a material. For fine-grained materials, the degree of saturation is also important.

Ke et al. (2000) studied the impacts of these items on parameters k_1 through k_3 in Equation 2.4. As reflected in Table 2.1, most parameters suggested by Hardin and Drnevich affect k_1. However, k_2 and k_3 are affected by fewer parameters. Therefore, determining k_1 in the laboratory is difficult. On the other hand determining k_2 and k_3 might seem relatively easy, but the testing process is time consuming and costly.

One of the purposes of this study is to relate seismic modulus with the load-induced nonlinear modulus while predicting k_2 and k_3 parameters considering state of stress under the external load imparted by a FWD or truck load. Ke et al. (2000) derived such a relationship, which is in the form of:

$$E = E_{seis}\left(\frac{\sigma_{c-ult}}{\sigma_{c-init}}\right)^{k_2}\left(\frac{\sigma_{d-ult}}{\sigma_{d-init}}\right)^{k_3} \tag{2.5}$$

where E is the resilient modulus at a given depth under FWD or truck load, E_{seis} is the seismic modulus of the layer, k_2 and k_3 are statically determined coefficients. $\sigma_{c\text{-}init}$ and $\sigma_{c\text{-}ult}$ are respectively initial and ultimate confining pressures. $\sigma_{d\text{-}init}$ and $\sigma_{d\text{-}ult}$ are the initial and ultimate deviatoric stresses, respectively. The derivation of Equation 2.5 is included in Appendix B.

One of the limitations of Equation 2.5 is that at very small or at very large deviatoric stresses the modulus tends to be infinity or zero, respectively. Many years of research (Kramer, 1996) have shown that below a certain strain level the modulus is constant and equal to the small-strain linear-elastic modulus of the material (see Figure 2.3). Similarly, at higher strain levels, the modulus approaches a constant value. Therefore, a set of boundary limitations is applied. If in Equation 2.5 the strain is small enough that the modulus becomes greater than the seismic modulus measured in the field, the seismic modulus will be adopted as the modulus of the material. On the other hand, if at higher vertical strain levels the modulus becomes lower than 5% of the seismic modulus measured in the field, 5% of seismic modulus will be adopted as the

Table 2.2 Parameters Affecting Modulus of Granular Base and Subgrade (after Hardin and Drnevich, 1972)

Parameter	Importance*		Parameter Affected in Equation 2.4		
	Coarse-Grained Materials	Fine-Grained Materials	k_1	k_2	k_3
Strain Amplitude	V	V			√
Effective Mean Principal Stress (Confining pressure)	V	V		√	√
Void Ratio	V	V	√		
Degree of Saturation	R	V	√	√	
Overconsolidation Ratio	R	V	√		
Effective Stress Envelop	R	L	√		
Octahedral Shear Stress	L	L	√		
Frequency of Loading	L	L	√		
Long-Term Time Effects (Thixotropy)	R	R	√		
Grain Characteristics	R	L	√		√
Soil Structures	R	R	√		√
Volume Change Due to Shear Strain	V	R	√		

* **V means important, L means less important, R means relatively unimportant.**

modulus of the material. As such, the upper and lower bounds of the modulus are:

$$E_{up} = E_{seis} \tag{2.6a}$$

$$E_{low} = 0.05E_{seis} \tag{2.6b}$$

Ishibashi and Zhang (1993) combined the effects of the confining pressure and plasticity index on modulus behavior in the form

$$\frac{E}{E_{seis}} = K(\gamma, PI)(\sigma'_m)^{m(\gamma,PI)-m_0} \tag{2.7}$$

where PI is the plasticity index of the base or subgrade material and γ is the shear strain and

$$K(\gamma, PI) = 0.5\left\{1 + \tanh\left[\ln\left(\frac{0.000102 + n(PI)}{\gamma}\right)^{0.492}\right]\right\} \tag{2.8}$$

$$m(\gamma, PI) - m_0 = 0.272\left\{1 - \tanh\left[\ln\left(\frac{0.000556}{\gamma}\right)^{0.4}\right]\right\}\exp(-0.0145PI^{1.3}) \tag{2.9}$$

$$n(PI) = \begin{cases} 0.0 & for PI = 0 \\ 3.37\times10^{-6}\,PI^{1.404} & for 0 < PI \le 15 \\ 7.0\times10^{-7}\,PI^{1.976} & for 15 < PI \le 70 \\ 2.7\times10^{-5}\,PI^{1.115} & for PI > 70 \end{cases} \tag{2.10}$$

Influence of the confining pressure on modulus reduction, E/E_{seis}, is also illustrated in Figure 2.3. At higher confining pressures, the modulus reduction, E/E_{seis}, becomes closer to one, meaning that modulus is closer to seismic modulus.

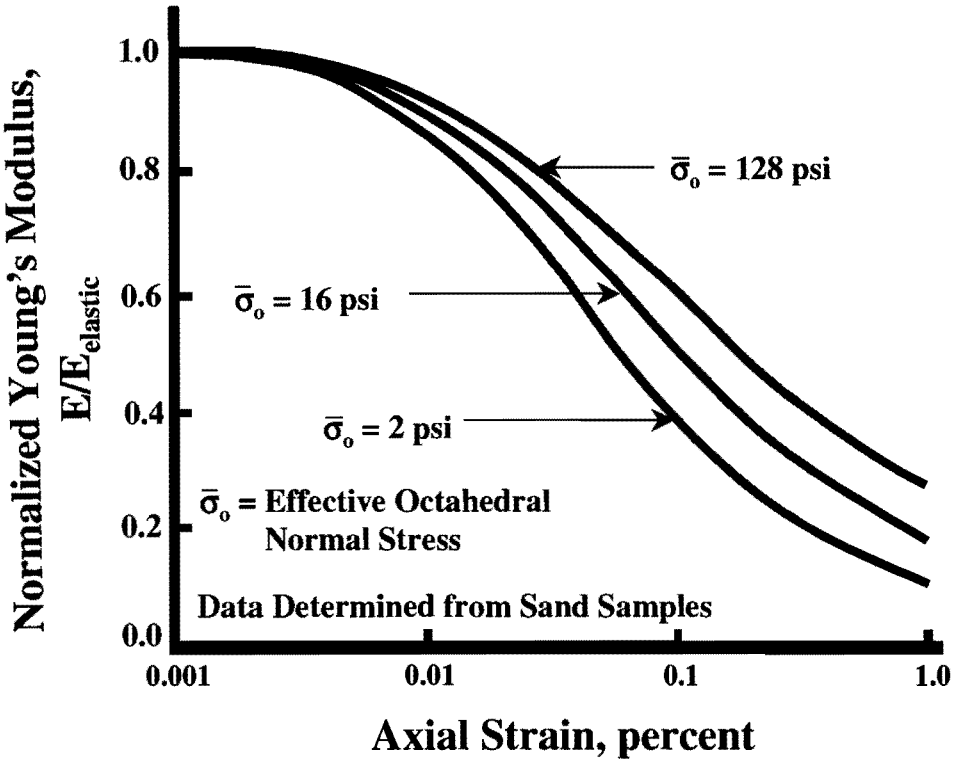

Figure 2.3 Influence of Effective Confining Pressure on Modulus Reduction Curve (from Ishibashi, 1992)

Bituminous Materials

Several parameters affect the modulus of bituminous materials. The most important parameters are the rate of the loading (i.e., frequency of loading), temperature and air void content.

The typical frequency range at which asphalt concrete (AC) moduli measured with seismic methods is about 10 KHz to 25 KHz; whereas, the actual traffic load has a dominant frequency of about 10 to 30 Hz. Aouad et al. (1993) clearly demonstrated the importance of considering the impact of frequency on modulus. As shown in Figure 2.4, depending on the temperature, the modulus measured with seismic methods should be reduced by a factor of about 3 to 15. Daniel and Kim (1998) and Kim and Lee (1995) used the results from several laboratory and field tests (such as FWD, ultrasonic, uniaxial sweep, and creep) to show the frequency dependence of modulus. The results from Daniel and Kim are shown in Figure 2.5. Again, the frequency dependence is temperature related.

The AC modulus is strongly dependent on temperature. Von Quintus and Kilingsworth (1998) demonstrated the importance of temperature gradient within a pavement section. Aouad et al. (1993), Li and Nazarian (1994) and several other investigators have studied the variation in modulus with temperature adjustment. With the advancement in measuring the modulus of pavements, methodology for temperature correction should be studied and improved.

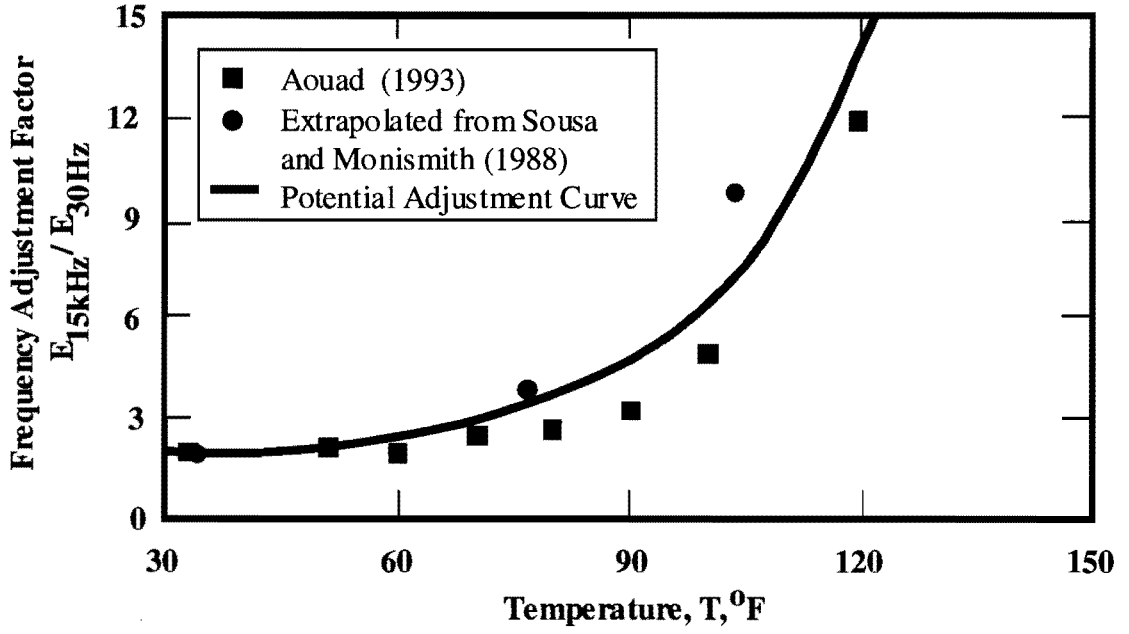

Figure 2.4 Variation in AC Modulus with Frequency and Temperature (from Aouad et al., 1993)

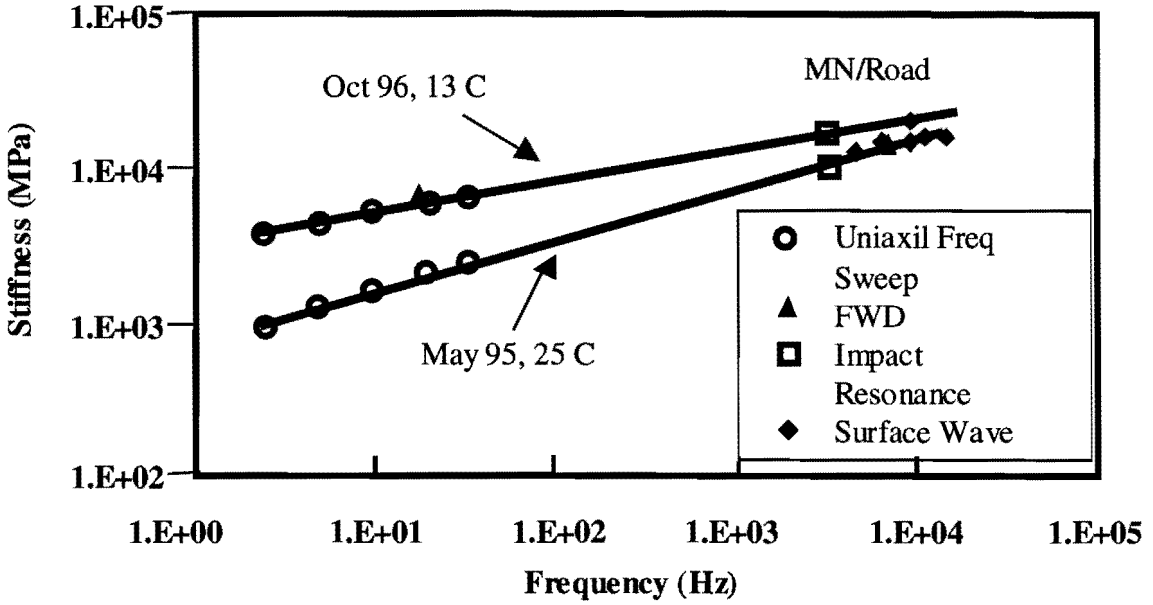

Figure 2.5 Frequency Dependency of AC Modulus (from Daniel and Kim, 1998)

Air void content has a significant impact on the modulus of AC as well. Rojas (1999) clearly demonstrated that the modulus of a mix is inversely proportional to the air void content of the mix (Figure 2.6). He also showed that aggregate gradation and the asphalt viscosity affect the modulus of the mix.

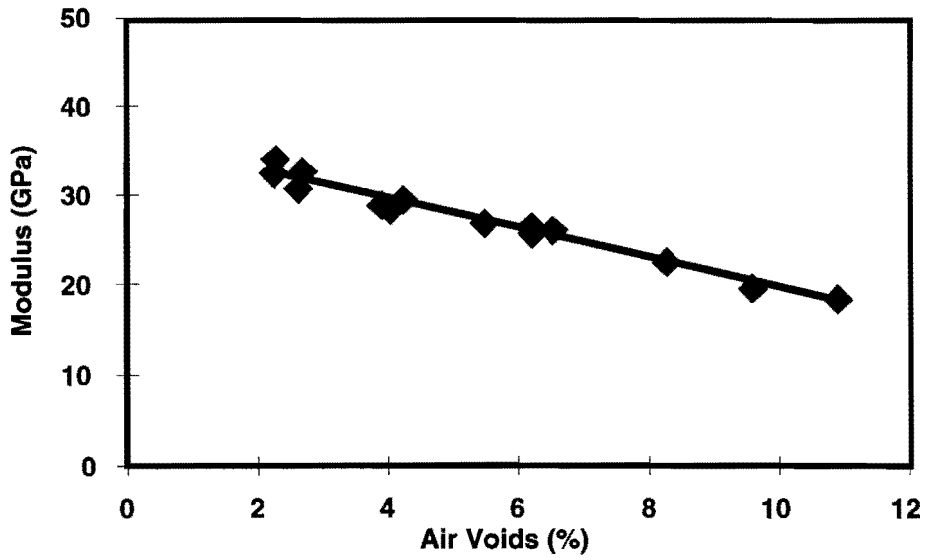

Figure 2.6 Impact of Air Void Content on AC Modulus (from Rojas, 1999)

PAVEMENT REMAINING LIFE

A pavement may develop several modes of failure during its service life. Therefore, its integrity at a given point in time depends on the type of failure occurring on it. Each failure criterion should be developed separately to take care of each specific type of failure. Since the most common structural failure modes observed in flexible pavements are rutting and fatigue cracking, these failure modes are adopted as pavement performance indicators.

According to Huang (1994), the failure criterion for fatigue cracking is expressed as:

$$N_f = f_1(\varepsilon_t)^{-f_2}(E_1)^{-f_3} \tag{2.11}$$

in which N_f is the allowable number of load repetitions to prevent fatigue cracking, ε_t is the tensile strain at the bottom of AC layer, E_1 is the elastic modulus of the AC layer, and f_1, f_2, and f_3 are constants determined from laboratory fatigue tests with f_1 modified to correlate with field performance observations. The Asphalt Institute recommends 0.0796, 3.291, and 0.854 for f_1, f_2, and f_3, respectively.

The failure criterion for rutting is expressed as:

$$N_r = f_4(\varepsilon_c)^{-f_5} \tag{2.12}$$

in which N_r is the allowable number of repetitions to limit rutting, ε_c is the compressive strain on the top of subgrade, and f_4 and f_5 are constants determined from road tests or field performance. The Asphalt Institute suggests that the values of f_4 and f_5 are 1.365×10^{-9} and 4.477, respectively.

CHAPTER THREE
PAVEMENT ANALYSIS MODELS

INTRODUCTION

Linear elastic models are the simplest models used to characterize the behavior of pavement systems. Several computer programs have been developed to analyze the structural response of pavement systems based on linear elastic theory (Uzan et al., 1989). Since some pavement materials may exhibit nonlinear behavior under actual wheel load, linear elastic models cannot rigorously consider such behavior.

Equivalent linear models can be used to consider the nonlinear behavior of pavement materials. These models are approximate since they cannot consider the variation in the stiffness of pavement layers in the lateral direction. By employing finite element methods, the variation in stiffness of pavement layers in horizontal and radial directions can be taken into consideration. In this chapter, each model is briefly discussed. Ke et al. (2000) extensively described the advantages and disadvantages of each model.

STRUCTURAL MODELS

Brown (1996) discusses a spectrum of analytical and numerical models that can be used in pavement design. These models estimate the critical stresses, strains and deformations within a pavement structure. The structural models used in this study are described in this section.

Layered Elastic Model

The layered elastic models are the simplest models for estimating the response of pavements under load, since the modulus of each layer is constant. Most algorithms used in pavement analysis and design, take advantage of these types of solutions. BISAR (De Jong et al., 1973) and WESLEA (Van Cauwelaert et al., 1989) are two of the popular linear elastic programs. These programs can rapidly yield results. However, if the loads are large enough for the material to exhibit nonlinear behavior, the results are approximate.

Equivalent-Linear Model

To approximate the load-induced nonlinear behavior of pavement materials, an equivalent linear model can be adopted. The equivalent-linear model is based on the static linear elastic layered

theory. The nonlinear behavior of the pavement materials is modeled through an iterative process employing any of the nonlinear constitutive models described in Chapter 2.

The implementation of the equivalent linear process is summarized in a flowchart shown in Figure 3.1. The layers that may experience nonlinear behavior are divided into several sublayers as shown in Figure 3.2. The number of sublayers is determined based on a compromise between the accuracy required and the computation time. Ke et al. (2000) demonstrate that three to five sub-layers are optimal for most typical pavements in Texas. Several radial points (called stress points) are chosen for each nonlinear sub- layer. An initial modulus is assigned to each stress point. The appropriate stresses and strains are calculated for all stress points using a multi-layer elastic layered solution. The calculated stresses and strains can be input to the appropriate constitutive model to calculate a modulus. The assumed modulus and the newly calculated modulus at each point are compared. If the difference is larger than a pre-assigned tolerance at any point, the process will be repeated using an updated assumed moduli. The above procedure is repeated until the modulus difference is within the tolerance and thus, convergence is reached. The required stresses and strains are computed using final moduli for all nonlinear sub-layers. This method is relatively rapid; however, the results are approximate. In a linear-elastic layered solution, the lateral variation of modulus within a layer cannot be considered. Practically speaking, this method may be quite reasonable for most pavement analyses.

Finite Element Models

To model the nonlinear behavior of pavement in the most comprehensive manner, finite element analysis methods can be used. Several software packages are capable of modeling the behavior of a pavement by selecting the most sophisticated constitutive models for each layer of pavement. The dynamic nature of the loading can also be considered. ABAQUS (Habbit, Karlsson & Sorensen, Inc) was used herein because of its flexibility. In nonlinear analysis using ABAQUS the constitutive model described in Equation 2.4 can be implemented in a user subroutine. Whenever an element in a nonlinear layer is involved, that subroutine is called to compute the nonlinear modulus related to its existing state of stress. The analytical solutions are highly efficient and are quite advanced. However, expertise is needed to review the input and output to ensure that all aspects of modeling are properly considered. Using the finite element methods can be very time consuming.

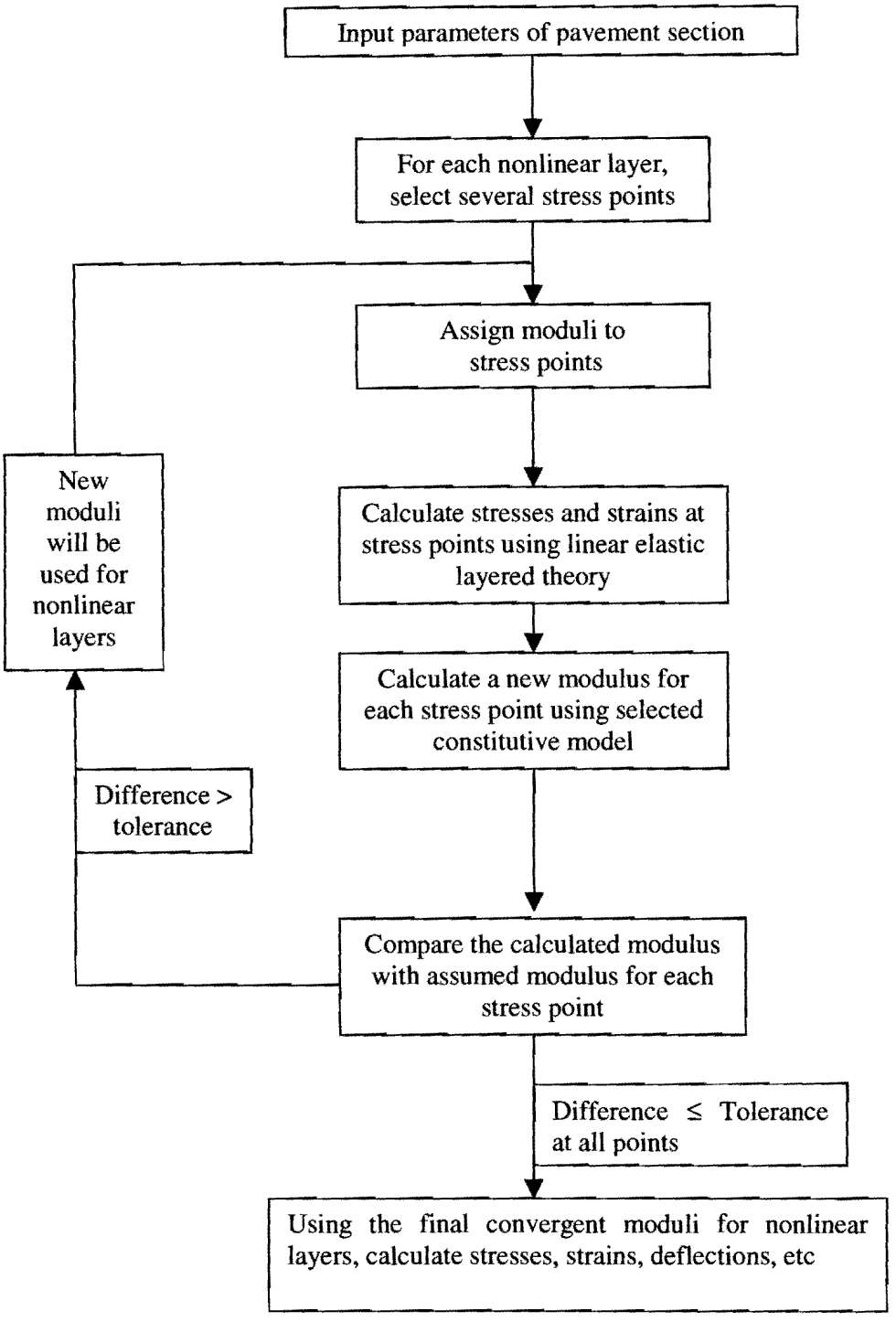

Figure 3.1 Flow Chart of Implementation of Equivalent-Linear Model

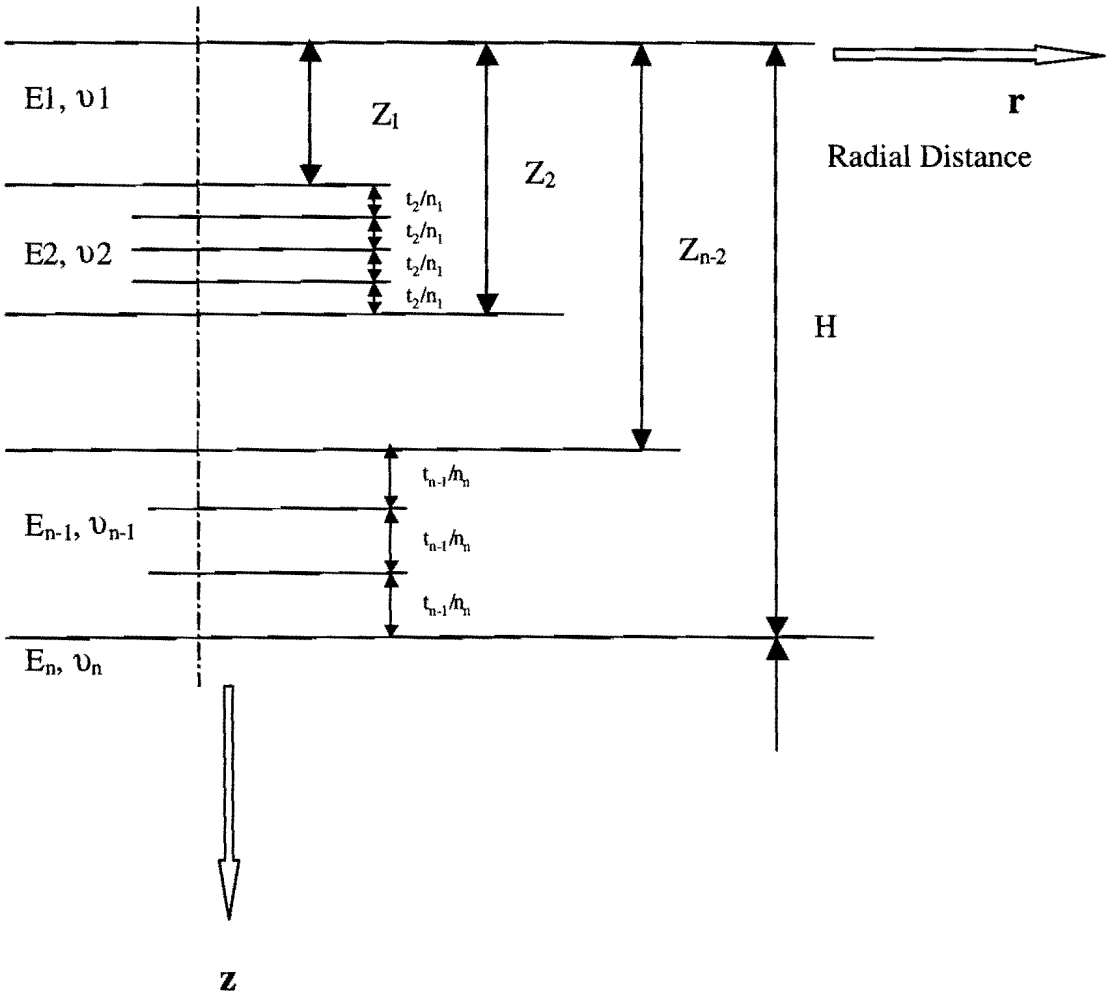

Figure 3.2 Typical Profile of a Pavement Section Used in Equivalent Linear Model

TYPICAL RESULTS

To observe the sensitivity of the equivalent linear model to the change of nonlinear parameters, four hypothetical pavement sections were assumed. The pavement sections used in this study are assumed to have four layers, an asphalt concrete layer over a base over a subgrade over bedrock. These pavement sections, which are shown in Figure 3.3 and their properties summarized in Tables 3.1, are meant to simulate primary, secondary, county roads and streets.

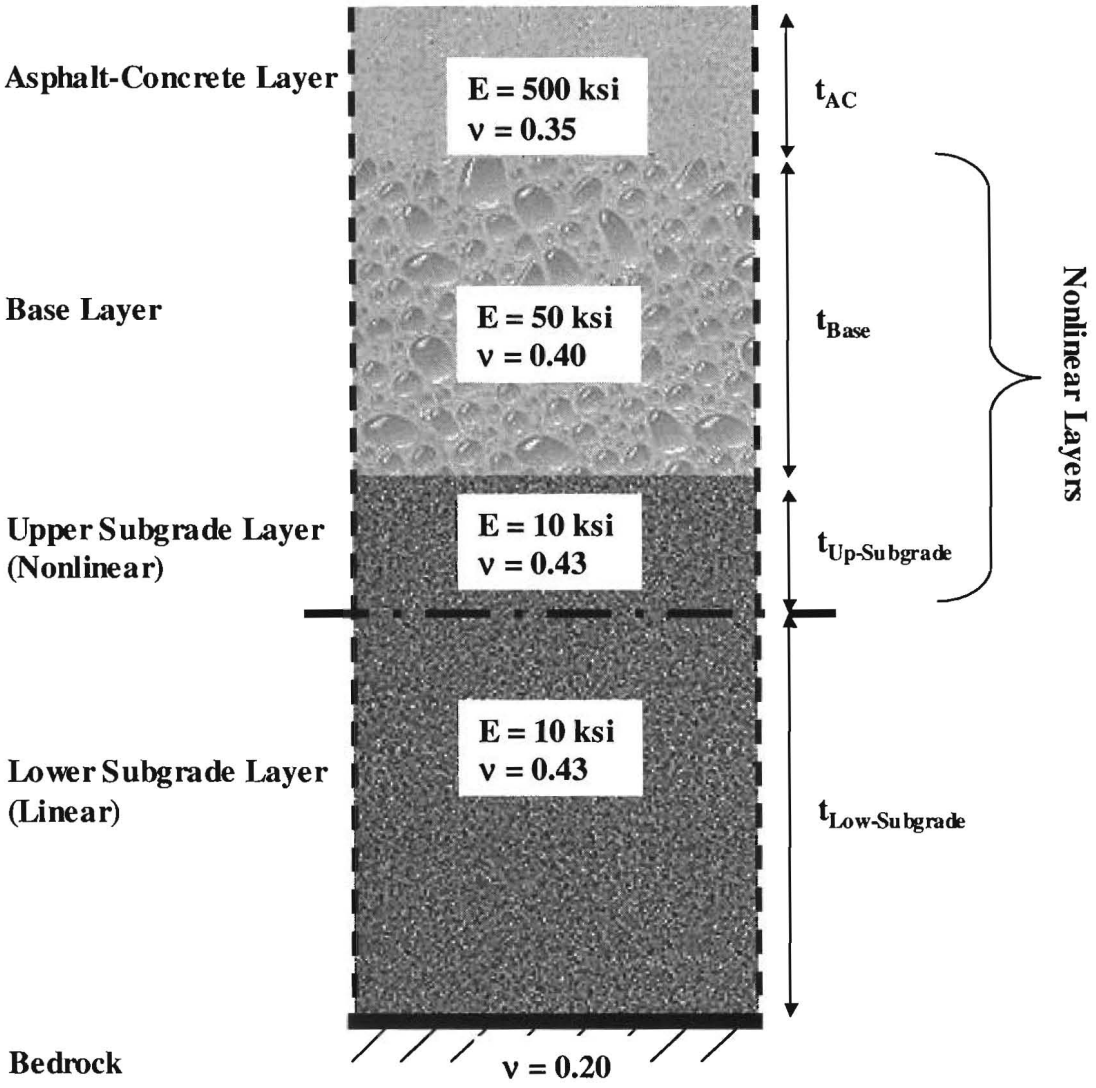

Figure 3.3 Profile of Pavement Sections Used in This Study

Table 3.1 Properties of Different Pavement Sections

	Layer	Modulus ksi	(MPa)	Poisson Ratio	Thickness (inch)	(mm)	Unit Weight (inch)	(KN/m^3)
Primary Road	**AC**	500	(3450)	0.35	5	(125)	140	(22.0)
	Base	50	(345)	0.35	12	(300)	120	(18.8)
	Upper Subgrade	10	(69)	0.4	43	(1075)	110	(17.2)
	Lower Subgrade	10	(69)	0.4	240	(6000)	110	(17.2)
	Bedrock	1000	(6900)	0.2	Infinity	(Infinity)		
Secondary Road	**AC**	500	(3450)	0.35	3	(75)	140	(22.0)
	Base	50	(345)	0.35	12	(300)	120	(18.8)
	Upper Subgrade	10	(69)	0.4	45	(1125)	110	(17.2)
	Lower Subgrade	10	(69)	0.4	240	(6000)	110	(17.2)
	Bedrock	1000	(6900)	0.2	Infinity	(Infinity)		
County Road	**AC**	500	(3450)	0.35	5	(125)	140	(22.0)
	Base	50	(345)	0.35	6	(150)	120	(18.8)
	Upper Subgrade	10	(69)	0.4	49	(1225)	110	(17.2)
	Lower Subgrade	10	(69)	0.4	240	(6000)	110	(17.2)
	Bedrock	1000	(6900)	0.2	Infinity	(Infinity)		
Street	**AC**	500	(3450)	0.35	3	(75)	140	(22.0)
	Base	50	(345)	0.35	6	(150)	120	(18.8)
	Upper Subgrade	10	(69)	0.4	51	(1275)	110	(17.2)
	Lower Subgrade	10	(69)	0.4	240	(6000)	110	(17.2)
	Bedrock	1000	(6900)	0.2	Infinity	(Infinity)		

In each pavement type, the top layer is an asphalt concrete pavement with a thickness of 3 in. (75 mm) or 5 in. (125 mm), a Poisson's ratio of 0.35 and unit weight of 140 pcf (22 KN/m^3). Under the asphalt concrete layer lays the base. The thickness of this layer is assumed to be either 6 in. (150 mm) or 12 in. (300 mm) with a Poisson's ratio of 0.35 and a unit weight of 120 pcf (18.8 kN/m^3). The third layer is the subgrade. Sensitivity studies by Ke et al. (2000) indicated that pavement materials might show nonlinear behavior down to a depth of 60 in. (1.5 m) from the surface. Therefore, the thickness of the nonlinear layer of subgrade is proportionate to the thickness of asphalt concrete and base layers. From a depth of 60 in. (1.5 m) to 240 in. (6 m) the subgrade layer is assumed to be linear. A Poisson's ratio of 0.4 was assigned to the nonlinear and linear layers of the subgrade. At the bottom of subgrade is an infinite layer of bedrock with a modulus value of 1000 ksi (69000 MPa), and a Poisson's ratio of 0.2.

Typical seismic moduli assigned to each layer are included in Table 3.1. A modulus of 500 ksi (3450 MPa) was assumed for the AC layer. It is assumed that the modulus is corrected for

temperature and rate of loading as discussed in Chapter 2. Typical seismic moduli of 50 ksi (345 MPa) and 10 ksi (69 MPa) were assumed for the base and subgrade.

In the equivalent linear and nonlinear analyses, two nonlinear constitutive models were considered. The first one is of the form of

$$E = k_1 \sigma_c^{k_2} \sigma_d^{k_3} \tag{3.1}$$

Equation 3.1 is identical to Equation 2.4 so its associated parameters are defined there. In this model, the base and the upper layer of subgrade are considered nonlinear. Parameters k_2 and k_3 need to be provided for each nonlinear layer. Based on a large number of tests with bender elements by Baig (1991), and recommendations from TxDOT Projects 0-1336 (Nazarian et al., 1996) and 0-1177 (Feliberti and Nazarian, 1993), typical k_2 and k_3 values for different pavement materials were estimated. Table 3.2 contains these values. Generally base materials are categorized as high quality, average, or poor quality, while subgrade materials are categorized as sandy, high plasticity clay and low plasticity clay.

The other constitutive model is in the form of

$$K(\gamma, PI) = 0.5\left\{1 + \tanh\left[\ln\left(\frac{0.000102 + n(PI)}{\gamma}\right)^{0.492}\right]\right\} \tag{3.2}$$

This model and its parameters are also described in Chapter 2. Typical PI values used in this study are shown in Table 3.2.

Table 3.2 Typical Nonlinear Values of Pavement Materials

Material	Classification	Nonlinear Parameters		
		k_2	k_3	PI
Base	High Quality	0.4	-0.2	0
	Average	0.2	-0.3	6
	Poor Quality	0.1	-0.4	12
Subgrade	Sandy	0.4	-0.2	0
	Low Plasticity Clay	0.1	-0.3	30
	High Plasticity Clay	0.0	-0.4	60

To demonstrate the importance of considering the nonlinear moduli in the analysis and design of pavements, the variation in modulus of the typical primary road under traffic load is shown in Figure 3.4. An extensive discussion of the impact of the nonlinear behavior of the pavement layers on the remaining life can be found in Nazarian et al. (1998b). Since the remaining life of a pavement is related to stresses at the interface of the layers, it is readily obvious that this parameter should be considered.

Different structural and material models were applied to a primary road using the typical values presented in this chapter. The two critical strains and remaining lives, as described in Chapter 2, for different conditions are summarized in Table 3.3. The estimated runtime for each condition is also included in the table.

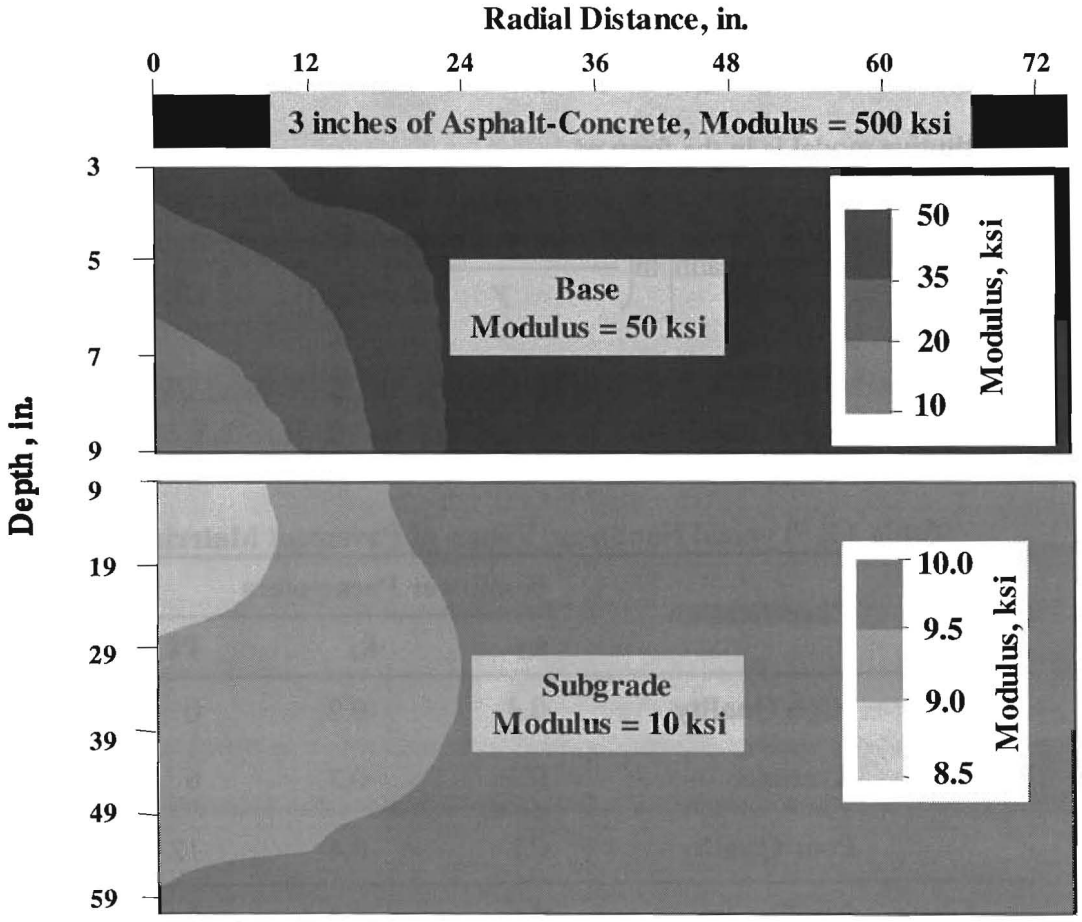

Figure 3.4 Variation of Modulus of Pavement Material Under Traffic Load

Table 3.3 Remaining Life of a Primary Road Applying Different Structural Models

Structure Model	Computation Time (sec)	Critical Strains (micro-strain)				Remaining Lives (10^3 ESALs)			
		Tensile	Error,%	Compressive	Error,%	Fatigue	Error,%	Rutting	Error,%
Linear Static	2	204	33	587	21	1505	271	401	185
Linear Dynamic	600	203	33	596	20	1532	278	373	165
PI Model	10	250	18	605	21	653	61	380	170
Equivalent Linear	120	282	7	844	14	518	28	79	44
Nonlinear Static	1500	307	1	702	5	392	3	120	28
Nonlinear Dynamic	2400	304	-	764	-	406	-	141	-

Since the dynamic nonlinear assumptions seem to represent the most realistic conditions, the results from other conditions are compared with the results from the nonlinear dynamic model. The errors represent the percent error of the results with respect to the results of the dynamic nonlinear model. Table 3.3 indicates that the equivalent linear model may not be the fastest or the most accurate structural model for predicting the remaining life of pavements. However, given the variability in material properties along the length of a given project, and given the uncertainties in the remaining life models typically used, the equivalent linear models may be the best compromise in terms of practicality of use and the accuracy of the results. Nonlinear static and nonlinear dynamic models may be more accurate models; however, given the personnel shortage and the state of practice in designing pavements by highway agencies, they may not be the most practical alternatives.

CHAPTER FOUR
PAVEMENT RESPONSE UNDER EQUIVALENT LINEAR MODEL

INTRODUCTION

Ke et al. (2000) conducted a preliminary sensitivity study related to all material and structural models described in Chapters 2 and 3. In this chapter, the sensitivity of the pavement responses to the nonlinear parameters of the base and subgrade for the assumed equivalent linear model is comprehensively studied. The sensitivity of pavement surface deflections, critical strains, and remaining lives of the four pavement sections described in Chapter 3 to the variations in nonlinear pavement parameters is studied. The iterative computer program based on the equivalent linear model, described in the previous chapter, was developed and used to estimate the deflections, critical strains, and remaining lives of the pavement sections. A 9000 lb (40 KN) load, uniformly distributed over a circular area with a radius of 6 in. (150 mm), is assumed for calculating the deflections. The critical strains and remaining lives were determined considering a standard 18-kip (80-KN) tandem load. The main reasons for this sensitivity study are (1) to investigate the impact of the nonlinear parameters of the base and subgrade layers on the FWD deflections and (2) to assess the effects of the nonlinear parameters of the base and subgrade on estimating the performance of pavements. In that manner, one would know which of the nonlinear parameters could be estimated with reasonable certainty and which ones cannot be accurately backcalculated. Similarly, one would know which of the nonlinear parameters should be known accurately and which ones are of no consequence on the calculated remaining lives of pavement.

SENSITIVITY STUDY

The variations in the deflections of the pavement surface, the two critical strains (tensile strain at the bottom of the AC layer, and compressive strain at the top of the subgrade) and fatigue and rutting remaining lives due to variations in nonlinear parameters, k_2 and k_3, for each layer are studied in this section. In each case, a particular parameter was allowed to vary while others were maintained constant. A data set containing 500 input data simulating different pavement sections was generated using a Monte Carlo simulation (Ang and Tang, 1984a, 1984b). For each data set, a normal distribution with a mean value equal to the values reported in Tables 3.2 and a standard deviation of 20% of the mean value were assumed. The equivalent linear program was then executed to obtain the deflections, critical strains, and the two remaining lives. Using the baseline values reported in Tables 3.2, the corresponding deterministic baseline value for each

response parameter was obtained. For each of the 500 cases, the variation from the baseline value, VB, was determined using the following relationship:

$$VB = \left| \frac{\bar{y} - y}{\bar{y}} \right| \tag{4.1}$$

where $\bar{y}$ is the target parameter derived from the equivalent linear model using the mean values for the nonlinear parameters, and y is the target parameter derived from the equivalent linear model using the varied parameter.

The variations in deflection, VB, from the baseline for the parameter k_3 of the base of the secondary road are depicted in Figure 4.1. This type of graph demonstrates the correlation between perturbed and target parameters. In Figure 4.1, deflections of the last four sensors vary slightly, while the perturbed parameter k_3 of the base is varied by 20%. The greater the spread in the variation from the baseline is, the more sensitive the parameter is to the variation of the target parameter. The spread of the target parameter is also an indication of the target parameter distribution. Another advantage of using this type of graph is that it shows the sensitivity of several target parameters at the same time at the same scale.

To quantify the sensitivity as qualitatively demonstrated in Figure 4.1, a sensitivity number was introduced. The effects of the perturbed input parameter on the response parameters can be assessed using the sensitivity number. To obtain the sensitivity number, a cumulative distribution from the baseline curve (Y-axis of Figure 4.1) was developed for each of the response parameters. Figure 4.2 demonstrates this concept. Another X-axis, which corresponds to the ratio of the target parameter calculated from the perturbed value (y) and the target parameter from the baseline value ($\bar{y}$) is added for clarity. The value at the 95 percentile of the variation from the baseline of each parameter is called the sensitivity number (SN). The larger the sensitivity number is, the more sensitive the target parameter will be to the input parameter. In this case, the sensitivity number as marked in Figures 4.1 and 4.2 is 13.

For practical purposes, several levels of sensitivity are defined. For deflections, these limits are derived from the precision of the FWD measurements. For the critical strains and remaining lives, the limits were set according to the nature of the parameters. These levels, which are defined in Table 4.1, are used throughout this study. From the sensitivity number determined in the previous paragraph, parameter k_3 of base is considered sensitive.

Similar to this example, the behavior of all pavement sections described in Chapter 3 is studied. The deflection, critical strains and remaining lives of all the pavement sections are analyzed. The results and figures of the sensitivity study are presented in Appendix C.

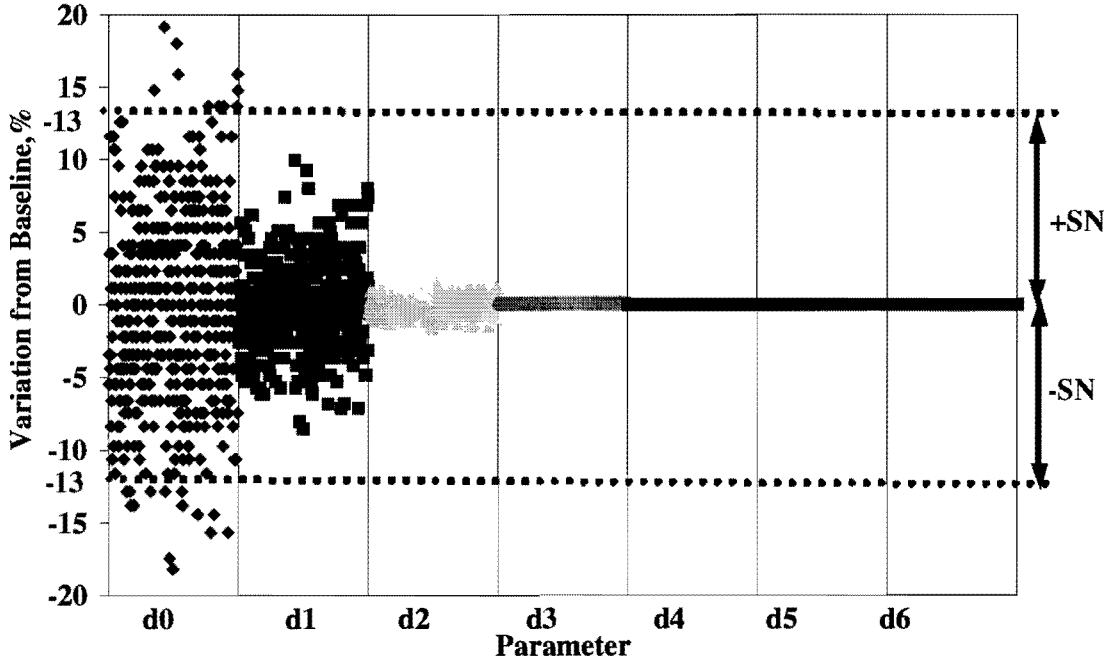

Figure 4.1 Variation of Deflection at Sensor Locations (d0-d6) due to Variation of k_3 of Base for a Hypothetical Pavement Section

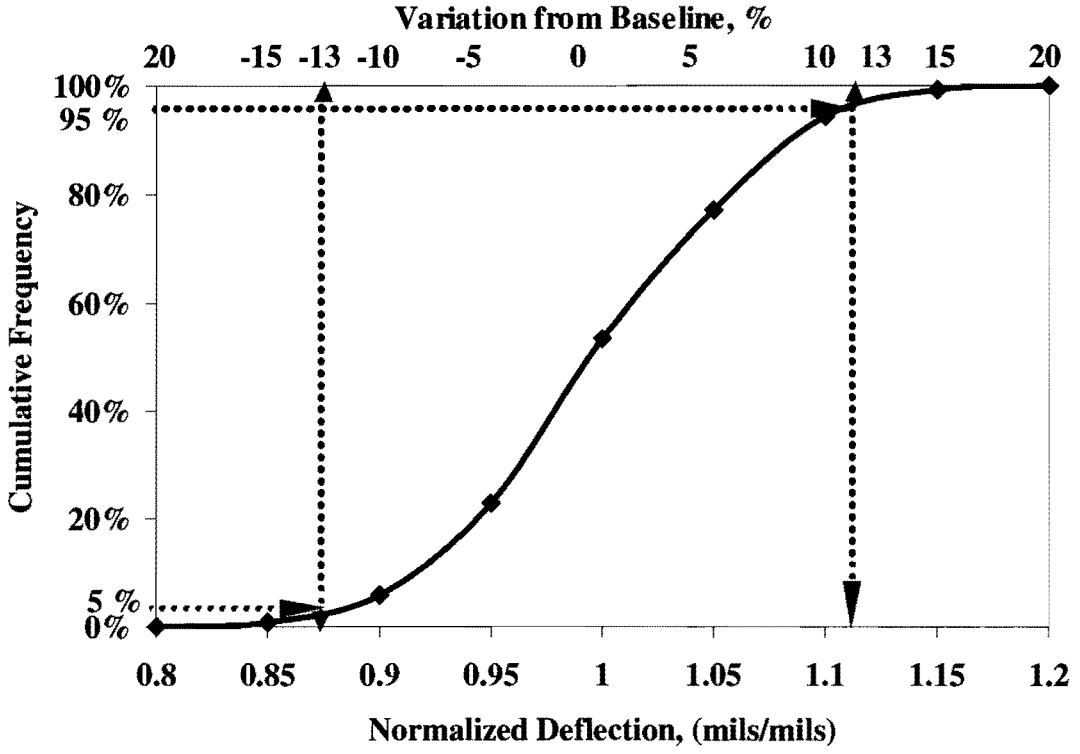

Figure 4.2 Cumulative Distribution of Deflection due to Variation of k3 of Base for a Hypothetical Pavement Section

Table 4.1 Levels of Sensitivity Based on Sensitivity Number of Each Parameter

Level of Sensitivity	Sensitivity Number (SN), %		
	Deflection	**Critical Strain**	**Remaining Life**
Not Sensitive (NS)	SN ≤ 10	SN ≤ 10	SN ≤ 25
Moderately Sensitive (MS)	10 < SN ≤ 20	10 < SN≤ 20	25 < SN≤ 50
Sensitive (S)	20 < SN≤ 30	20 < SN≤ 40	50 <SN≤ 100
Very Sensitive (VS)	30 < SN	40 < SN	100 < SN

Sensitivity of Deflection

The baseline values of the nonlinear parameters used in this study are presented in Table 4.2. Following the procedure described above, four sets of 500 input data points were generated by varying one nonlinear parameter at a time, another 500 sets of data were generated varying all the nonlinear parameters.

Table 4.2 Nonlinear Properties of Nonlinear Layers for "Primary Road Average Quality Base and Low Plasticity Clay Subgrade"

Nonlinear Layer	k_2	k_3
Average Quality Base	0.2	-0.3
Low Plasticity Clay Subgrade	0.1	-0.3

The variations from the baseline for seven deflections from the primary road constructed on average quality base and low plasticity clay subgrade are shown in Figure 4.3. The sensors are placed under the load and 12 in. (305 mm), 24 in. (610 mm), 36 in. (914 mm), 48 in. (60 in.) and 72 in. (1524 mm) from the load. Each of the nonlinear parameters k_2 and k_3 are varied. As a reminder, the corresponding k_2 and k_3 values are shown in Table 4.2. As reflected in Figure 4.3, the deflection under the load is impacted the most by the nonlinear parameters of the base and subgrade. As the distance from the load increases, the impact of the nonlinear parameters on the surface deflection decreases. Hence, throughout this study deflection under the load is primarily used to indicate the sensitivity level. From Figure 4.3, parameter k_3 of the base and subgrade is the most dominant parameter impacting the deflections.

The variations from the baseline for the seven deflections, when all nonlinear variables are perturbed, are shown in Figure 4.4. This condition better corresponds to the actual field condition. The cumulative distributions of absolute values of the variations from the baseline for the deflection under the load for each nonlinear parameter, and when all nonlinear parameters are

simultaneously perturbed, are shown in Figure 4.5. For the typical secondary road (as defined in Chapter 3) the surface deflection of the pavement is most sensitive to the parameters k_3 of subgrade and base and is less sensitive to the parameters k_2 of those layers. Comparing the cumulative curves when each individual parameter was varied with those when all parameters are perturbed would permit one to visually draw these conclusions. The closer a cumulative distribution curve is to the solid line (corresponding to the case when all parameters are perturbed), the more sensitive the desired output parameter will be to the selected input parameter.

Using the sensitivity numbers and their associated levels of sensitivity (Table 4.1), the sensitivity of the deflection under the load to the nonlinear parameters of base and subgrade are categorized for this case as well as all other pavement structures and base and subgrade types in Table 4.3. The obvious conclusion from Table 4.3 is that the thinner the pavement structures are, the more the deflections will be impacted by the nonlinear parameters. The not as obvious conclusion is that the type of base and subgrade also impact the sensitivity of the surface deflection to the nonlinear behavior of the base and subgrade. In general, thicker pavement structures, built with high quality base materials underlain by sandy subgrade are least impacted by the nonlinear behavior of the base and subgrade. On the contrary, thinner pavement structures, built from low quality base on clayey subgrades are significantly impacted by the nonlinear behavior of the pavement. In practical terms, for thicker, high quality pavements, the modulus of the subgrade determined by the SPA should be closer to those backcalculated by the FWD. Thinner, lower quality pavements, there should be significant differences between the SPA and FWD moduli. Another important implication of Table 4.3 is that when FWD tests are conducted on sandy subgrade or high quality base, the backcalculation of nonlinear parameters is rather difficult. On the other hand, for the lower quality base materials and clayey subgrades, the FWD deflections near the load are impacted by the nonlinear behavior of the materials.

Sensitivity of Strains

Using the procedure described for the deflections, the variations of tensile strain at the bottom of the AC layer, and compressive strain at the top of the subgrade are also studied. The variations in critical strains from the baseline strains when each nonlinear parameter was varied individually, and when all parameters were perturbed simultaneously, are shown in Figures 4.6 and 4.7, respectively. The cumulative distributions of the absolute values of the variations from the baseline for tensile and compressive strains are shown in Figure 4.8. From Figure 4.8, parameters k_3 of the base and subgrade are the most dominant parameter impacting tensile strain and compressive strain respectively.

Tables 4.4 and 4.5 summarize the sensitivity levels of tensile and compressive strains to the nonlinear parameters of the base and subgrade, respectively. According to Table 4.4, the critical tensile strain is very sensitive to the variation of k_2 of the base, while it is sensitive to the k_3 of the base and is moderately sensitive to k_2 and k_3 of the subgrade. Since the tensile strain is estimated at the bottom of the AC layer, it is reasonable to be sensitive to the nonlinear parameters of the base layer. The critical compressive strain is estimated at the top of the subgrade layer; therefore, this target parameter is very sensitive to nonlinear parameters of the subgrade layer.

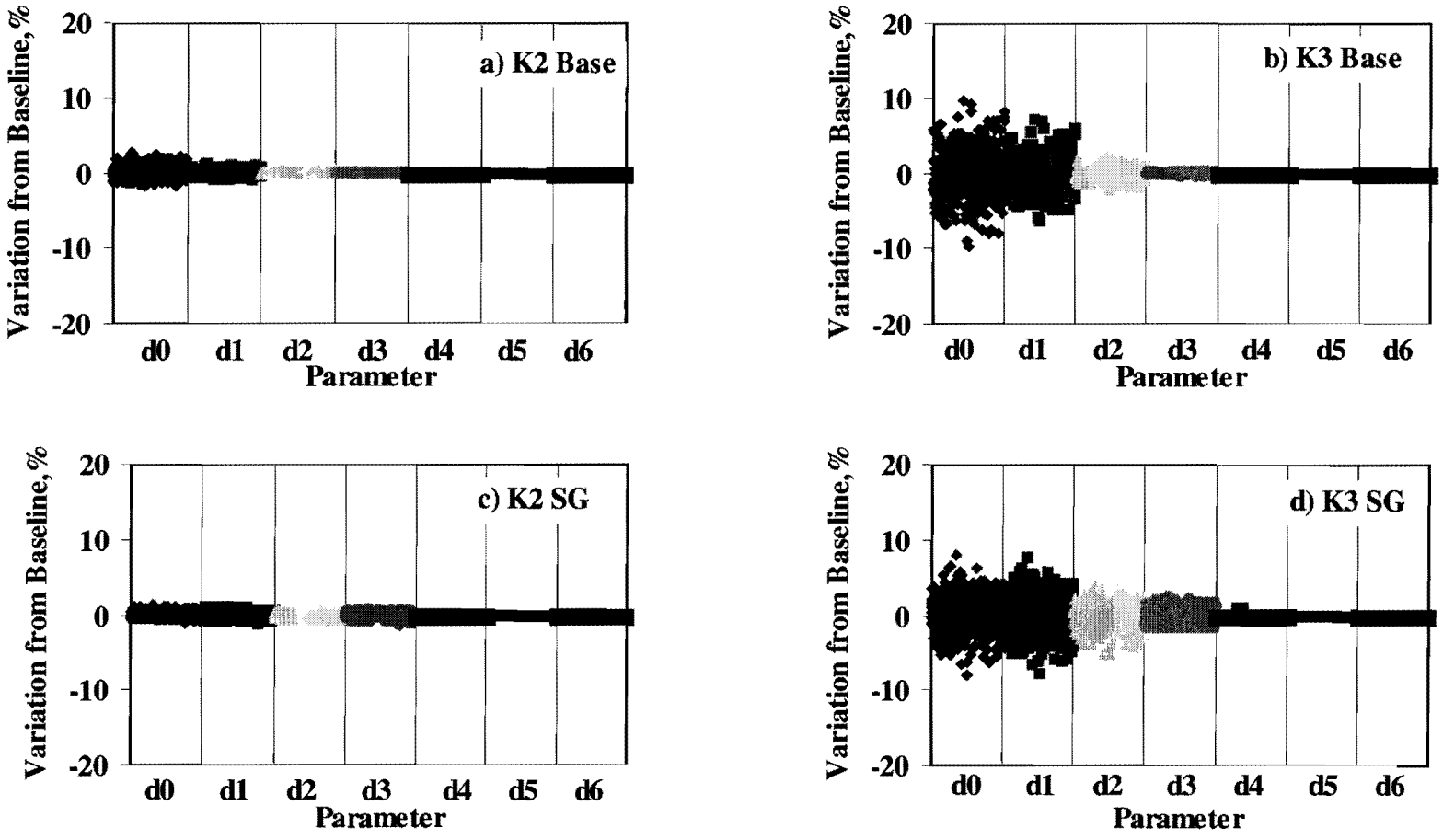

Figure 4.3 Variation of Deflection at Sensor Locations (d0-d6) due to Variation of Nonlinear Parameters for "Primary Road, Average Quality Base and Low Plasticity Clay Subgrade"

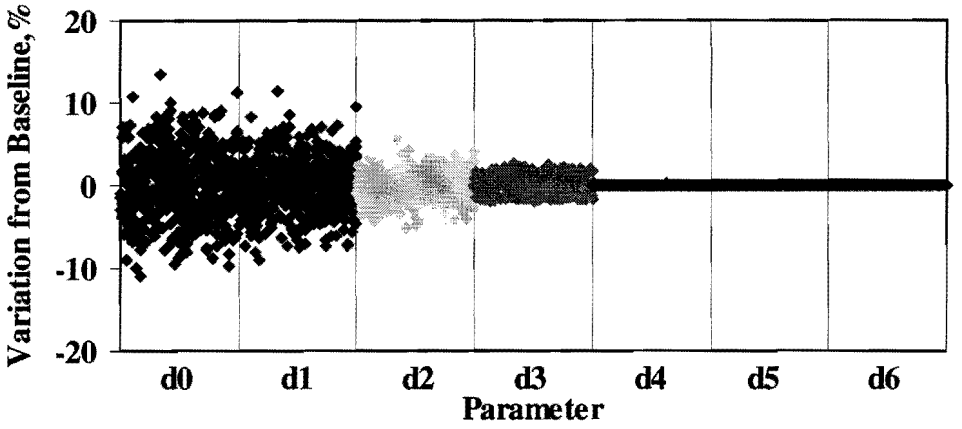

Figure 4.4 Variation of Deflection at Sensor Locations (d0-d6) due to Variation of All Nonlinear Parameters for "Primary Road, Average Quality Base and Low Plasticity Clay Subgrade"

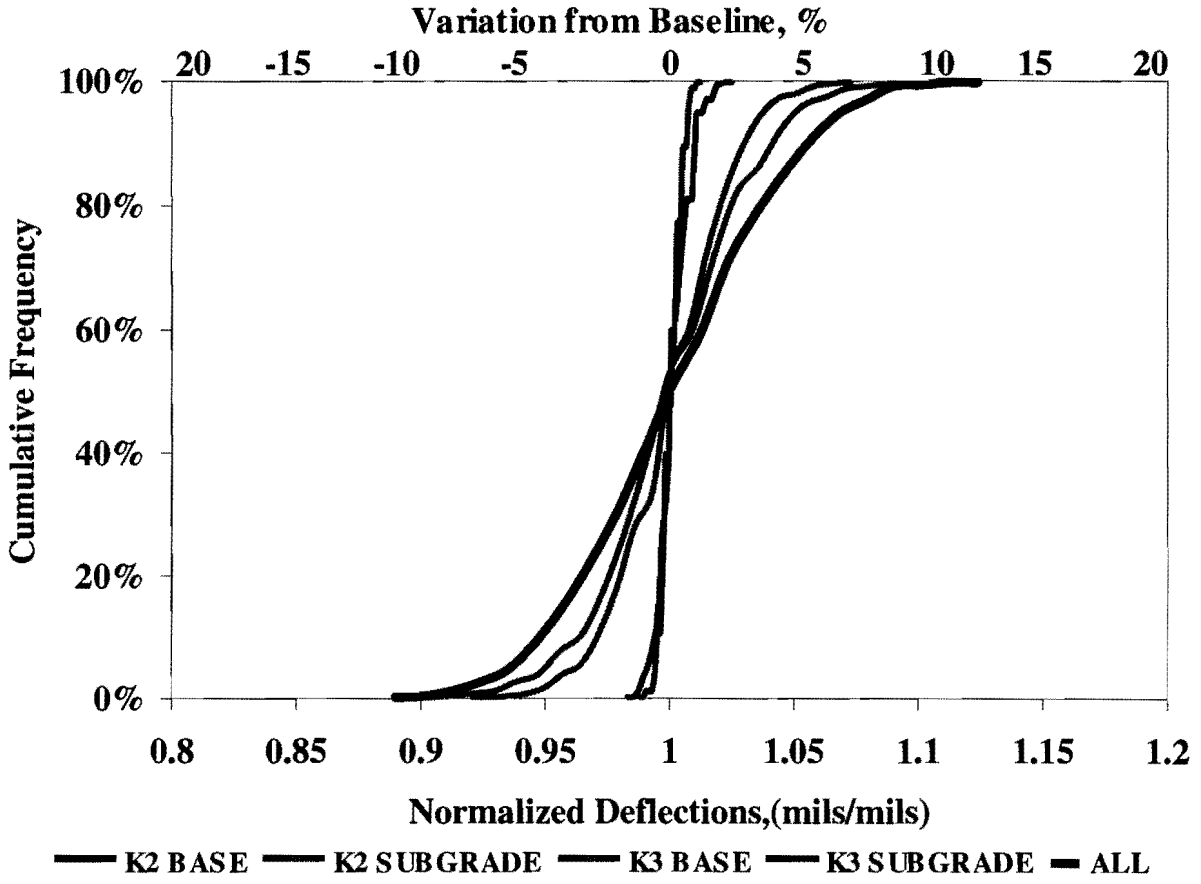

Figure 4.5 Cumulative Distribution of Deflection under the Load for "Primary Road, Average Quality Base and Low Plasticity Clay Subgrade"

Table 4.3 Sensitivity Level of Deflection Under the Load When K2 and K3 Parameters Are Perturbed

Pavement Profile	Base Layer	High Quality			Average Quality			Poor Quality		
	Subgrade Layer	Sandy	Clay Low PI	Clay High PI	Sandy	Clay Low PI	Clay High PI	Sandy	Clay Low PI	Clay High PI
Primary Road	K_2 Base	NS			NS	NS	NS	NS	NS	NS
	K_2 Subgrade		NS			NS		NS	NS	
	K_3 Base									
	K_3 Subgrade									
	All									
Secondary Road	K_2 Base	NS			NS	NS	NS		NS	NS
	K_2 Subgrade		NS			NS			NS	
	K_3 Base									
	K_3 Subgrade									
	All									
County Road	K_2 Base	NS	NS		NS	NS	NS	NS	NS	NS
	K_2 Subgrade		NS			NS			NS	
	K_3 Base	NS	NS	NS	NS					
	K_3 Subgrade									
	All									
Street	K_2 Base	NS			NS	NS	NS	NS	NS	NS
	K_2 Subgrade									
	K_3 Base									
	K_3 Subgrade									
	All									

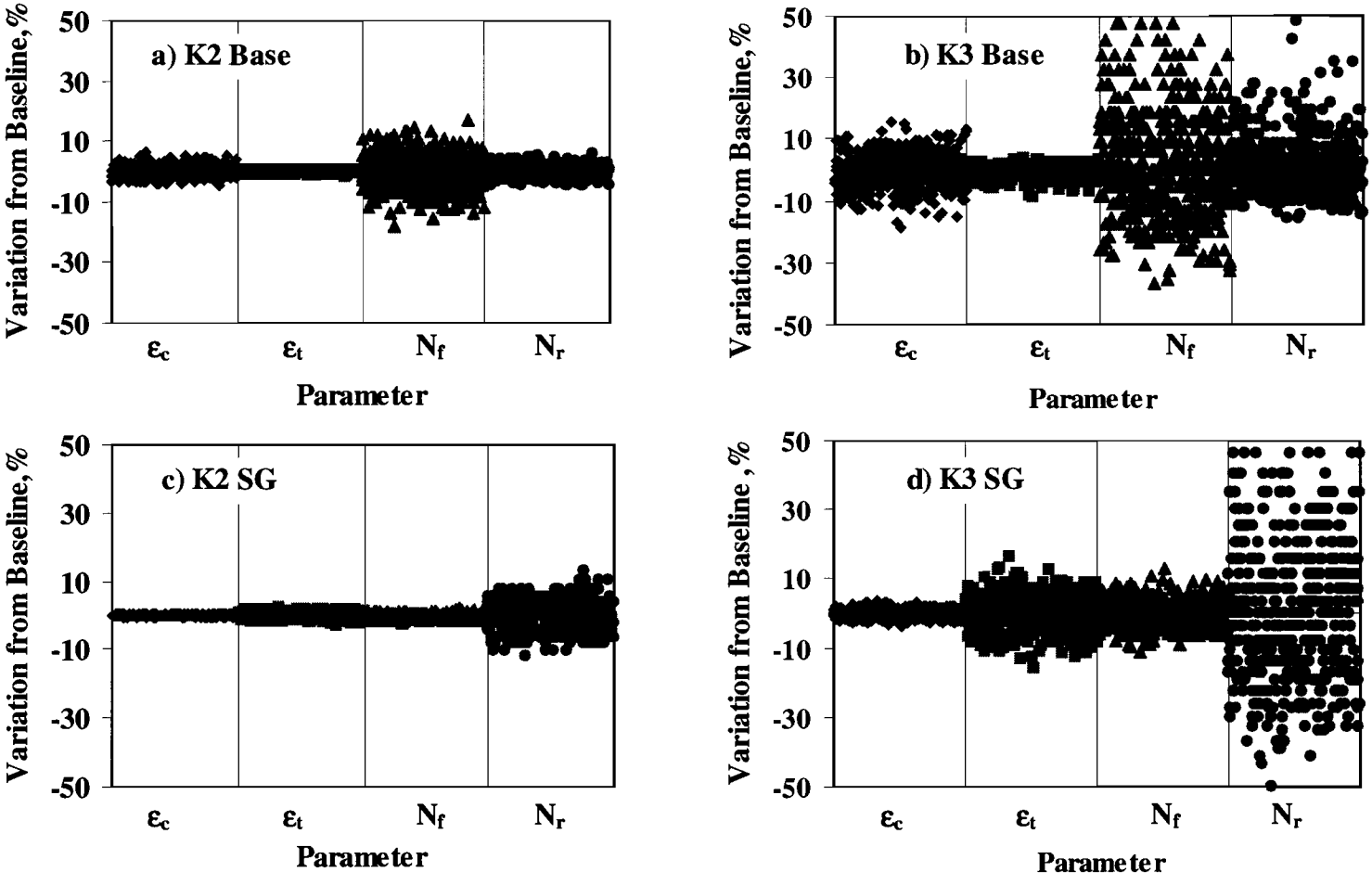

Figure 4.6 Variation of Tensile Strain (ε_t), Compressive Strain (ε_c), Fatigue (N_f), and Rutting (N_r) Remaining Lives for "Primary Road, Average Quality Base and Low Plasticity Clay Subgrade"

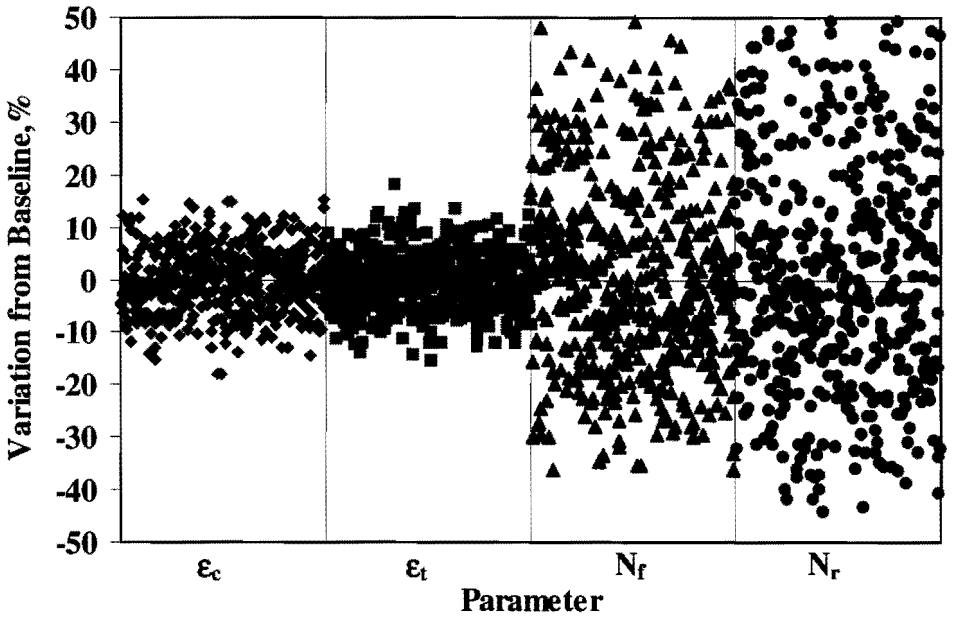

Figure 4.7 Variation of Tensile Strain (ε_t), Compressive Strain (ε_c), Fatigue (N_f), and Rutting (N_r) Remaining Lives Due to Variation of All Nonlinear Parameters for "Primary Road, Average Quality Base and Low Plasticity Clay Subgrade"

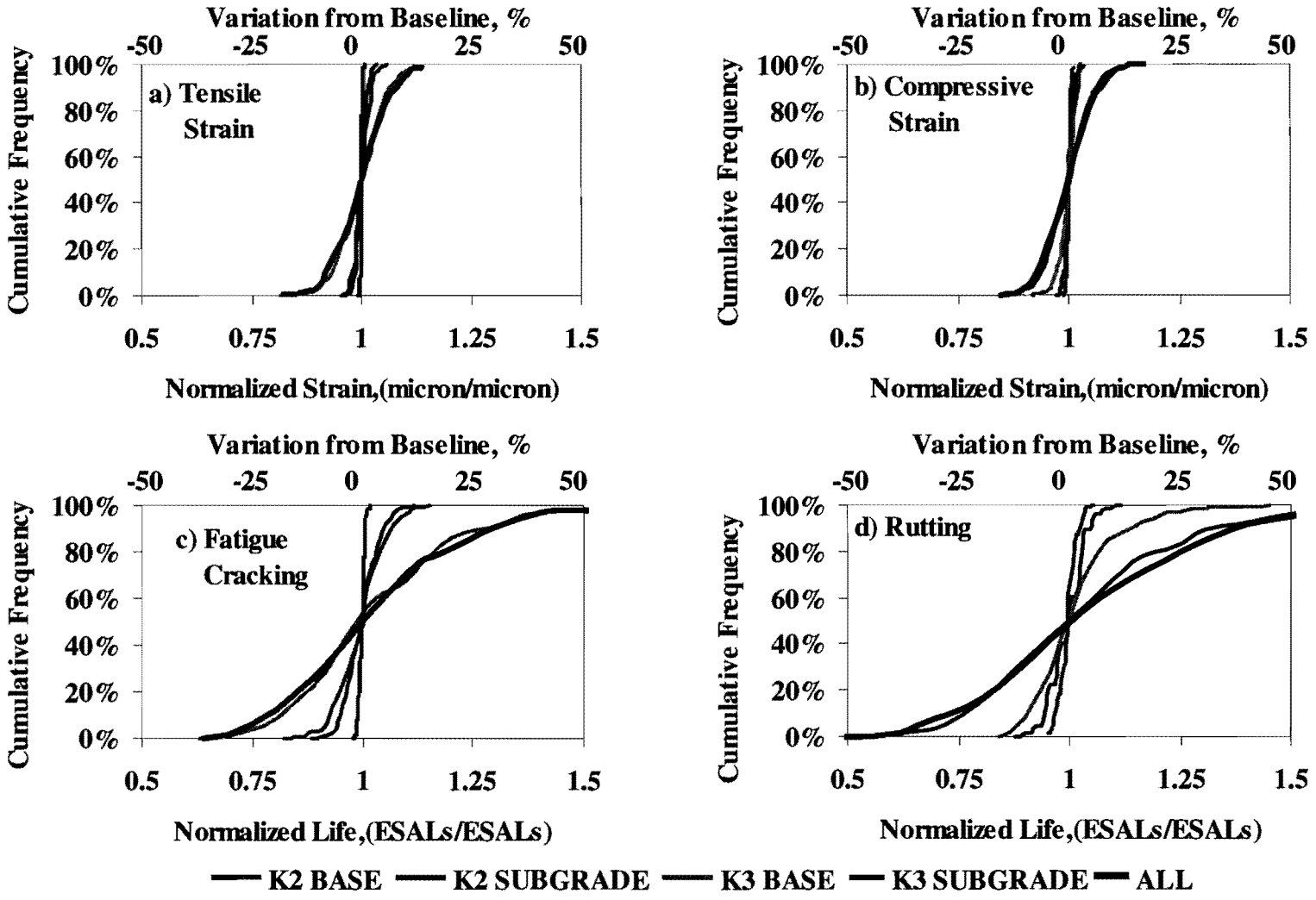

Figure 4.8 Cumulative Distribution of Critical Strains and Remaining Lives for "Primary Road, Over Average Quality Base and Low Plasticity Clay Subgrade"

Table 4.4 Sensitivity Level of Critical Tensile Strain When k2 and k3 Parameters are Perturbed

Pavement Profile	Base Layer	High Quality			Average Quality			Poor Quality		
	Subgrade Layer	Sandy	Clay Low PI	Clay High PI	Sandy	Clay Low PI	Clay High PI	Sandy	Clay Low PI	Clay High PI
Primary Road	K_2 Base	NS	S	VS	NS	NS	NS	NS	NS	NS
	K_2 Subgrade	NS	NS	MS	NS	NS	MS	NS	NS	NS
	K_3 Base	MS	S	S	VS	VS	VS	VS	VS	VS
	K_3 Subgrade	MS	MS	MS	NS	NS	MS	NS	NS	NS
	All	S	S	VS	VS	VS	VS	VS	VS	VS
Secondary Road	K_2 Base	MS	S	VS	S	S	MS	MS	MS	MS
	K_2 Subgrade	S	NS	S	NS	NS	MS	NS	NS	MS
	K_3 Base	VS	VS	VS	VS	VS	VS	VS	VS	VS
	K_3 Subgrade	S	S	S	NS	MS	MS	NS	NS	MS
	All	VS	VS	VS	VS	VS	VS	VS	VS	VS
County Road	K_2 Base	NS	MS	MS	NS	NS	NS	NS	NS	NS
	K_2 Subgrade	NS	NS	MS	NS	NS	MS	NS	NS	MS
	K_3 Base	NS	MS	MS	S	S	S	S	S	S
	K_3 Subgrade	NS	MS	MS	NS	MS	MS	NS	MS	MS
	All	MS	S	S	S	S	S	S	S	S
Street	K_2 Base	NS	MS	S	NS	NS	MS	MS	NS	NS
	K_2 Subgrade	S	NS	S	MS	NS	S	NS	NS	S
	K_3 Base	S	S	S	VS	VS	VS	VS	VS	S
	K_3 Subgrade	MS	S	S	NS	S	S	NS	S	S
	All	S	VS	VS	VS	VS	VS	VS	VS	VS

Table 4.5 Sensitivity Level of Critical Compressive Strain When k2 and k3 Parameters are Perturbed

Pavement Profile	Base Layer	High Quality			Average Quality			Poor Quality		
	Subgrade Layer	Sandy	Clay Low PI	Clay High PI	Sandy	Clay Low PI	Clay High PI	Sandy	Clay Low PI	Clay High PI
Primary Road	K_2 Base	NS	MS	VS	NS	NS	NS	NS	NS	NS
	K_2 Subgrade	S	NS	VS	S	NS	VS	S	NS	VS
	K_3 Base	MS	MS	MS	S	S	S	S	S	S
	K_3 Subgrade	S	S	VS	S	S	VS	S	VS	VS
	All	VS	VS	VS	VS	VS	VS	VS	VS	VS
Secondary Road	K_2 Base	NS	S	S	NS	NS	NS	NS	NS	NS
	K_2 Subgrade	S	MS	VS	S	MS	VS	S	MS	VS
	K_3 Base	S	S	S	VS	VS	VS	VS	VS	VS
	K_3 Subgrade	S	VS	VS	S	VS	VS	S	VS	VS
	All	VS	VS	VS	VS	VS	VS	VS	VS	VS
County Road	K_2 Base	NS	NS	NS	NS	NS	NS	NS	NS	NS
	K_2 Subgrade	MS	MS	VS	MS	MS	VS	MS	MS	VS
	K_3 Base	NS	NS	NS	NS	NS	MS	NS	NS	MS
	K_3 Subgrade	MS	VS	VS	MS	VS	VS	MS	VS	VS
	All	S	VS	VS	S	VS	VS	S	VS	VS
Street	K_2 Base	NS	MS	MS	NS	NS	NS	NS	NS	NS
	K_2 Subgrade	S	MS	VS	S	MS	VS	MS	MS	VS
	K_3 Base	NS	MS	MS	MS	S	S	MS	S	S
	K_3 Subgrade	MS	VS	VS	MS	VS	VS	NS	VS	VS
	All	VS	VS	VS	S	VS	VS	S	VS	VS

Sensitivity of Remaining Life

Using the previous procedure, the variations of the remaining lives due to the perturbation of the nonlinear parameters of the base and subgrade are also determined. The variations from the base line as well as the cumulative distribution of the absolute values of the variations are included in Figures 4.6 through 4.8. The impact of different nonlinear parameters for different pavement structures, and different base and subgrade types are summarized in Tables 4.6 and 4.7. for rutting and cracking, respectively. The sensitivity levels for the remaining lives are very similar to those of the corresponding strains, as expected. The fatigue cracking is very sensitive to the parameter k_2 of the base layer and moderately to the other parameters (Table 4.6). The rutting of the pavement section is significantly impacted by the parameter k_3 of the subgrade (Table.4.7).

GENERAL OBSERVATIONS AND PRACTICAL RECOMMENDATIONS

Based on this sensitivity study, the following conclusions can be drawn:

a. The deflections under the load, 12in. (305 mm) and 24in. (610 mm) from the load (similar to the first three sensors of the FWD), may be sensitive to the variations of the nonlinear parameters, k_2 and k_3 of the base and subgrade. Deflections farther than 24 in. (610 mm) are generally not impacted by the nonlinear parameters of the base and subgrade.

b. The deflections under the load for the primary and secondary roads with thicker base layers (12 in., 305mm), are very sensitive to the parameter k_3 of the base with the exception of high quality base materials. In this case, the deflections under the load are very sensitive or sensitive to the parameter k_3 of the subgrade.

c. The deflections under the load for county and street roads, with a thin base layer (6in., 150mm), are very sensitive to the parameter k_3 of the subgrade. The deflections under the load for the county and street roads, with thin base layer (6in., 150mm), are very sensitive to the parameter k_3 of the subgrade, with an exception of the sandy subgrades. When the subgrade material is sandy, the deflections under the load are very sensitive to the parameter k_3 of the base.

c. The critical tensile strains for secondary and street roads with a thin layer of AC (3in., 75mm), are very sensitive to the parameter k_3 of the base. For the primary and county roads in pavement sections with a thick layer of AC (6in., 150mm), these strains are sensitive to the parameter k_3 of the base.

e. In most cases, the parameters k_2 of the base and subgrade do not significantly impact the critical tensile strains of the pavement sections.

f. Critical compressive strain is very sensitive to the parameter k_3 of the subgrade, with an exception of sandy subgrades. In this case, the compressive strain is moderately sensitive to the parameter k_3 of the subgrade.

Table 4.6 Sensitivity Level of Fatigue Remaining Life When k2 and k3 Parameters are Perturbed

Pavement Profile	Base Layer	High Quality			Average Quality			Poor Quality		
	Subgrade Layer	Sandy	Clay Low PI	Clay High PI	Sandy	Clay Low PI	Clay High PI	Sandy	Clay Low PI	Clay High PI
Primary Road	K_2 Base	NS	MS	VS	NS	NS	NS	NS	NS	NS
	K_2 Subgrade	NS	NS	MS	NS	NS	NS	NS	NS	NS
	K_3 Base	MS	MS	MS	VS	VS	VS	VS	VS	VS
	K_3 Subgrade	NS	NS	MS	NS	NS	NS	NS	NS	NS
	All	MS	S	S	VS	VS	VS	VS	VS	VS
Secondary Road	K_2 Base	NS	S	VS	MS	MS	NS	MS	MS	NS
	K_2 Subgrade	MS	NS	S	NS	NS	NS	NS	NS	NS
	K_3 Base	S	VS	VS	VS	VS	VS	VS	VS	VS
	K_3 Subgrade	MS	MS	S	NS	NS	NS	NS	NS	NS
	All	VS	VS	VS	VS	VS	VS	VS	VS	VS
County Road	K_2 Base	NS	NS	MS	NS	NS	NS	NS	NS	NS
	K_2 Subgrade	NS	NS	MS	NS	NS	MS	NS	NS	MS
	K_3 Base	NS	NS	NS	MS	MS	MS	S	S	S
	K_3 Subgrade	NS	MS	MS	NS	MS	MS	NS	NS	MS
	All	MS	MS	MS	MS	MS	S	S	S	S
Street	K_2 Base	NS	MS	S	NS	NS	NS	NS	NS	NS
	K_2 Subgrade	MS	NS	S	NS	NS	S	NS	NS	MS
	K_3 Base	MS	MS	S	VS	VS	VS	VS	VS	VS
	K_3 Subgrade	MS	S	S	NS	S	S	NS	MS	MS
	All	S	VS	VS	VS	VS	VS	VS	VS	VS

42

Table 4.7 Sensitivity Level of Rutting Remaining Life When k2 and k3 Parameters are Perturbed

Pavement Profile	Base Layer	High Quality			Average Quality			Poor Quality		
	Subgrade Layer	Sandy	Clay Low PI	Clay High PI	Sandy	Clay Low PI	Clay High PI	Sandy	Clay Low PI	Clay High PI
Primary Road	K_2 Base	NS	MS	VS	NS	NS	NS	NS	NS	NS
	K_2 Subgrade	S	NS	VS	MS	NS	VS	MS	NS	VS
	K_3 Base	MS	MS	MS	S	VS	VS	S	VS	VS
	K_3 Subgrade	S	VS	VS	S	VS	VS	MS	VS	VS
	All	VS	VS	VS	VS	VS	VS	VS	VS	VS
Secondary Road	K_2 Base	NS	S	VS	NS	NS	NS	NS	NS	NS
	K_2 Subgrade	S	MS	VS	S	MS	VS	S	NS	VS
	K_3 Base	MS	S	VS	VS	VS	VS	VS	VS	VS
	K_3 Subgrade	S	VS	VS	S	VS	VS	S	VS	VS
	All	VS	VS	VS	VS	VS	VS	VS	VS	VS
County Road	K_2 Base	NS	NS	NS	NS	NS	NS	NS	NS	NS
	K_2 Subgrade	MS	MS	VS	MS	MS	VS	MS	MS	VS
	K_3 Base	NS	NS	NS	NS	NS	MS	NS	NS	MS
	K_3 Subgrade	MS	VS	VS	MS	VS	VS	NS	VS	VS
	All	S	VS	VS	S	VS	VS	S	VS	VS
Street	K_2 Base	NS	MS	MS	NS	NS	NS	NS	NS	NS
	K_2 Subgrade	S	MS	VS	MS	MS	VS	MS	MS	VS
	K_3 Base	NS	MS	MS	MS	S	VS	MS	S	VS
	K_3 Subgrade	MS	VS	VS	MS	VS	VS	NS	VS	VS
	All	VS	VS	VS	S	VS	VS	S	VS	VS

g. Fatigue cracking of pavement sections is very sensitive to the parameter k_3 of the base. When the base material is of high quality, the fatigue cracking is moderately sensitive and sometimes sensitive to the parameters k_3 of the base and subgrade.

h. Rutting is very sensitive to the parameter k_3 of the subgrade. When subgrade material is clayey with high plasticity, the parameter k_3 of the base is very sensitive when base is average to poor quality. The parameter k_3 is moderately sensitive to sensitive when the base is high quality.

i. Generally, the performance of the pavement seems to not be very sensitive to the parameters k_2, and appears to be sensitive to the parameters k_3 of the base and subgrade.

j. Since the deflections of most pavements are not sensitive to the parameters k_2 of the base and subgrade, the backcalculation of these parameters may not result in a unique answer. The performance of the pavement is sensitive to the parameters k_3; therefore, these parameters can be backcalculated from the pavement FWD deflections with more confidence.

CHAPTER FIVE
BACKCALCULATION OF NONLINEAR PARAMETERS

INTRODUCTION

As previously indicated, the FWD moduli correspond to strain levels that are closer to strains imposed by traffic. Seismic moduli obtained from the SPA are the linear elastic moduli. A constitutive model that relates the SPA and FWD moduli was described in Chapter 2 and Appendix B. As a reminder, this relationship is in the form of

$$E = E_{seis}\left(\frac{\sigma_{c-ult}}{\sigma_{c-init}}\right)^{k_2}\left(\frac{\sigma_{d-ult}}{\sigma_{d-init}}\right)^{k_3} \tag{5.1}$$

Since Equation 5.1 is the same as Equation 2.5, the reader is referred to Chapter 2 for the definitions of the parameters of this equation. Ke et al. (2000) demonstrated the feasibility of using this relationship to estimate the appropriate design moduli for the base and subgrade layers from the seismic moduli. In this chapter, an algorithm for estimating the nonlinear parameters k_2 and k_3 of the base and/or subgrade by combining the deflection basin from the FWD, with the linear elastic moduli from the SPA, is described. A case study is used to demonstrate the process of determining the nonlinear parameters of a pavement section. Finally, the strengths and limitations of the algorithm are addressed.

DESCRIPTION OF ALGORITHM

Backcalculation (inversion) is an iterative process that allows the user to extract information from an observed response. In this process, one attempts to determine the most appropriate input parameters to a model so that the differences between an observed response and calculated response from the model are minimum. From this general statement, any backcalculation process requires two general algorithms: 1) an algorithm to calculate the desired responses given the input parameters (called the forward model) and 2) an algorithm that adjusts the input parameters so that the error between the observed and the calculated responses are minimized (called the optimization process). In this study, the observed response is the FWD deflection bowl, and the input parameters are the nonlinear parameters k_2 and k_3 of the base and subgrade. The multi-layered equivalent linear program described in Chapter 3 was adopted as the forward model that relates the nonlinear parameters of the base and subgrade to the surface deflection.

The algorithm needed to minimize the errors between the measured and calculated deflections (the optimization process) is described below. Figure 5.1 contains a flow chart of the process.

The optimization process used in this study is based on singular value decomposition. Singular value decomposition (SVD) (Golub and Reinsch, 1970) is a powerful set of techniques for dealing with sets of equations that are either singular or numerically very close to singular. SVD is the method of choice for most linear least-squares problems.

When a FWD test is carried out on a pavement, about seven deflections are collected. These seven or so deflections are represented as a vector, $\mathbf{d}^{\mathbf{FWD}}$. Assuming initial values for the nonlinear parameters k_2 and k_3 of the base and subgrade, and knowing the seismic moduli of all layers from SPA, a set of deflections can be calculated using the adapted forward model. The set of deflections calculated in this manner can also be represented as the vector represented by $\mathbf{d}^{\mathbf{Seismic}}$. For mathematical convenience, the first set of assumed nonlinear parameters (k_2 and k_3) of each layer is also represented as a matrix called $\mathbf{k}^0$.

The goal is to determine a matrix $\mathbf{k}^{\mathbf{f}}$ that minimizes the difference between the deflections measured by the FWD, $\mathbf{d}^{\mathbf{FWD}}$, and the calculated $\mathbf{d}^{\mathbf{Seismic}}$. The governing equation of the inversion problem can be expressed as:

$$d_i^{FWD} - d_i^{Seismic} = \sum_{j=1}^{M} \frac{\partial d_i^{Seismic}}{\partial k_j} \Delta k_j \qquad i = 1,\ldots,N \qquad (5.2)$$

which N is the number of the FWD sensors. Parameters $\partial d_i^{Seismic} / \partial k_j^0$ are the partial derivatives of each measured deflection with respect to each nonlinear parameter of each nonlinear layer. Equation 5.2 can be expressed in the matrix form as

$$\mathbf{\Delta c} = \mathbf{A}\,\mathbf{\Delta k} \qquad (5.3)$$

where

$$\mathbf{\Delta c} = (\Delta c_1\ \Delta c_2\ \ldots.\Delta c_N)^T \qquad (5.4)$$

where N is the number of the FWD sensors and $\Delta c_i = d_i^{FWD} - d_i^{Seismic}$. $\mathbf{\Delta k}$ is defined as a modification matrix that is added to matrix $\mathbf{k}^0$ to determine the matrix of unknowns $\mathbf{k}^i$ for the next iteration, and can be expressed as

$$\mathbf{\Delta k} = \begin{bmatrix} (\Delta k_2)_1 & (\Delta k_3)_1 \\ (\Delta k_2)_2 & (\Delta k_3)_2 \\ \ldots. & \ldots. \\ (\Delta k_2)_M & (\Delta k_3)_M \end{bmatrix}^T \qquad (5.5)$$

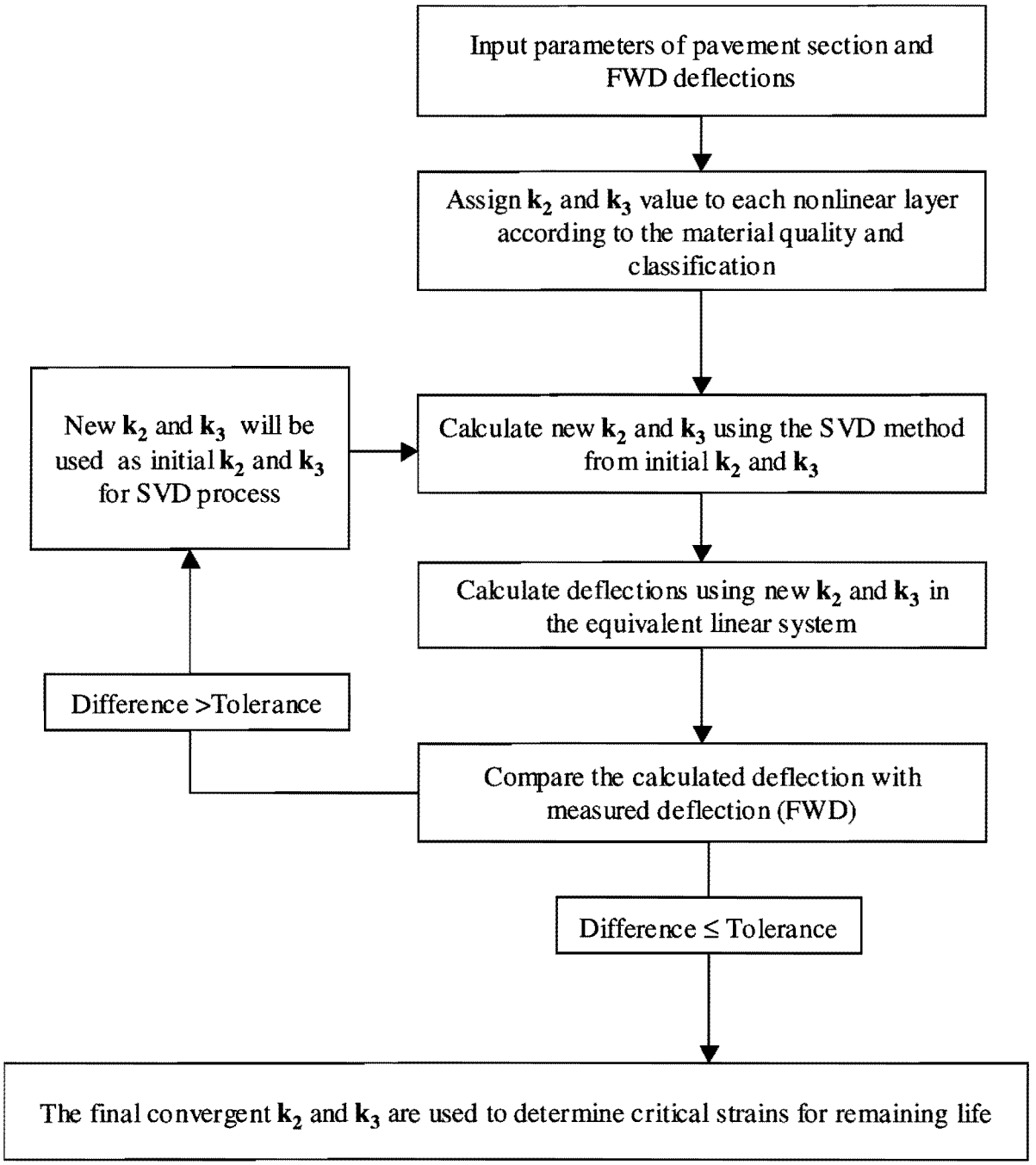

Figure 5.1 Flow Chart of Implementation of Backcalculation Process

where M is the number of nonlinear layers. Matrix **A** is a 2M × N matrix of partial derivatives whose elements $A_{ij} = \partial d_i^{Seismic} / \partial k_j^0$. Matrix $\mathbf{k}^i$ is considered the solution to the unknown parameters (k_2 or k_3) when it yields a vector $\Delta\mathbf{c}$ in Equation 5.3 that is sufficiently small. In practice, it is assumed that N (number of FWD sensors) is greater than 2M (number of unknown k parameters). Thus, the problem defined by Equation 5.3 is over-constrained.

Equation 5.3 cannot be solved through calculating the conventional inverse of matrix **A**, $\mathbf{A}^{-1}$. Matrix $\mathbf{A}^{-1}$ exists only if **A** is square and nonsingular. An approach to solving Equation 5.3 is to construct its normal or Gaussian-Newton equation. This results in the classical least-square solution where

$$\Delta\mathbf{k} = (\mathbf{A}^T\mathbf{A})^{-1}\,\mathbf{A}^T\Delta\mathbf{c} \tag{5.6}$$

subject to minimization of $(\Delta\mathbf{c} - \mathbf{A}\,\Delta\mathbf{k})^T(\Delta\mathbf{c} - \mathbf{A}\,\Delta\mathbf{k})$ with respect to $\Delta\mathbf{k}$. This solution is also known as the optimization solution.

The computation of the matrix $\mathbf{A}^T\mathbf{A}$ may involve numerical inaccuracy, which can be troublesome when the number of sensors or the number of layers is large. To avoid this drawback, the singular value decomposition of a matrix (Golub and Reinsch, 1970) approach has been utilized to develop the generalized inverse solution of Equation 5.3.

The decomposition of matrix A leads to a product of three matrices:

$$\mathbf{A} = \mathbf{U}\mathbf{S}\mathbf{V}^T \tag{5.7}$$

where **U** is a 2M × N matrix whose columns are eigenvectors, u_j (j=1,..., N), of length 2M, associated with the columns of **A**. Similarly, **V** is an N× N matrix whose columns are eigenvectors, v_j (j=1,..., N), of length N, associated with rows of **A**. Matrix **S** is a diagonal matrix with N elements with diagonal entries, s_{ij} (j=1,...,N), which are nonnegative square roots of the eigenvalues of the symmetric matrix $\mathbf{A}^T\mathbf{A}$, and known as the singular values of **A**.

By substituting Equation 5.7 into Equation 5.3, and utilizing the orthonormal property of **U** and **V** [i.e. $\mathbf{U}^T\mathbf{U} = \mathbf{V}^T\mathbf{V} = \mathbf{V}\mathbf{V}^T = \mathbf{I}$ (unit matrix)], it is easy to show that

$$\Delta\mathbf{k} = \mathbf{V}\mathbf{S}^{-1}\,\mathbf{U}^T\Delta\mathbf{c} \tag{5.8}$$

This expression gives the generalized inverse solution of Equation 5.3.

Adding $\Delta\mathbf{k}$ to $\mathbf{k}^0$ yields updated parameters k (i.e. k_2 and k_3) from a new set of deflections, and a new set of partial derivatives can be calculated. This procedure is repeated until Δc_is are sufficiently small. At this time, values of k_2 and k_3 that satisfy the given data are found.

The convergence of successive iterations is monitored by the following root-mean-square (RMS) error criterion:

$$\varepsilon = \sqrt{\frac{1}{N}\sum_{i=1}^{N}\Delta c_i} \tag{5.9}$$

The procedure is terminated when ε reaches an acceptably small value or when all elements of vector **Δc** are within the standard error bounds of FWD precision or other pre-specified limits.

IMPLEMENTATION OF ALGORITHM

A computer program based on the backcalculation algorithm described in the previous section has been developed in two programming languages. The front-end of the program including the Graphical User Interface (GUI), and the control structure were packaged using C++. The brain of the program, which is mainly the backcalculation procedure, was developed in Fortran language and linked in C++. The backcalculation program was easier to develop in Fortran since part of the backcalculation algorithm, the equivalent linear procedure, was based on BISAR (De Jong et al., 1973), an existing layered linear elastic program developed in Fortran.

The first set of required inputs for this program are the FWD deflection basins, the corresponding applied load, seismic moduli of pavement layers collected by the SPA, as well as layer properties such as thickness, and Poisson's ratio of each layer. The second set of inputs is the pavement material properties, which will determine the layers exhibiting load-induced nonlinear behavior. The user also selects the number of sub-layers for each nonlinear layer used in the modulus backcalculation. Ke et al. (2000) have discussed and made recommendations on the number of sub-layers for generating adequate results.

The initial ("seed") nonlinear parameters of the pavement layers (i.e. k_2 and k_3) are determined based on the material property selected for each nonlinear layer. Typical values of different material types are presented in Table 3.2. The program only considers two nonlinear layers. The two common nonlinear layers are the base and upper part of the subgrade layer. The program is capable of three backcalculation alternatives. The nonlinear parameter that is backcalculated is parameter k_3 for both base and subgrade. The user selects to backcalculate either or both parameters.

When the program is executed, the nonlinear layers are divided into the user-specified number of sub-layers. The layer properties (e.g. seismic modulus, Poisson's ratio, k_2, and k_3) are assigned to each nonlinear sub-layer. Then using the equivalent linear procedure, a modulus of each nonlinear layer is calculated from seismic moduli and the nonlinear parameters k_2 and k_3 of the corresponding layers. The optimization process discussed in the previous section is then used to calculate the nonlinear parameter(s) k_3 of the base and (or) subgrade depending on the user selection.

The output of the program is comprised of the backcalculated nonlinear parameter(s) k_3 of the base and (or) subgrade, the calculated deflection basin and the deflection's RMS error. Layer moduli and the critical strains for the fatigue cracking and rutting remaining lives of the pavement are also reported.

As indicated before, it does not seem that the parameters k_2 of the base and subgrade can be reliably backcalculated because they do not significantly impact the deflection basin.

VERIFICATION OF ALGORITHM

The four typical pavement sections described in Chapter 3 were used to verify the accuracy and stability of the backcalculation procedure. Since for each of the four pavement types, three types of base and three types of subgrade are considered, nine sets of deflection basins were calculated using the forward model. Each deflection basin, along with its associated seismic moduli, were input into the backcalculation program to estimate one or more nonlinear parameters of the base and/or subgrade. The backcalculation was carried out for three scenarios. Each scenario is described below. In all cases the backcalculation process was terminated when the deflection RMS error was less than 0.05 or when the number of iterations exceeded 10.

First, only the parameter k_3 of the base was varied and backcalculated while the other potential parameter (i.e. k_3 of subgrade) was considered as constant. The backcalculated k_3 parameters and the expected values for the four typical pavement sections are presented in Table 5.1. In the table, the term "Iteration" represents the number of iterations after which the backcalculation procedure was terminated. The deflection RMS errors were calculated in the same manner as described in Equation 5.9. Also included in the table are the backcalculated errors. These errors measure the absolute ratio of the difference between the expected and calculated k_3 values to the expected k_3 value. Figure 5.2 graphically represents the backcalculated errors for the nine sets of pavement materials in Table 5.1. The errors, when the base material is average or poor quality over a clayey subgrade, are less than 5% indicating a reasonable and stable process. As a general trend (see Figure 5.2), when the subgrade material is sandy the backcalculated errors are large and the number of iterations exceed the specified limit. As such, predicting the parameter k_3 of the base for pavement sections constructed with high quality base over sandy subgrade may not be feasible. A close comparison of the errors associated with predicting the parameter k_3 of the base (Table 5.1) and the levels of sensitivity for the same parameter (Table 4.3) indicates that accurately predicting the parameters, which are not impacting the deflection basin, is not feasible or practical. For sandy subgrades this seems to be the case.

Table 5.1 Backcalculation of the Parameter k_3 of the Base for the Four Typical Pavement Sections

Pavement Profile	Base Layer	High Quality			Average Quality			Poor Quality		
	Subgrade Layer	Sandy	Clay Low PI	Clay High PI	Sandy	Clay Low PI	Clay High PI	Sandy	Clay Low PI	Clay High PI
Primary Road	Iteration	1	4	2	11	6	6	11	7	8
	RMS Error	0.69	0.26	0.20	0.69	0.26	0.19	0.70	0.27	0.19
	k_3 Base Actual	-0.20	-0.20	-0.20	-0.30	-0.30	-0.30	-0.40	-0.40	-0.40
	k_3 Base Measured	-0.10	-0.19	-0.21	-0.26	-0.29	-0.30	-0.37	-0.39	-0.40
	Backcalculation Error	50.00	4.44	6.89	11.89	1.77	1.53	6.73	1.45	0.85
Secondary Road	Iteration	11	5	2	11	6	8	11	8	9
	RMS Error	0.55	0.27	0.26	0.76	0.25	0.25	0.74	0.24	0.25
	k_3 Base Actual	-0.20	-0.20	-0.20	-0.30	-0.30	-0.30	-0.40	-0.40	-0.40
	k_3 Base Measured	-0.15	-0.17	-0.18	-0.28	-0.30	-0.30	-0.38	-0.40	-0.40
	Backcalculation Error	25.25	15.55	10.54	6.77	0.61	0.47	3.98	0.45	0.32
County Road	Iteration	11	4	3	11	5	6	11	7	7
	RMS Error	0.73	0.22	0.25	0.66	0.22	0.25	0.70	0.22	0.25
	k_3 Base Actual	-0.20	-0.20	-0.20	-0.30	-0.30	-0.30	-0.40	-0.40	-0.40
	k_3 Base Measured	0.00	-0.19	-0.17	-0.19	-0.29	-0.29	-0.33	-0.39	-0.39
	Backcalculation Error	100.00	6.32	14.97	37.71	3.24	3.43	16.57	1.93	2.45
Street	Iteration	11	9	6	11	7	9	11	8	9
	RMS Error	0.74	0.18	0.16	0.70	0.19	0.16	0.73	0.18	0.16
	k_3 Base Actual	-0.20	-0.20	-0.20	-0.30	-0.30	-0.30	-0.40	-0.40	-0.40
	k_3 Base Measured	0.00	-0.20	-0.21	-0.25	-0.29	-0.30	-0.37	-0.40	-0.40
	Backcalculation Error	99.99	0.30	6.79	17.19	2.81	0.52	8.50	0.58	0.38

* Errors larger than 10% are highlighted.

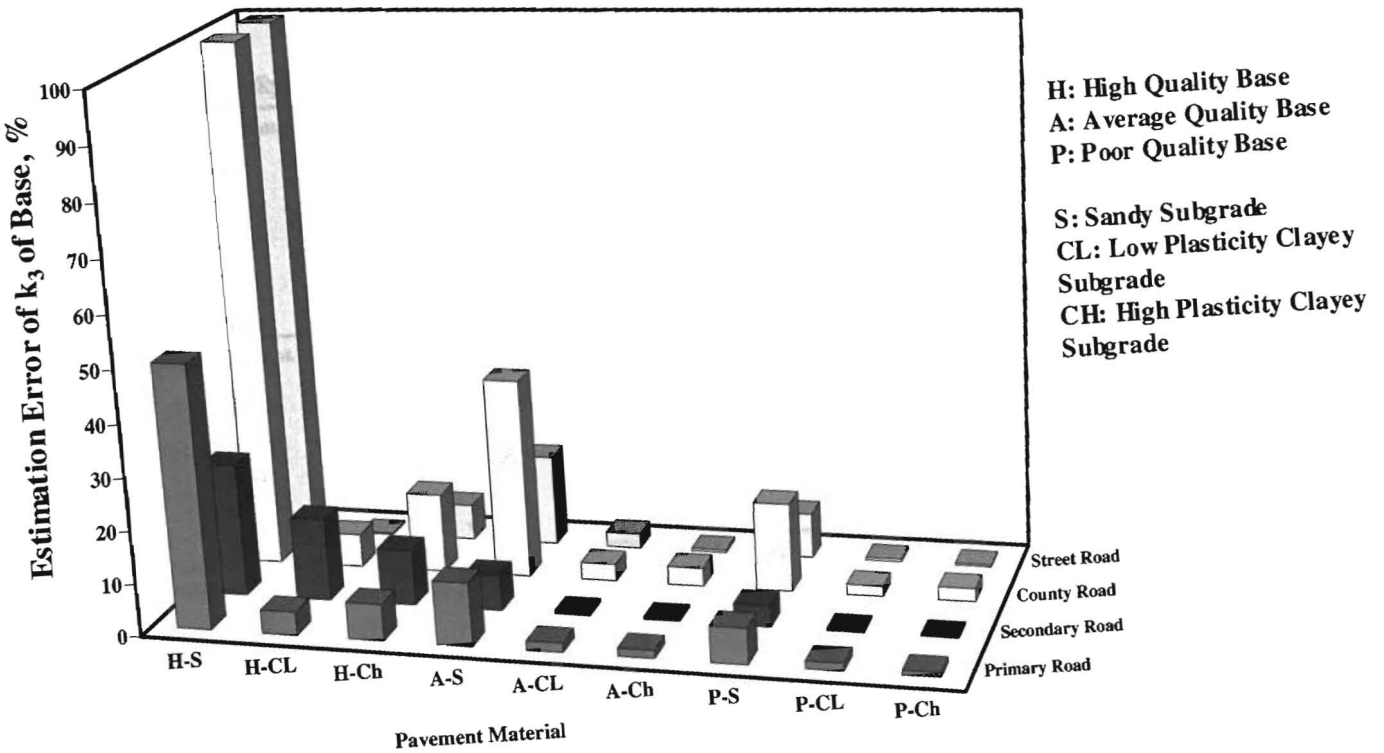

Figure 5.2 Backcalculation Error for the Parameter k_3 of the Base for the Four Typical Pavement Sections

In the same manner, the parameter k_3 of the subgrade was varied and estimated while the parameter k_3 of the base was maintained as constants. Table 5.2 summarizes the backcalculated and the expected values for the parameter k_3 of subgrade layer, as well as the number of iterations and deflection RMS errors. In most cases, the backcalculated errors are less than 5%, indicating a reasonable and stable process. However, for a number of cases, the errors are unacceptably large. This is illustrated well in Figure 5.3. The figure graphically shows that for all types of base material, when the subgrade is sandy, predicting the parameter k_3 of the subgrade is not feasible. Once again, the accuracy of the backcalculated values is directly correlated to the results from the sensitivity study.

Finally, the nonlinear parameters k_3 of the base and subgrade were simultaneously varied and backcalculated. The results are summarized in Table 5.3. The backcalculated errors are larger than when the parameter k_3 is backcalculated for each layer separately. Figure 5.4 graphically shows the backcalculated errors when both parameters k_3 of base and subgrade were backcalculated. Since the pavement sections with sandy subgrade resulted in very large errors, they were not included in Figure 5.4. The figure shows that the backcalculation of parameter k_3 of base and subgrade, at the same time, may result in small errors for certain pavement sections such as street road with poor base and clayey subgrade. However, the majority of the pavement sections produced large errors when backcalculated. This suggests that backcalculation of both parameters simultaneously is not practical.

The results of the sensitivity study in Chapter 4 indicate that the nonlinear parameters k_2 of the base and subgrade do not substantially influence the FWD deflections. As such, it may not be feasible to accurately and robustly backcalculate these parameters. Also, as the pavements are constructed from thicker and higher quality materials, the backcalculation of the parameters k_3 of the base and subgrade becomes exceedingly more difficult.

In general, it seems that backcalculating the nonlinear parameters of the base and subgrade from FWD deflections should be avoided or done with extreme caution.

Table 5.2 Backcalculation of the Parameter k_3 of the Subgrade for the Four Typical Pavement Sections

Pavement Profile	Base Layer	High Quality			Average Quality			Poor Quality		
	Subgrade Layer	Sandy	Clay Low PI	Clay High PI	Sandy	Clay Low PI	Clay High PI	Sandy	Clay Low PI	Clay High PI
Primary Road	Iteration	11	7	7	11	6	7	11	6	7
	RMS Error	1.21	0.26	0.19	0.79	0.27	0.20	0.87	0.26	0.19
	k_3 Subgrade Actual	-0.20	-0.30	-0.40	-0.20	-0.30	-0.40	-0.20	-0.30	-0.40
	k_3 Subgrade Measured	-0.27	-0.29	-0.39	-0.23	-0.29	-0.39	-0.27	-0.29	-0.39
	Backcalculation Error	33.31	2.29	1.67	16.07	3.73	1.99	32.79	3.36	1.80
Secondary Road	Iteration	11	7	7	11	7	8	11	7	8
	RMS Error	1.14	0.24	0.25	0.80	0.24	0.26	0.80	0.24	0.25
	k_3 Subgrade Actual	-0.20	-0.30	-0.40	-0.20	-0.30	-0.40	-0.20	-0.30	-0.40
	k_3 Subgrade Measured	0.00	-0.29	-0.39	-0.23	-0.30	-0.40	-0.23	-0.30	-0.40
	Backcalculation Error	100.00	2.38	2.16	12.53	1.19	1.20	13.50	1.40	1.00
County Road	Iteration	11	7	7	11	7	7	11	7	7
	RMS Error	2.47	0.22	0.26	1.16	0.22	0.26	1.17	0.22	0.26
	k_3 Subgrade Actual	-0.20	-0.30	-0.40	-0.20	-0.30	-0.40	-0.20	-0.30	-0.40
	k_3 Subgrade Measured	-0.35	-0.30	-0.39	-0.29	-0.30	-0.39	-0.25	-0.30	-0.39
	Backcalculation Error	76.77	1.43	1.69	43.64	1.32	1.33	23.15	1.38	1.44
Street	Iteration	11	9	8	11	7	9	11	8	8
	RMS Error	1.06	0.18	0.16	2.12	0.19	0.16	1.81	0.18	0.16
	k_3 Subgrade Actual	-0.20	-0.30	-0.40	-0.20	-0.30	-0.40	-0.20	-0.30	-0.40
	k_3 Subgrade Measured	-0.23	-0.30	-0.40	-0.32	-0.30	-0.40	-0.32	-0.30	-0.40
	Backcalculation Error	15.46	0.12	0.32	60.94	0.61	0.16	61.70	0.51	0.42

* Errors larger than 10% are highlighted.

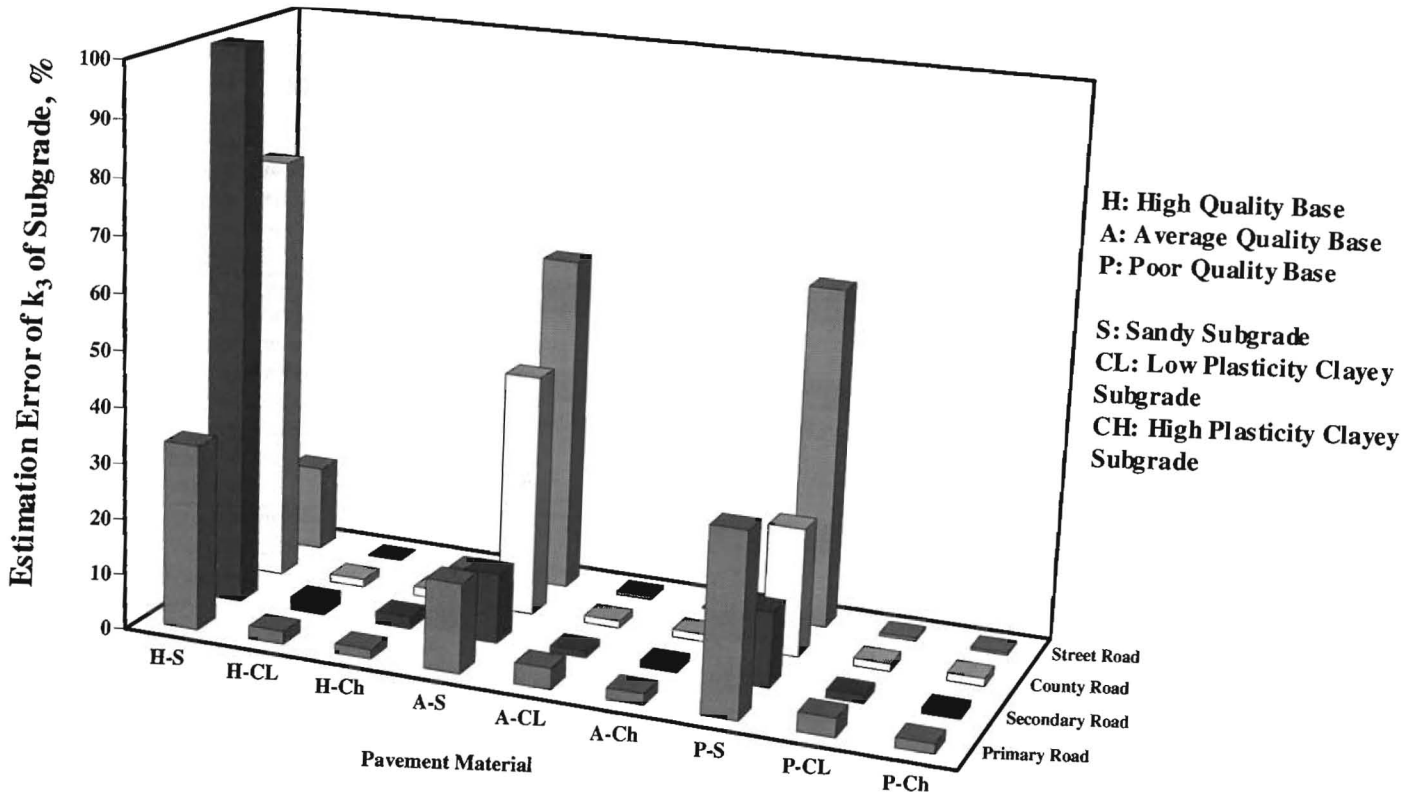

Figure 5.3 Backcalculation Error for the Parameter k_3 of the Subgrade for the Four Typical Pavement Sections

Table 5.3 Backcalculation of the Parameters k3 of the Base and Subgrade for the Four Typical Pavement Sections

Pavement Profile	Base Layer	Sandy			Average			Poor		
	Subgrade Layer	Sandy	Clay Low PI	Clay High PI	Sandy	Clay Low PI	Clay High PI	Sandy	Clay Low PI	Clay High PI
Primary Road	Iteration	11	4	5	4	5	3	11	3	4
	RMS Error	0.58	0.23	0.18	0.75	0.00	0.26	0.52	0.55	0.27
	k_3 Base Actual	-0.20	-0.20	-0.20	-0.30	-0.30	-0.30	-0.40	-0.40	-0.40
	k_3 Base Measured	0.00	-0.29	-0.35	-0.14	-0.35	-0.35	-0.31	-0.48	-0.45
	Back Calculation Error	100.00	44.70	77.34	54.11	15.99	15.94	22.90	18.89	12.66
	k_3 Subgrade Actual	-0.20	-0.30	-0.40	-0.20	-0.30	-0.40	-0.20	-0.30	-0.40
	k_3 Subgrade Measured	-0.26	-0.25	-0.31	-0.41	-0.24	-0.34	-0.33	-0.17	-0.33
	Back Calculation Error	31.30	16.68	22.48	103.00	18.47	16.12	66.99	43.86	18.63
Secondary Road	Iteration	11	5	6	8	6	5	7	6	6
	RMS Error	0.56	0.24	0.26	0.71	0.23	0.32	0.72	0.23	0.26
	k_3 Base Actual	-0.20	-0.20	-0.20	-0.30	-0.30	-0.30	-0.40	-0.40	-0.40
	k_3 Base Measured	0.00	-0.26	-0.18	-0.25	-0.31	-0.32	-0.36	-0.41	-0.41
	Back Calculation Error	100.00	31.87	11.43	18.11	4.15	8.23	9.26	1.94	2.34
	k_3 Subgrade Actual	-0.20	-0.30	-0.40	-0.20	-0.30	-0.40	-0.20	-0.30	-0.40
	k_3 Subgrade Measured	-0.24	-0.27	-0.4	-0.30	-0.28	-0.36	-0.30	-0.29	-0.38
	Back Calculation Error	20.71	9.93	0.26	48.45	5.09	9.42	51.75	4.99	4.63
County Road	Iteration	11	5	3	10	5	4	4	3	4
	RMS Error	1.57	0.25	0.34	0.54	0.00	0.25	0.64	0.31	0.24
	k_3 Base Actual	-0.20	-0.20	-0.20	-0.30	-0.30	-0.30	-0.40	-0.40	-0.40
	k_3 Base Measured	-0.04	-0.58	-0.65	-0.05	-0.44	-0.29	-0.14	-0.49	-0.42
	Back Calculation Error	80.47	188.09	226.23	83.51	45.60	2.15	65.36	23.54	4.13
	k_3 Subgrade Actual	-0.20	-0.30	-0.40	-0.20	-0.30	-0.40	-0.20	-0.30	-0.40
	k_3 Subgrade Measured	-0.32	-0.22	-0.31	-0.31	-0.26	-0.40	-0.33	-0.25	-0.39
	Back Calculation Error	59.27	25.67	21.33	53.00	14.75	0.36	64.81	16.50	1.91
Street	Iteration	11	6	6	11	3	6	11	6	4
	RMS Error	2.45	0.26	0.18	0.70	0.18	0.16	0.66	0.19	0.16
	k_3 Base Actual	-0.20	-0.20	-0.20	-0.30	-0.30	-0.30	-0.40	-0.40	-0.40
	k_3 Base Measured	0.00	-0.41	-0.21	-0.14	-0.26	-0.29	-0.35	-0.39	-0.39
	Back Calculation Error	100.00	104.93	6.20	54.21	12.69	2.93	13.03	1.81	1.40
	k_3 Subgrade Actual	-0.20	-0.30	-0.40	-0.20	-0.30	-0.40	-0.20	-0.30	-0.40
	k_3 Subgrade Measured	-0.34	-0.27	-0.40	-0.29	-0.31	-0.40	-0.26	-0.30	-0.40
	Back Calculation Error	69.37	10.99	0.54	42.93	3.53	0.92	32.49	1.37	0.59

* Errors larger than 10% are highlighted.

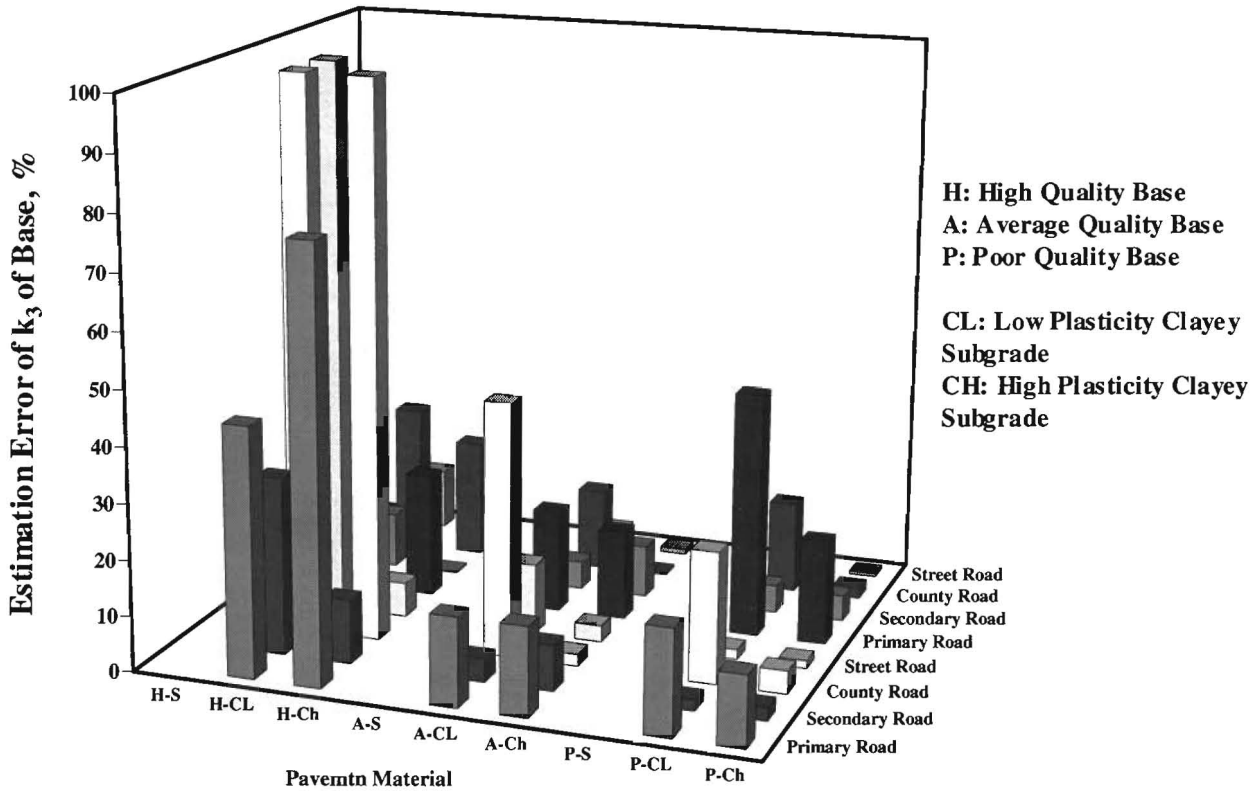

Figure 5.4 Backcalculation Error for the Parameter k_3 of the Base and Subgrade for the Four Typical Pavement Sections

CHAPTER SIX
CASE STUDY

INTRODUCTION

A case study is presented to demonstrate the use of the equivalent linear program described in Chapter 5. The two processes shown in Figure 6.1 were considered. First, the forward process was considered. In that process, one combines the seismic moduli and laboratory-derived nonlinear parameters to determine the design moduli that can be used in current mechanistic design procedures. The algorithm used in the forward process is detailed in Chapter 3 and Ke et al. (2000). Second, the backcalculation process is discussed. As a reminder, in that process the FWD deflections and seismic moduli are used as input to determine the nonlinear parameters of the base and subgrade.

SITE DESCRIPTION

The data used are from the WesTrack project funded by the Federal Highway Administration. WesTrack is an experimental test facility designed to provide early verification of the Strategic Highway Research Program (SHRP) hot mix asphalt mixture design procedures, and to continue the development of performance related specifications (PRS) for hot-mix asphalt pavement structures. The facility consists of 1.7 miles (2.8 Km) of two-lane oval track, with the straight sections used for pavement testing. The two straight sections of the track are divided into 26 different pavement sections. An aerial photograph of the track and a schematic of the test sites are shown in Figure 6.2. Detailed description of the WesTrack can be found in www.westrack.com.

The typical cross-section of the test track is shown in Figure 6.3. The pavement structures for all experimental sections are similar (Seeds et al., 2000). The HMA surface layer consists of two 3 in. (75 mm) lifts, placed according to the specifications of the experimental design for each section. The unbound aggregate base course consists of two 6 in. (150 mm) lifts and is a high quality granular material. The engineering fill is 18 in. (450 mm) thick, placed in three separate 6 in. (150 mm) lifts. The natural soil that underlies the pavement structure consists of a mixture of fine-grained materials, mostly clay with significant amounts of sand and silt.

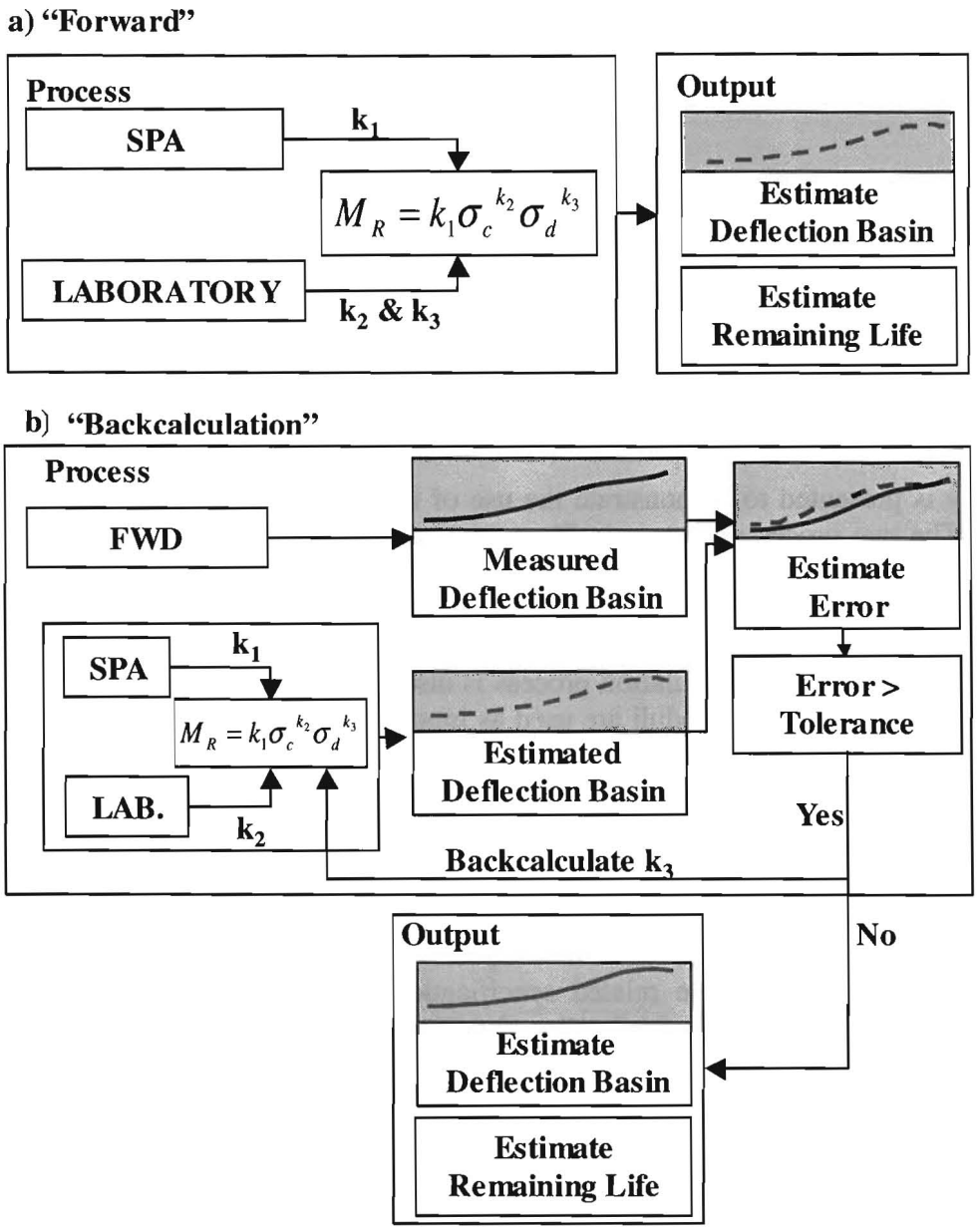

Figure 6.1 Flowchart of Forward and Backcalculation Processes Demonstrated Using This Case Study

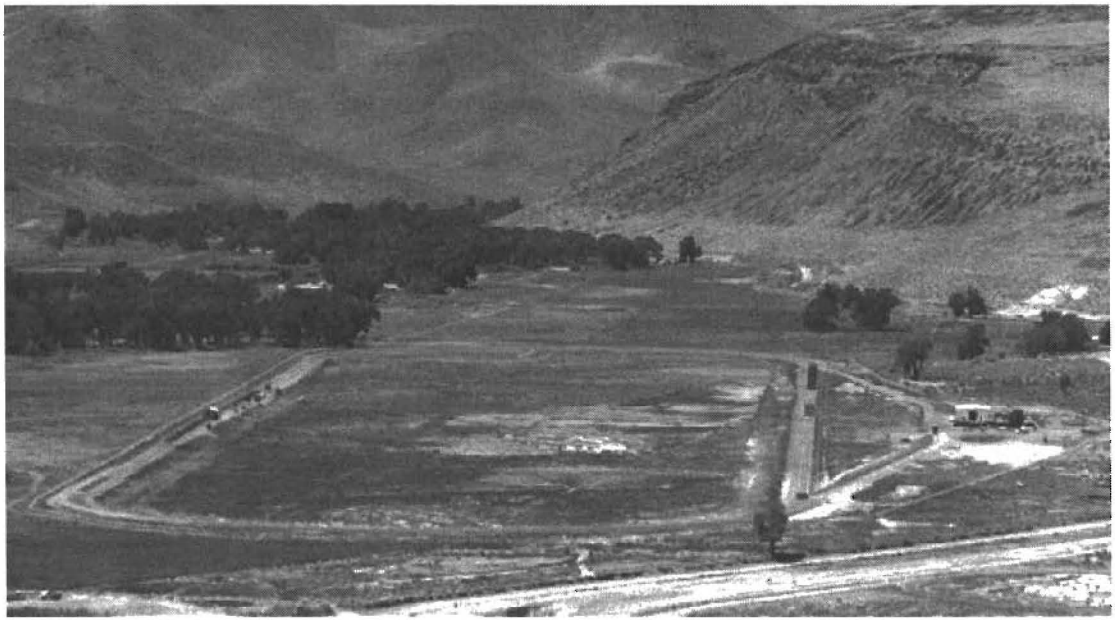

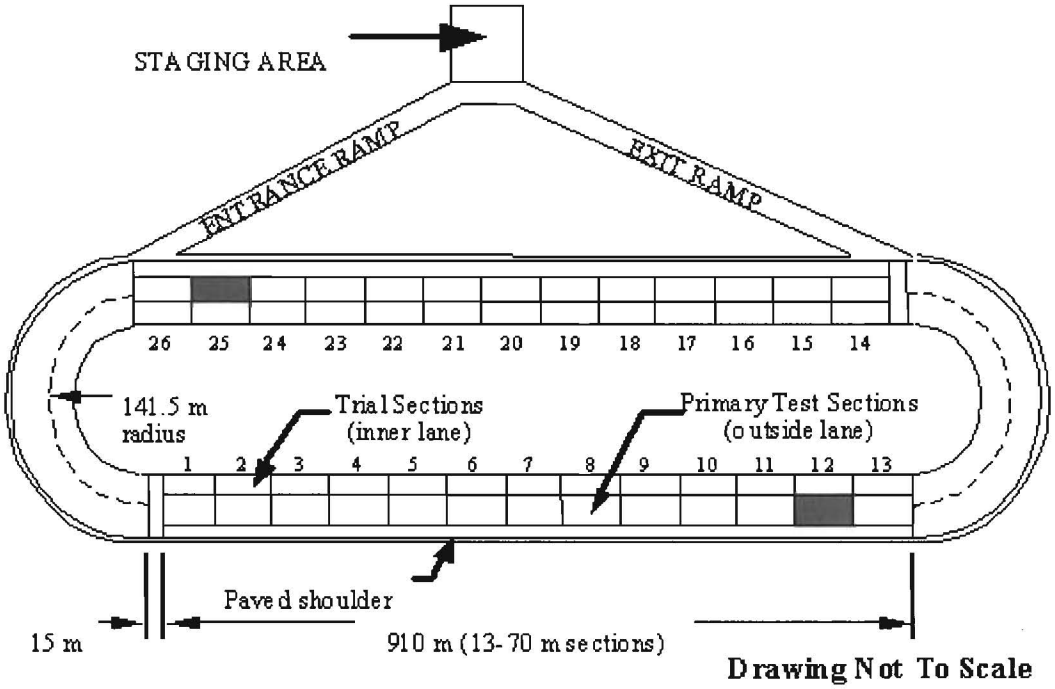

Figure 6.2 Layout and Schematic of WesTrack Site

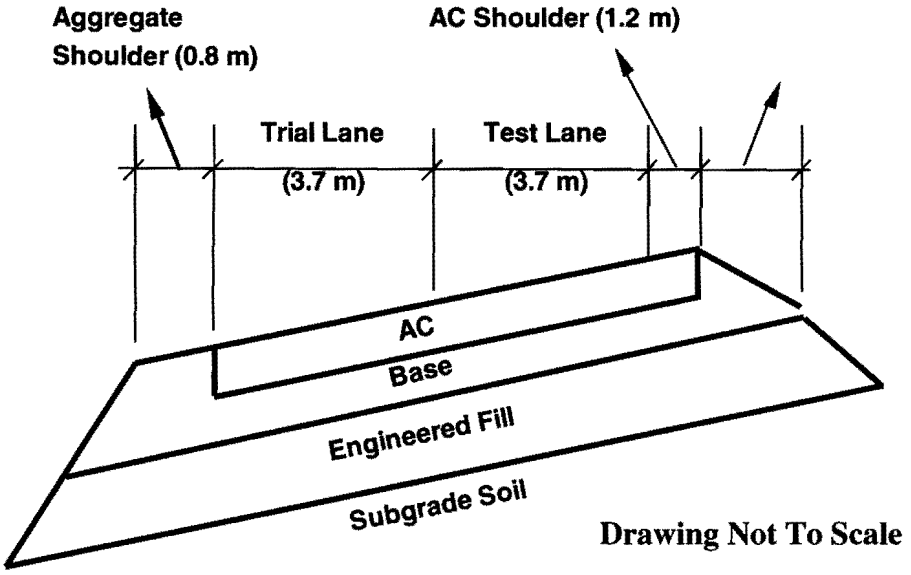

Figure 6.3 Cross-Section of Test Track

Sections 12 and 25 of the track are considered in this study (see Figure 6.2) because they are the closest to the two Long Term Pavement Performance (LTPP) seasonal monitoring sites (Mikhail et al., 1999). All field test results used here are from data collected in March 1996 shortly before the loading of the facility.

FWD RESULTS

The FWD measurements were carried out along Sections 12 and 25 at 33-ft (10 m) intervals. The FWD sensors were spaced at 0 in., 8 in. (203 mm), 12 in. (305 mm), 24 in. (610 mm), 36 in. (914 mm), 48 in. (1219 mm), and 60 in. (1524 mm) from the FWD load plate. Seeds et al. (2000) and Mikhail et al. (1999) both reported different receiver spacings for the second and third sensors at 12 in. (305) and 18 in. (475 mm). However, since this was a SHRP test site SHRP spacing was used.

The FWD deflections and their corresponding FWD loads measured at both sections are summarized in Table 6.1. For Section 12, the five deflection basins are quite similar. However, for Section 25, the last two deflection measurements are quite different than the others.

Seeds et al. (2000) and Mikhail et al. (1999) have reported overall variations in modulus with depth from the WesTrack sections. However, since this is a case study, the backcalculation process was repeated for the specific set of data used. For this study, two computer programs, MODULUS 5.0 and EVERCALC 5.0, were used to backcalculate the layer moduli. Michalak and Scullion (1995) developed the MODULUS 5.0 program for TxDOT. Sivaneswaran et al. (1999) developed the EVERCALC 5.0 program for the Washington State Department of Transportation. Both programs are widely used. Seeds et al. (2000) and Mikhail et al. (1999) reported the degree of difficulty associated with backcalculating the modulus values. Since the

Table 6.1 FWD Deflections for WesTrack Sites 12 and 25

Section	Location	Load, lbs	Deflection, mils d0	d1	d2	d3	d4	d5	d6
	25	8664	13.0	10.1	8.2	6.6	4.2	2.9	2.1
	35	8680	12.4	9.5	7.8	6.2	4.0	2.8	2.1
12	45	8684	12.6	9.5	7.6	6.1	3.8	2.7	2.0
	55	8680	12.5	9.5	7.7	6.2	3.8	2.7	2.0
	65	8577	12.9	10.2	8.3	6.7	4.3	3.1	2.2
	25	8926	13.7	11.2	9.5	8.0	5.3	3.4	2.4
	35	8918	13.4	11.0	9.3	7.7	5.2	3.5	2.4
25	45	8891	12.8	10.4	8.9	7.3	4.8	3.2	2.2
	55	8922	9.8	7.8	6.5	5.3	3.5	2.5	1.9
	65	8902	10.9	9.0	7.6	6.4	4.4	3.2	2.4

two strategies shown in Figure 6.1 require the use of the deflection basins, it is important to quantify the different parameters that impact the deflection basins.

The FWD backcalculation was performed using the two cross-sections shown in Figure 6.4. In one cross section, the engineering fill and the subgrade were maintained as separate layers as normally done in the FWD analysis. However, Mikhail et al. (1999) indicated that the extraction of reasonable moduli with that cross-section was not possible. They recommended the cross-

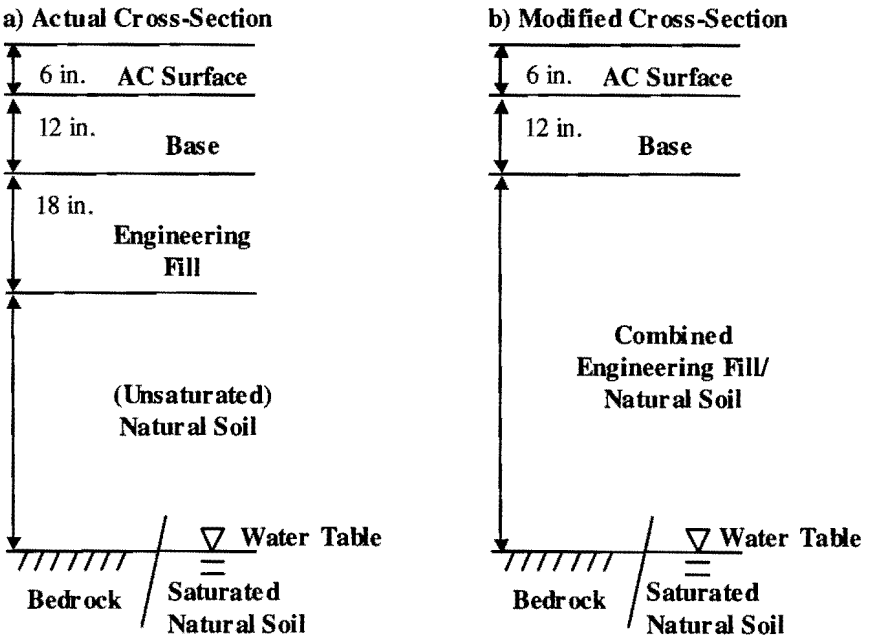

Figure 6.4 WesTrack Actual Pavement Cross-Section and Simplified Cross-Section Used in this Study

section shown in Figure 6.4b where the engineering fill and subgrade are combined into one layer. Based on extensive geotechnical coring, the presence of shallow bedrock could not be verified at the site. However, the water table could have existed at some depth (Seeds et al. 2000). This matter was investigated by analyzing the deflections using bedrock or the water table at varying depths.

The results from the backcalculation process are summarized in Tables 6.2 through 6.7. Each table shows the deflection bowls after the completion of backcalculation for the five locations tested along each test section of the track. The corresponding RMS errors, which provide indication of the closeness of fit between the measured FWD deflections and calculated deflections, are also included.

Tables 6.2 and 6.3 contain the results from the analyses of the FWD defections with MODULUS using the two cross-sections in Figure 6.4. In Table 6.2a, where the analyses are based on a four-layer system with bedrock, a reasonably good fit between the measured and calculated deflections was achieved. The RMS errors are close to 5%. However, the backcalculated layer moduli presented in Table 6.2b, are not representative of the in-situ conditions. In most cases, the moduli of the base layer are very high and those of the engineering fill are very low. The analyses were repeated using the modified cross-section where the engineering fill and the unsaturated subgrade are combined. Table 6.3 shows the results from those analyses. The RMS errors range from 4% to 9% and the corresponding layer moduli are still not representative of actual conditions with high base moduli and much lower AC modulus. The deflections of these two cases were also analyzed with EVERCALC and similar results were obtained.

To follow up on the recommendations of Seeds et al. (2000) and Mikhail et al. (1999), the bedrock was replaced with a water-saturated layer. For the saturated layer, a substantially smaller modulus (see discussion in the next section) and a Poisson's ratio of 0.47 were assumed. Tables 6.4 through 6.7 summarize the results of the analyses based on three and four layer systems with water table. In Table 6.4 and 6.5 the results are based on backcalculating all layers. Even though the calculated deflections are within an RMS error of 4%, the backcalculated moduli are unreasonable. To obtain a more reasonable fit, the procedure was repeated fixing the water saturated layer modulus at 30 ksi (207 MPa) for section 12 and 20 ksi (138 MPa) for section 25 based on recommendations of Seeds et al. (2000) and Mikhail et al. (1999). Tables 6.6 and 6.7 summarize the results from those analyses. Again the results indicate a poor depiction of the layer moduli that existed at the site.

Overall, after several backcalculation attempts using both programs, the moduli do not seem reasonable. As indicated by Mikhail et al. (1999), the results cannot be supported by nondestructive and destructive tests. This could be due to the weakness inherent in the backcalculation procedure using FWD data. The problem could also be associated with the WesTrack pavement structure and underlying support conditions (Seeds et al. 2000). The final solution pursued by Mikhail, et al. (1999) and Seeds et al. (2000) was to use the seismic moduli described next to constrain the backcalculation results.

Table 6.2 Analyses of FWD Deflections with Program MODULUS Based on a Four-Layer System with Bedrock Option

a) Deflection

Section	Location	Deflection, mils d0	d1	d2	d3	d4	d5	d6	RMS Error
12	25	13.1	9.9	8.6	6.1	4.3	3.0	2.0	4 %
	35	12.4	9.3	8.1	5.8	4.1	2.9	2.0	4 %
	45	12.6	9.3	8.0	5.7	4.0	2.7	1.9	4 %
	55	12.6	9.3	8.1	5.7	4.0	2.7	1.9	5 %
	65	12.9	9.9	8.7	6.2	4.4	3.1	2.2	4 %
25	25	13.7	11.2	9.9	7.2	5.2	3.7	2.6	6 %
	35	13.4	10.9	9.7	7.1	5.2	3.7	2.6	5 %
	45	12.8	10.4	9.2	6.7	4.8	3.4	2.4	5 %
	55	9.8	7.6	6.8	5.0	3.6	2.5	1.7	5 %
	65	11.0	8.9	7.9	6.0	4.4	3.3	2.3	3 %

b) Modulus

Section	Location	Modulus, ksi AC	Base	Eng. Fill *	Subgrade
12	25	222	111	5	18
	35	214	126	6	19
	45	200	120	6	20
	55	204	120	6	20
	65	239	113	5	17
25	25	372	94	4	16
	35	351	105	4	16
	45	383	103	4	18
	55	316	190	4	30
	65	367	162	4	19

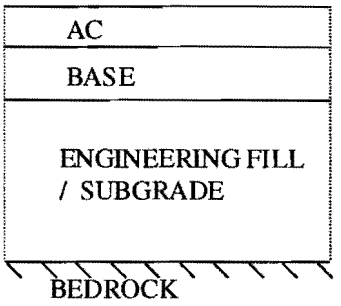

* Eng. Fill: Engineering Fill

Table 6.3 Analyses of FWD Deflections with Program MODULUS Based on a Three-Layer System with Bedrock Option

a) Deflection

Section	Location	Deflection, mils							RMS Error
		d0	d1	d2	d3	d4	d5	d6	
12	25	13.0	10.0	8.6	5.9	4.3	3.1	2.3	6 %
	35	12.4	9.4	8.1	5.6	4.1	3.0	2.2	5 %
	45	12.6	9.4	8.0	5.5	3.9	2.8	2.1	5 %
	55	12.5	9.4	8.0	5.5	3.9	2.9	2.1	6 %
	65	12.9	10.0	8.7	6.1	4.4	3.3	2.4	6 %
25	25	13.5	11.4	10.1	7.1	5.1	3.8	2.8	9 %
	35	13.3	11.0	9.8	7.0	5.1	3.8	2.8	8 %
	45	12.6	10.6	9.3	6.6	4.7	3.5	2.6	9 %
	55	9.8	7.7	6.8	4.8	3.6	2.6	2.0	5 %
	65	10.9	8.9	7.9	5.9	4.4	3.3	2.5	4 %

b) Modulus

Section	Location	Modulus, ksi		
		AC	Base	Eng. Fill / Subgrade *
12	25	278	76	13
	35	269	85	14
	45	231	85	14
	55	256	81	14
	65	292	78	12
25	25	614	52	11
	35	514	65	11
	45	600	58	12
	55	418	115	16
	65	479	108	12

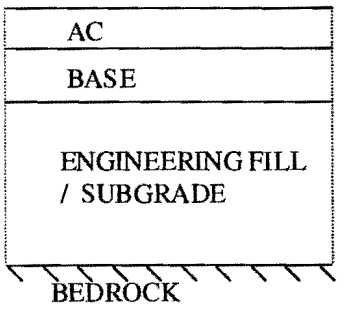

* Eng. Fill: Engineering Fill

Table 6.4 Analyses of FWD Deflections with Program EVERCALC Based on a Four-Layer System with Water Table Option

a) Deflection

Section	Location	Deflection, mils							RMS Error
		d0	d1	d2	d3	d4	d5	d6	
	25	13.1	9.9	8.6	6.1	4.3	3.0	2.1	4 %
	35	12.5	9.3	8.1	5.8	4.1	2.3	2.1	3 %
12	45	12.6	9.3	8.0	5.6	3.9	2.7	2.0	4 %
	55	12.6	9.3	8.1	5.7	3.9	2.7	2.0	4 %
	65	13.0	9.9	8.7	6.2	4.4	3.1	2.2	3 %
	25	13.8	11.2	9.9	7.3	5.2	3.6	2.4	4 %
	35	13.5	10.8	9.7	7.2	5.2	3.6	2.4	3 %
25	45	12.9	10.3	9.2	6.8	4.9	3.3	2.2	3 %
	55	9.9	7.7	6.8	4.9	3.6	2.6	1.9	3 %
	65	11.0	8.8	7.9	6.0	4.5	3.2	2.3	3 %

b) Modulus

Section	Location	Modulus, ksi				
		AC	Base	Eng. Fill *	Sub.*	Sat. Sub.*
	25	208	121	3	73	18
	35	208	130	3	500	7
12	45	200	122	3	500	7
	55	201	123	3	500	76
	65	218	126	2	500	9
	25	303	120	2	24	132
	35	273	144	2	49	188
25	45	303	136	2	104	75
	55	331	171	3	1000	8
	65	339	176	2	1000	9

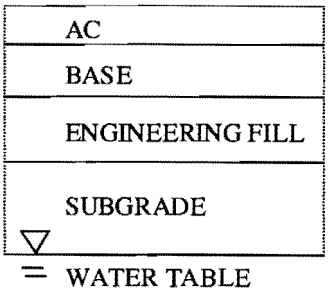

* Eng. Fill: Engineering Fill, Sub.: Subgrade, Sat. Sub.: Saturated Subgrade

Table 6.5 Analyses of FWD Deflections with Program EVERCALC Based on a Three-Layer System with Water Table Option

a) Deflection

Section	Location	Deflection, mils d0	d1	d2	d3	d4	d5	d6	RMS Error
12	25	13.1	9.9	8.6	6.0	4.3	3.0	2.1	4 %
	35	12.5	9.4	8.1	5.7	4.1	2.9	2.1	4 %
	45	12.7	9.3	8.0	5.5	3.9	2.8	1.9	4 %
	55	12.6	9.4	8.0	5.6	3.9	2.8	2.0	5 %
	65	13.0	10.0	8.7	6.2	4.4	3.1	2.2	4 %
25	25	13.0	11.4	10.3	7.4	5.1	3.5	2.4	5 %
	35	13.0	11.2	10.0	7.1	5.0	3.5	2.5	5 %
	45	12.3	10.6	9.5	6.7	4.7	3.3	2.2	5 %
	55	9.8	7.7	6.8	4.9	3.6	2.6	1.9	4 %
	65	11.0	8.9	7.9	5.9	4.4	3.3	2.3	4 %

b) Modulus

Section	Location	Modulus, ksi AC	Base	Eng. Fill / Sub.*	Sat. Sub.*
12	25	234	96	10	5000
	35	237	101	11	116
	45	207	99	12	99
	55	232	94	12	117
	65	247	100	9	5000
25	25	1132	36	9	1000
	35	782	55	9	1000
	45	957	47	10	1000
	55	375	136	13	135
	65	388	138	9	1000

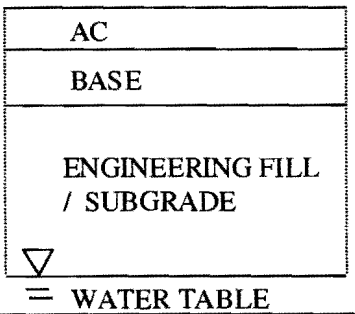

* Eng. Fill: Engineering Fill, Sub: Subgrade, Sat. Sub: Saturated Subgrade

Table 6.6 Analyses of FWD Deflections with Program EVERCALC Based on a Four-Layer System with Water Table Option at Fixed Value

a) Deflection

Section	Location	Deflection, mils							RMS Error
		d0	d1	d2	d3	d4	d5	d6	
12	25	13.1	9.9	8.6	6.1	4.3	3.0	2.1	4 %
	35	12.5	9.3	8.1	5.8	4.1	2.9	2.1	4 %
	45	12.6	9.3	8.0	5.6	3.9	2.8	2.0	4 %
	55	12.6	9.3	8.0	5.6	4.0	2.8	1.9	4%
	65	13.0	9.9	8.7	6.2	4.5	3.1	2.2	4 %
25	25	13.0	11.4	10.3	7.4	5.1	3.5	2.4	5 %
	35	13.5	10.9	9.7	7.1	5.1	3.6	2.4	3 %
	45	12.9	10.4	9.3	6.7	4.8	3.3	2.2	4 %
	55	9.9	7.7	6.8	5.0	3.6	2.6	1.9	3 %
	65	11.0	8.8	7.9	6.0	4.5	3.3	2.3	3 %

b) Modulus

Section	Location	Modulus, ksi				
		AC	Base	Eng. Fill *	Sub. *	Sat. Sub. *
12	25	209	119	4	25	30
	35	216	120	5	21	30
	45	200	114	6	21	30
	55	210	113	6	22	30
	65	224	119	4	21	30
25	25	969	55	3	78	20
	35	307	122	2	1000	20
	45	347	116	2	1000	20
	55	334	167	4	52	20
	65	339	176	2	84	20

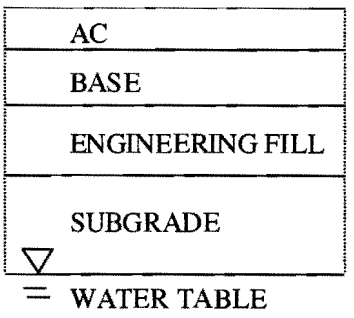

* Eng. Fill: Engineering Fill, Sub.: Subgrade, Sat. Sub.: Saturated Subgrade

Table 6.7 Analyses of FWD Deflections with Program EVERCALC Based on a Three-Layer System with Water Table Option at Fixed Value

a) Deflection

Section	Location	Deflection, mils							RMS Error
		d0	d1	d2	d3	d4	d5	d6	
12	25	12.6	10.2	8.9	5.9	4.1	2.9	2.2	6 %
	35	12.3	9.6	8.2	5.5	3.9	2.9	2.2	5 %
	45	12.6	9.5	8.0	5.3	3.8	2.8	2.1	5 %
	55	12.4	9.6	8.2	5.4	3.8	2.8	2.1	6 %
	65	12.7	10.2	8.9	6.0	4.3	3.1	2.3	5 %
25	25	12.7	11.4	10.5	7.5	5.1	3.5	2.4	6 %
	35	12.3	11.2	10.2	7.4	5.1	3.5	2.4	5 %
	45	11.8	10.6	9.7	6.9	4.8	3.2	2.2	5 %
	55	9.1	7.9	7.1	4.9	3.4	2.5	1.9	5 %
	65	10.2	9.1	8.3	6.0	4.3	3.2	2.4	5 %

b) Modulus

Section	Location	Modulus, ksi			
		AC	Base	Eng. Fill /Sub. *	Sat. Sub. *
12	25	504	47	14	30
	35	343	66	14	30
	45	278	67	15	30
	55	361	59	15	30
	65	438	55	13	30
25	25	1872	5	19	20
	35	1997	5	19	20
	45	1970	5	23	20
	55	1624	25	22	20
	65	1756	24	16	20

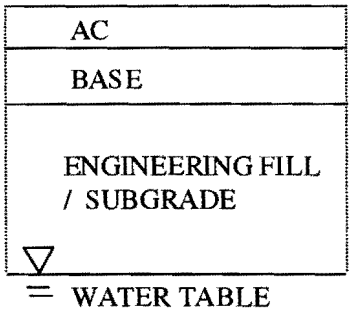

* Eng. Fill: Engineering Fill, Sub.: Subgrade, Sat. Sub.: Saturated Subgrade

SPA RESULTS

The SPA was used to perform SASW tests on the two pavement sections in March 1996. The intention was to conduct the SPA and FWD tests simultaneously before the loading of the testing facility. Because of time limitations, the SPA tests were carried out during a snowstorm where the ambient temperature was slightly above freezing. The FWD tests were carried out a few days later when the ambient conditions were more favorable.

Based on the SASW tests, the seismic moduli and layer thickness shown in Table 6.8 were determined. The profile was modeled as a five-layer system. The AC layer was modeled as two individual layers because of significant differences in the moduli of the lower and upper lifts. The moduli of the AC layers reported are those adjusted to a temperature of 77 °F (25 °C) and a frequency of 30 Hz using relationships discussed in Chapter 2. The moduli and thicknesses are reasonably similar for the five points tested.

Table 6.8 Seismic Moduli and Thickness from SPA for WesTrack Sites 12 and 25

Parameter	Section	Location	Top AC	Bottom AC	Base	Eng. Fill *	Subgrade
Modulus, ksi	12	25	805	417	36	21	15
		35	794	387	34	23	14
		45	797	436	32	20	12
		55	779	411	39	21	14
		65	758	360	32	19	13
	25	25	829	503	54	22	14
		35	801	446	42	20	13
		45	857	494	52	25	16
		55	840	489	50	23	15
		65	794	467	46	21	14
Thickness, in.	12	25	3.1	2.9	12	18	-
		35	3.0	3.0	12	18	-
		45	3.1	2.8	12	18	-
		55	3.0	3.0	12	18	-
		65	3.3	2.6	12	18	-
	25	25	3.3	2.6	12	18	-
		35	3.0	2.9	12	18	-
		45	3.3	2.8	12	18	-
		55	3.2	2.7	12	18	-
		65	3.0	3.0	12	18	-

* Eng. Fill: Engineering Fill

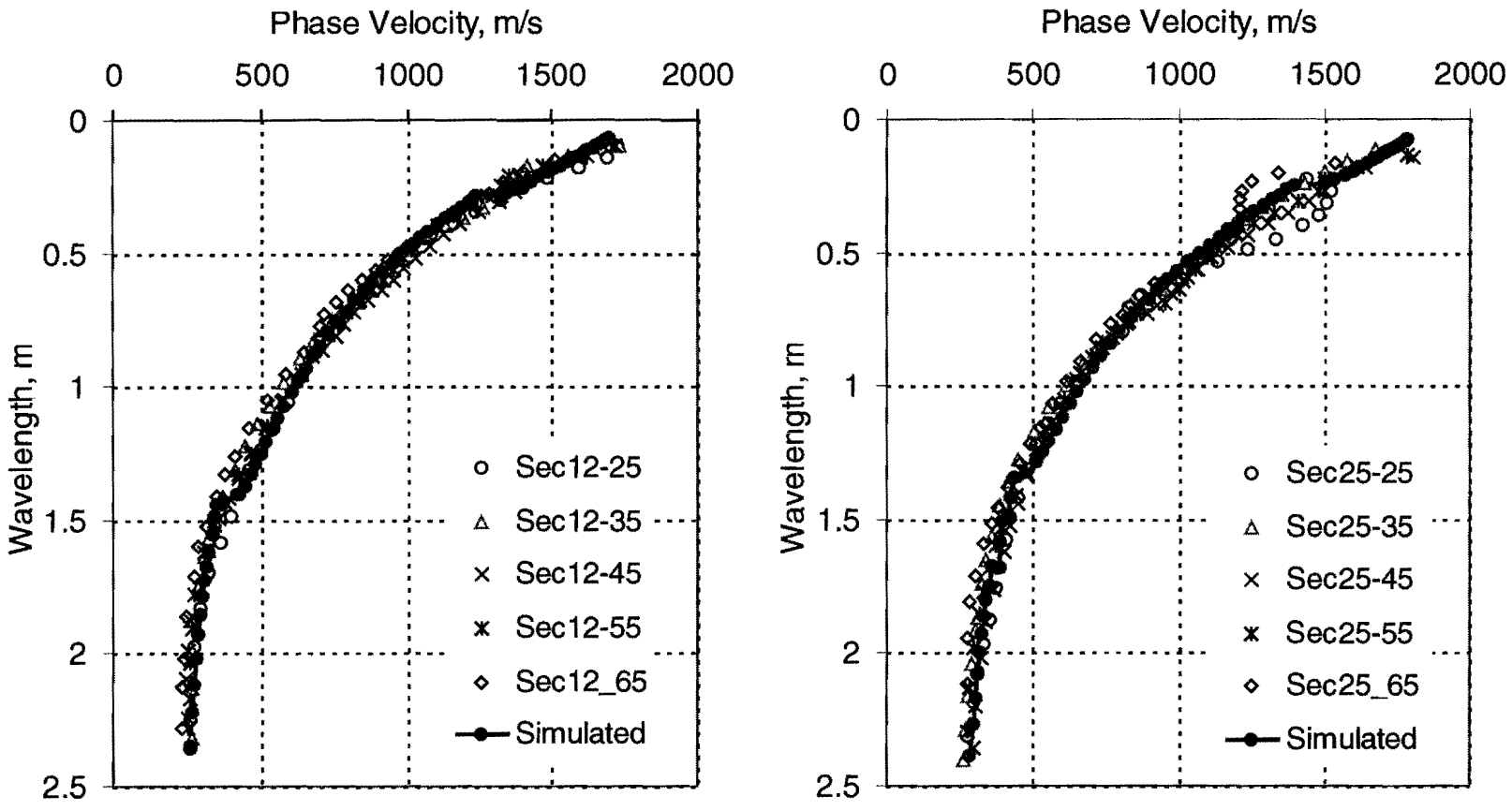

Figure 6.5 Comparison of Experimental and Theoretical Dispersion Curves from SASW Tests Performed with SPA

Dispersion curves containing the raw data from the SASW tests, from all points tested, are shown in Figure 6.5. In general, the curves for each section are similar. Also included in each figure is the theoretical dispersion curve obtained from the average properties of the five test locations at each section. The experimental curves and the theoretical one compare quite favorably. As with the FWD, there is some non-uniqueness associated with the results from the SASW moduli. As extensively discussed in Nazarian et al. (1993), the modulus and thickness of the AC layer are well constrained and for all practical purposes are unique. The modulus of the subgrade is also well constrained and should be determined with reasonably high certainty. The least certain parameters are the thickness of the engineering fill and the base. The thicknesses of the base and engineering fill were maintained as constants of 12 in. and 18 in. to ensure reasonable results.

LABORATORY RESULTS

Soil Specimens from different layers along the two sites were collected and tested by a commercial laboratory. Aside from index tests, the resilient modulus tests were performed. We reanalyzed the resilient modulus test results to determine the nonlinear parameters k_1 through k_3. The nonlinear parameters k_1 through k_3 for sections 12 and 25 are shown in Table 6.9. Laboratory tests performed on all specimens suggest k_2 of 0.45 and 0.17 for base and engineering fill, and k_3 of - 0.15 and 0.0 for base and engineering fill, respectively.

Table 6.9 Constitutive Parameters Determined from Laboratory Test Results

Material	Sample ID	k_1, psi	k_2	k_3	R^2
Base	b011116	4887	0.46	0.20	0.996
	b012424	6915	0.46	0.11	0.997
	b010620	4568	0.47	0.20	0.994
	b012213	10202	0.29	0.15	0.988
Engineering Fill or Subgrade	012213	20380	0.15	0.02	0.955
	012424	18214	0.16	-0.01	0.971
	012525	17848	0.13	0.05	0.978
	011217	19521	0.17	0.04	0.952
	011116	15463	0.22	0.01	0.988
	011318	4319	0.46	0.01	0.963
	011015	14012	0.18	-0.02	0.965
	012626	2785	0.27	0.49	0.905
	lift1-012011	16611	0.14	-0.01	0.968
	lift1-011607	18311	0.13	0.00	0.975
	lift2-011708	16661	0.15	0.04	0.973
	lift2-011809	18582	0.11	0.03	0.957
	lift2-010914	12838	0.20	-0.01	0.986

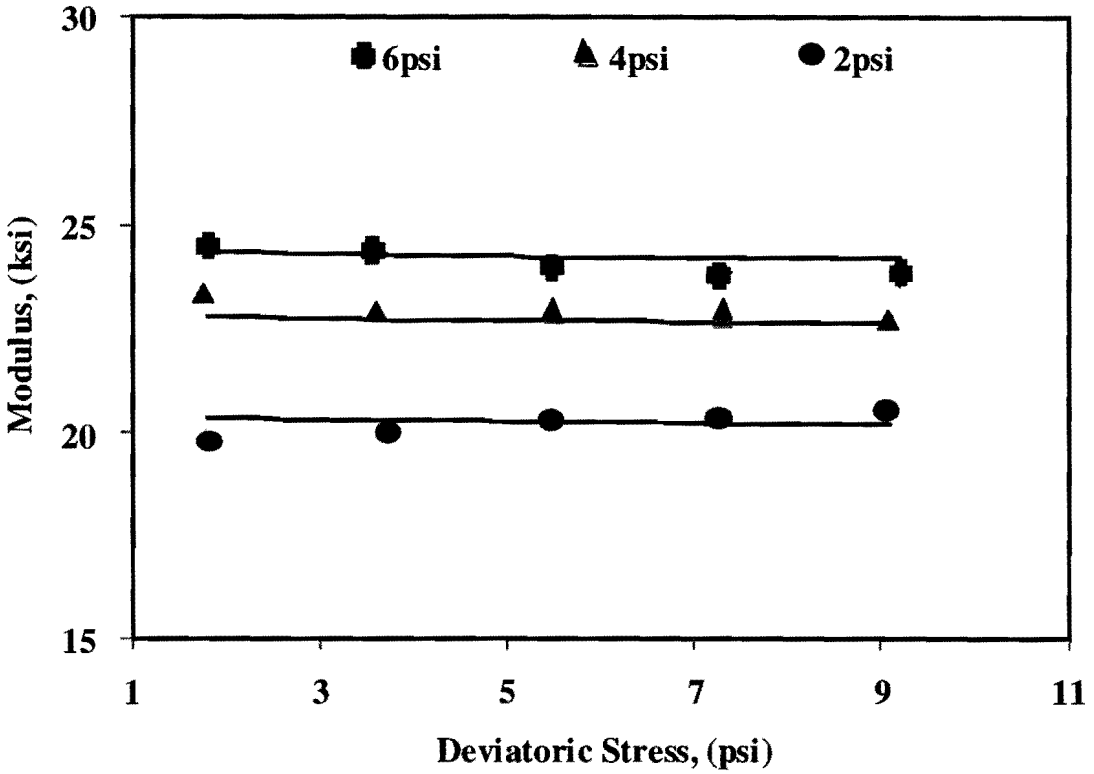

Figure 6.6 Typical Variation in Modulus with Confining Pressure and Deviatoric Stress for Base used in WesTrack

The extracted nonlinear parameters describe all materials quite well, as judged by the R^2 values (Table 6.9). All base materials exhibit a behavior similar to the one shown in Figure 6.6. The clayey engineering fill and the clayey subgrade behave similarly. In most cases, the modulus slightly increases with confining pressure (k_2 of about 0.15). The modulus is hardly affected by the deviatoric stress (k_3 of about zero), which is unexpected.

As indicated in Chapter 4, the parameters k_2 of the base and subgrade do not impact the deflection basins in a significant manner. In this case study, the parameters k_3 are equal or close to zero for all layers indicating that the nonlinear behavior should be small.

ANALYSIS OF RESULTS (LINEAR ELASTIC MODELS)

One of the goals of this project is to determine how well the deflection basin measured with the FWD can be determined when the seismic moduli along with the nonlinear parameters of the base and subgrade are known. To achieve this goal, the linear elastic program BISAR as well as the equivalent linear program developed here were used. Since a stiff layer was not detected at the site during the geotechnical exploration, the last layer of the profile was modeled as a saturated subgrade below the water table as recommended by Seeds et al. Seeds et al. reported that the water table was located at a depth of 120 in. to 160 in. depending on the time of year with an unknown modulus for the subgrade below the water table. To evaluate the impact of these two parameters on the estimated deflections, a sensitivity study was conducted by varying the depth of the water table and the modulus of the saturated subgrade. For ease of calculation, the linear elastic program BISAR (De Jong et al., 1973) was used. The seismic moduli of

different layers were input into BISAR to calculate deflections corresponding to the FWD measurements at all test points along Sections 12 and 25. The variations in the RMS errors with depth to bedrock for a modulus of subgrade of 1000 ksi (6.9 GPa) are shown in Figure 6.7. The RMS errors were determined by comparing the deflections actually measured with the FWD and those calculated using the seismic modulus, and were calculated using Equation 5.9. The RMS errors do not vary significantly when the depth of the water table is varied in the ranges of 140 in. to 340 in. and are about 10% for Section 12 and 20% for Section 25. The results from Point 45 of both sections deviate from the typical trends. Aside from uncertainties in the determination of the seismic moduli or differences in the testing location, the reason for such a deviation is not known. Based on Figure 6.7, an ideal depth for Sections 12 and 25 is 144 in. (3.5 m) from the surface. Coincidentally, this depth is similar to the depth suggested by EVERCALC.

In the second sensitivity study, the modulus of the saturated subgrade was varied while the depth to the water table was maintained at 144 in. (3.5 m) as determined from the previous section. The variations in the deflection RMS errors with the moduli of the subgrade are shown in Figure 6.8 for both sections. The RMS errors decrease quite rapidly when the modulus of the saturated subgrade is increased from 10 ksi (70 MPa) to 20 ksi (140 MPa). For a modulus of about 20 ksi (140 MPa) and 30 ksi (210 MPa) the RMS errors are reasonably constant. Above a modulus of 30 ksi (210 MPa), the RMS errors increase slightly. The majority of the test points exhibit minimum RMS errors at a modulus of saturated subgrade of about 20 ksi (140 MPa) to 25 ksi (175 MPa). These values are reasonably close to the modulus reported by Seeds et al., (2000).

Inspecting Table 6.8, the modulus of the subgrade above the water table is about 13 ksi (90 MPa) from seismic tests. Depending on the layering considered, the modulus of the subgrade above the water table is between 10 ksi (70 MPa) to 15 ksi (100 MPa). There is no plausible reason for the modulus of the subgrade below the water table to be greater than those above the water table at this site. Never the less, to analyze the FWD data considering the layered elasto-static models such as BISAR, such a layer has to be considered.

The deflections calculated with BISAR for all test points using seismic modulus profiles and the corresponding RMS errors when the depth to the water table of 144 in. (3.5 m) and a modulus of saturated subgrade of about 22 ksi (150 MPa) are listed in Table 6.10. For Section 12, the RMS errors are about 10% (except for Location 45). For Section 25, the differences are about 10% to 20%. The RMS errors are larger than those from different scenarios of the FWD backcalculation process. However, in this case the moduli are quite reasonable as indicated by Seeds et al. (2000).

These differences can be attributed to several sources. These sources include the following items:

1. Uncertainties in determining seismic modulus.
2. Uncertainties in the temperature and strain-rate adjustment algorithms.
3. Ignoring the dynamic nature of the problem.
4. Uncertainties in the values of Poisson's ratio of the layers.
5. Uncertainties associated with the location and properties of the assumed stiff layer.
6. Uncertainties in the measured load and deflections with the FWD.

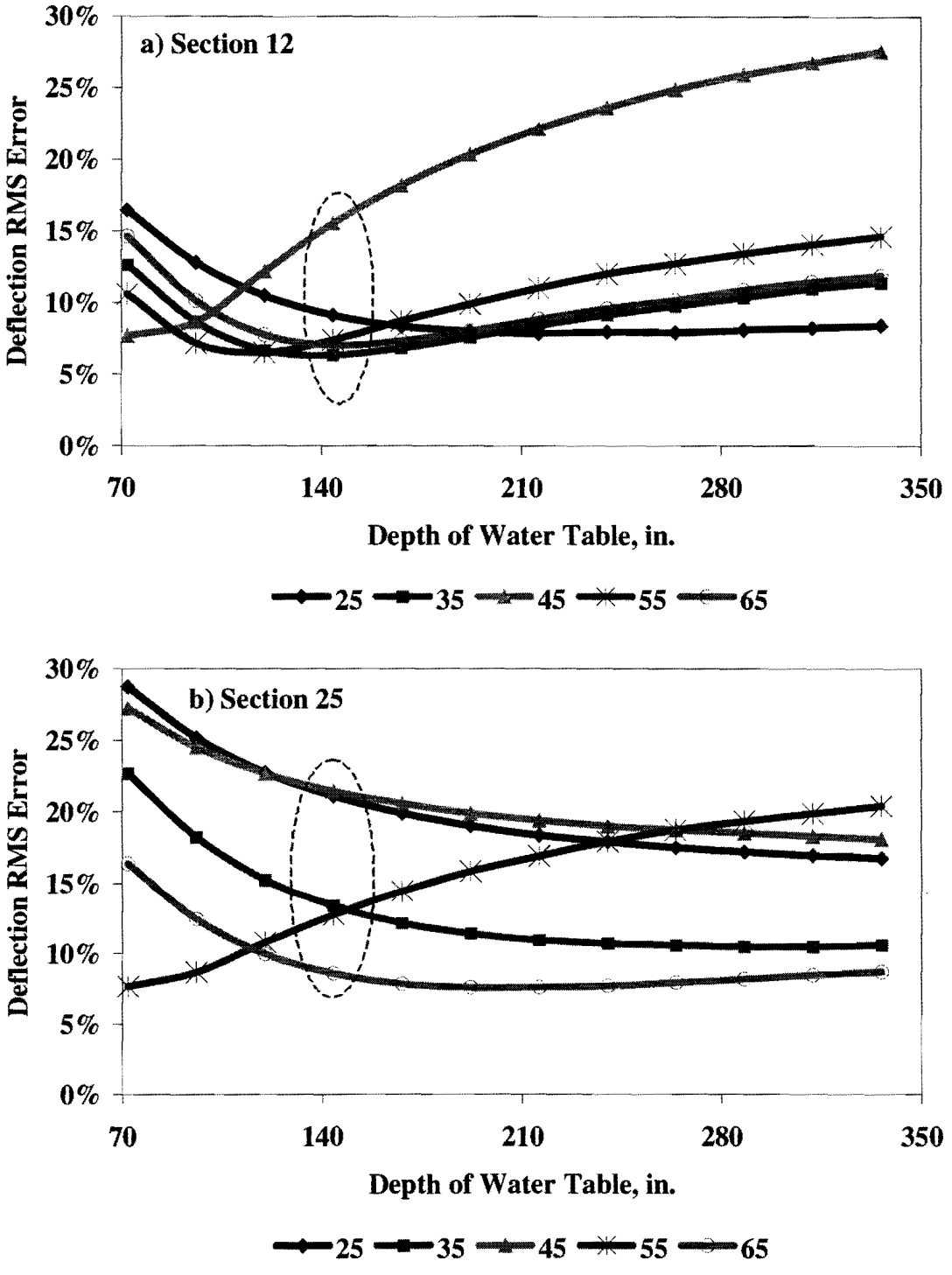

Figure 6.7 Effects of Depth to Water Table on Deflection RMS Errors Using Linear Elastic Analysis

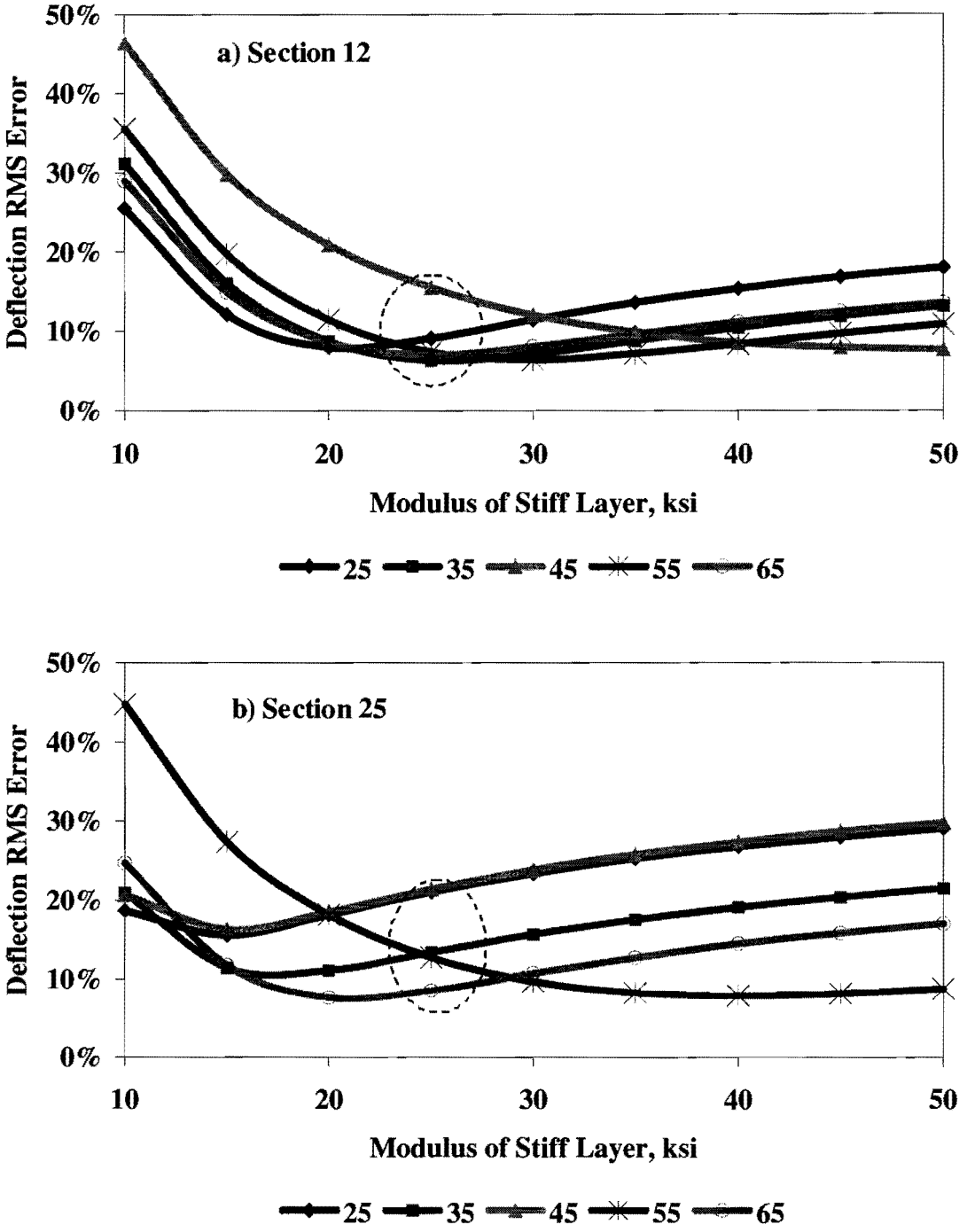

Figure 6.8 Effects of Modulus of Saturated Subgrade on Deflection RMS Errors Using Linear Elastic Analysis

One of the main reasons for the determination of the modulus profile of a given site is to estimate the stresses and strains within a pavement section so that the remaining life of the pavement can be estimated. Ke et al. (2000) demonstrated that even though the deflection basin may vary significantly with the variation in the depth to a rigid layer (or water table) at a given site, the two critical strains (i.e. compressive strain on top of subgrade and tensile strain at the bottom of the AC) do not change at all. As such, if the depth to the rigid layer (or water table) is known accurately, one should be theoretically able to backcalculate appropriate moduli from the deflection bowl. However, if the depth to the rigid layer (or water table) is not properly known, one may backcalculate erroneous moduli which may lead to erroneous critical strains. Looking at Tables 6.2 through 6.7, it is obvious that depending on the scenario selected by the engineer a completely different set of critical strains are obtained. However, for seismic methods, the critical strains should not change with the location of the rigid layer or water table. To verify these results, the critical strains (tensile strain at the bottom of the AC layer and compressive at the top of the subgrade) were calculated from the program BISAR using the seismic moduli at Location 35 of Section 12. The variation in critical strains and the remaining life based on fatigue cracking and rutting failure as a function of depth to water table is shown in Figure 6.9. It is evident that the variation in depth to the water table has little to no effect on the structural condition of the pavement.

Table 6.10 Deflections from BISAR (Linear Elastic) Using Seismic Moduli with Water Table at 144 in. (3.5 m)

Section	Location	Deflections, mils							RMS Error
		d0	d1	d2	d3	d4	d5	d6	
12	25	11.9	9.7	8.3	5.4	3.7	2.8	2.1	9%
	35	12.3	10.0	8.5	5.5	3.8	2.8	2.2	6%
	45	13.2	10.9	9.4	6.1	4.3	3.2	2.4	16%
	55	12.0	9.8	8.4	5.5	3.9	2.9	2.2	7%
	65	13.2	10.8	9.2	5.9	4.1	3.0	2.3	7%
25	25	11.2	9.3	8.1	5.6	4.1	3.2	2.5	18%
	35	12.6	10.4	9.0	6.1	4.4	3.3	2.6	11%
	45	10.4	8.6	7.5	5.1	3.8	2.9	2.3	19%
	55	11.1	9.2	8.0	5.4	4.0	3.0	2.4	18%
	65	11.8	9.7	8.4	5.7	4.2	3.2	2.5	8%

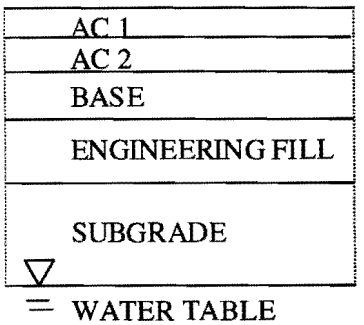

ANALYSES OF RESULTS (EQUIVALENT LINEAR ELASTIC MODELS)

The next set of analyses was performed using the equivalent linear procedure with the seismic modulus profiles. To demonstrate the forward process in Figure 6.1, three approaches were followed. The PI model described in Chapter 2 was used as the nonlinear material model first. The only required input to the PI model, aside from the seismic moduli, is the Plasticity Index (PI) of each nonlinear layer (in this case the base and engineering fill). In the second approach, the laboratory-derived nonlinear parameters k_2 and k_3 for the base and engineering fill and the seismic moduli were used along with Equation 2.5. The last approach was similar to the second with one difference. The nonlinear parameters k_2 and k_3 of the base and engineering fill were selected based on the values determined from the literature. The results from all test points are summarized in Table 6.11 for Section 12 and Table 6.10 for Section 25.

Deflections determined for Section 12 from the three approaches described above and their corresponding RMS errors are included in Table 6.11. The largest RMS errors were typically obtained when the PI model was used. In this case, the RMS errors range from 12% to 30%. It seems that the PI model over-emphasized the nonlinear behavior of the layer. This trend may be understandable for this site. The values of k_2 and k_3 of the subgrade are engineering fill from laboratory tests are much less than those typically encountered for those types of materials.

The lowest RMS errors were obtained when the nonlinear parameters k_2 and k_3 from the laboratory tests were used. Since the parameters k_3 of the engineering fill and base are rather small, and since the pavement structure (especially the AC layer) is thick, those results are quite similar to the linear elastic results with similar RMS errors of generally about 8%. When the k_2 and k_3 values from the literature were used, the impact of the nonlinear behavior of the base and subgrade were more pronounced on the deflections, but not as much as when the PI model was used.

Table 6.12 similarly compares the deflections from the three approaches as applied to Section 25 and the measured deflections with the FWD. The RMS errors from the PI model are somewhat higher than those from the other two approaches. On the other hand, the RMS errors from the nonlinear parameters based on the laboratory test and literature are similar to those calculated with the linear elastic model shown in Table 6.10. Location 55 exhibited larger RMS errors than those from the other deflection basins. This occurs primarily because the measured FWD deflection basins are largely different at this point. Such a difference is neither supported by the construction records, nor by the seismic data collected at these locations. In general the average RMS error is about 15% at this section.

To illustrate the load-induced nonlinearity that the base and engineering fill experience, a contour plot of the spatial variation in modulus is presented in Figure 6.10 for Location 35 of Section 12. The nonlinear parameters k_2 and k_3 of the engineering fill and base obtained from the literature were used. To develop reasonable curves, each nonlinear layer was divided into 12 sublayers. The base experiences localized reduction in modulus with depth in the vicinity of the load. At the boundary of the base and engineering fill, the modulus is about 75% of the seismic modulus of the layer. The engineering fill experiences very little localized load-induced nonlinearity close to the subgrade. The subgrade, as expected, experiences negligibly small load-induced nonlinear behavior.

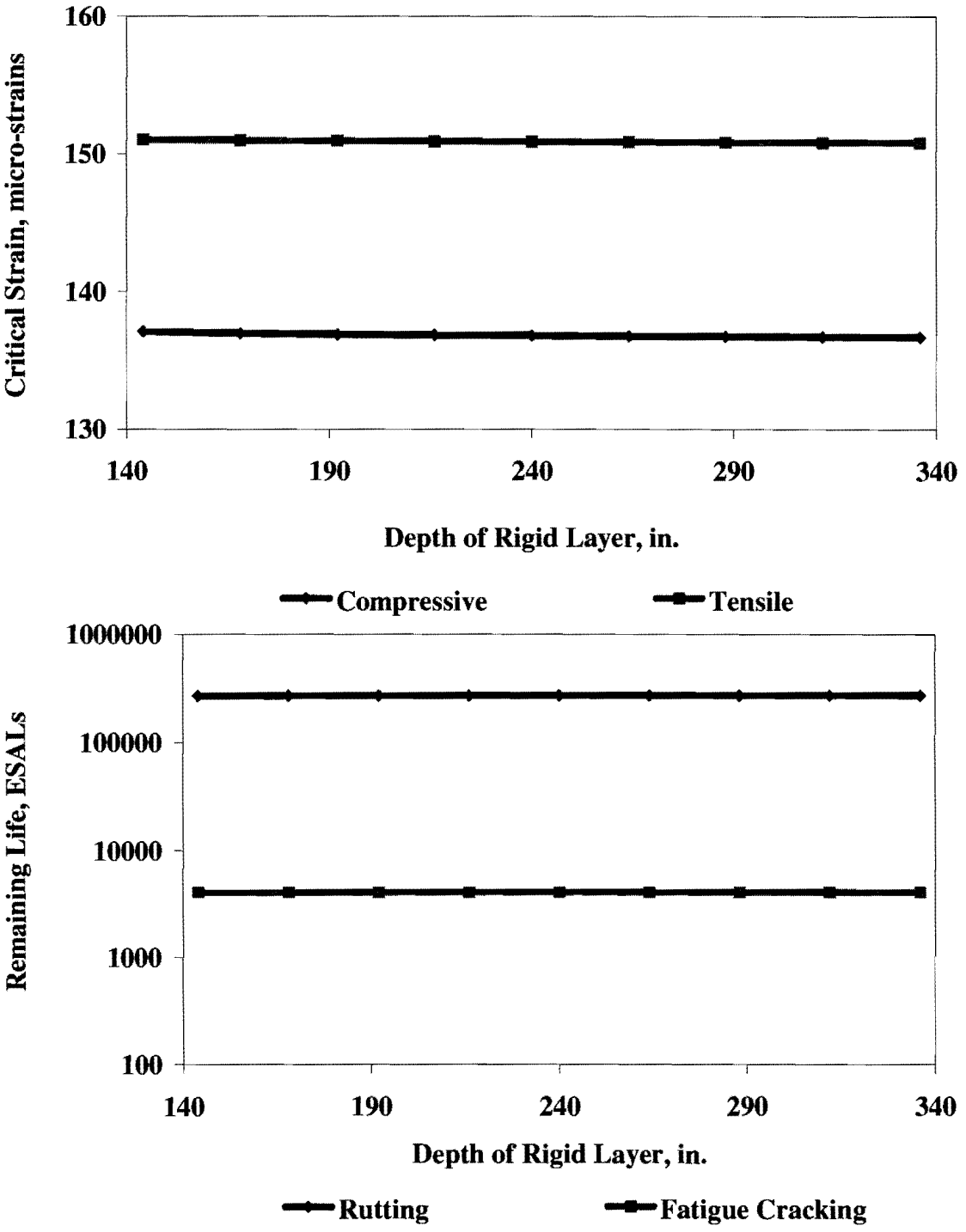

Figure 6. 9 Effects of Depth of Rigid Layer (Water Table/ Bedrock) on Critical Strains and Remaining Lives at Section 12 Location 35

Table 6.11 Deflections From Equivalent Linear Procedure Using Seismic Moduli along Section 12

Model Used	Location	Deflection, mils							RMS Error
		d0	d1	d2	d3	d4	d5	d6	
PI	25	14.5	11.7	9.8	5.8	3.8	2.7	2.1	12%
	35	15.0	12.1	10.1	5.9	3.9	2.8	2.2	17%
	45	16.1	13.2	11.1	6.7	4.4	3.2	2.4	28%
	55	14.6	11.8	9.9	5.9	3.9	2.9	2.2	16%
	65	16.4	13.3	11.1	6.4	4.1	3.0	2.3	20%
k_2 and k_3 from Laboratory	25	12.2	9.9	8.5	5.5	3.8	2.8	2.1	8%
	35	12.5	10.2	8.7	5.6	3.9	2.9	2.2	7%
	45	13.5	11.1	9.6	6.3	4.3	3.2	2.4	17%
	55	12.3	10.0	8.6	5.6	3.9	2.9	2.2	8%
	65	13.6	11.0	9.4	6.0	4.1	3.0	2.3	8%
k_2 and k_3 from Literature	25	13.3	10.7	9.1	5.6	3.8	2.8	2.1	9%
	35	13.6	11.0	9.2	5.7	3.9	2.8	2.2	10%
	45	14.6	12.0	10.2	6.4	4.3	3.2	2.4	21%
	55	13.4	10.9	9.2	5.7	3.9	2.9	2.2	11%
	65	14.7	11.9	10.1	6.2	4.1	3.0	2.3	12%

Table 6.12 Deflection Results from Equivalent Linear Procedure Using Seismic Moduli along Section 25

Model Used	Location	Deflections, mils							RMS Error
		d0	d1	d2	d3	d4	d5	d6	
PI	25	13.3	10.9	9.3	5.9	4.1	3.2	2.5	13%
	35	15.3	12.5	10.6	6.5	4.4	3.3	2.6	13%
	45	12.3	10.0	8.5	5.4	3.8	2.9	2.3	14%
	55	13.3	10.8	9.2	5.7	4.0	3.0	2.4	29%
	65	14.2	11.6	9.8	6.1	4.2	3.2	2.5	19%
k_2 and k_3 from Laboratory	25	11.7	9.7	8.4	5.7	4.2	3.2	2.5	16%
	35	13.0	10.7	9.3	6.2	4.4	3.4	2.6	10%
	45	10.7	8.9	7.7	5.2	3.8	2.9	2.3	17%
	55	11.5	9.5	8.2	5.5	4.0	3.0	2.4	20%
	65	12.2	10.0	8.7	5.8	4.2	3.2	2.5	9%
k_2 and k_3 from Literature	25	12.8	10.5	9.0	5.9	4.2	3.2	2.5	14%
	35	14.2	11.7	10.0	6.4	4.4	3.3	2.6	10%
	45	11.8	9.6	8.2	5.3	3.8	2.9	2.3	15%
	55	12.6	10.3	8.8	5.7	4.0	3.0	2.4	26%
	65	13.4	10.9	9.4	6.0	4.2	3.2	2.5	15%

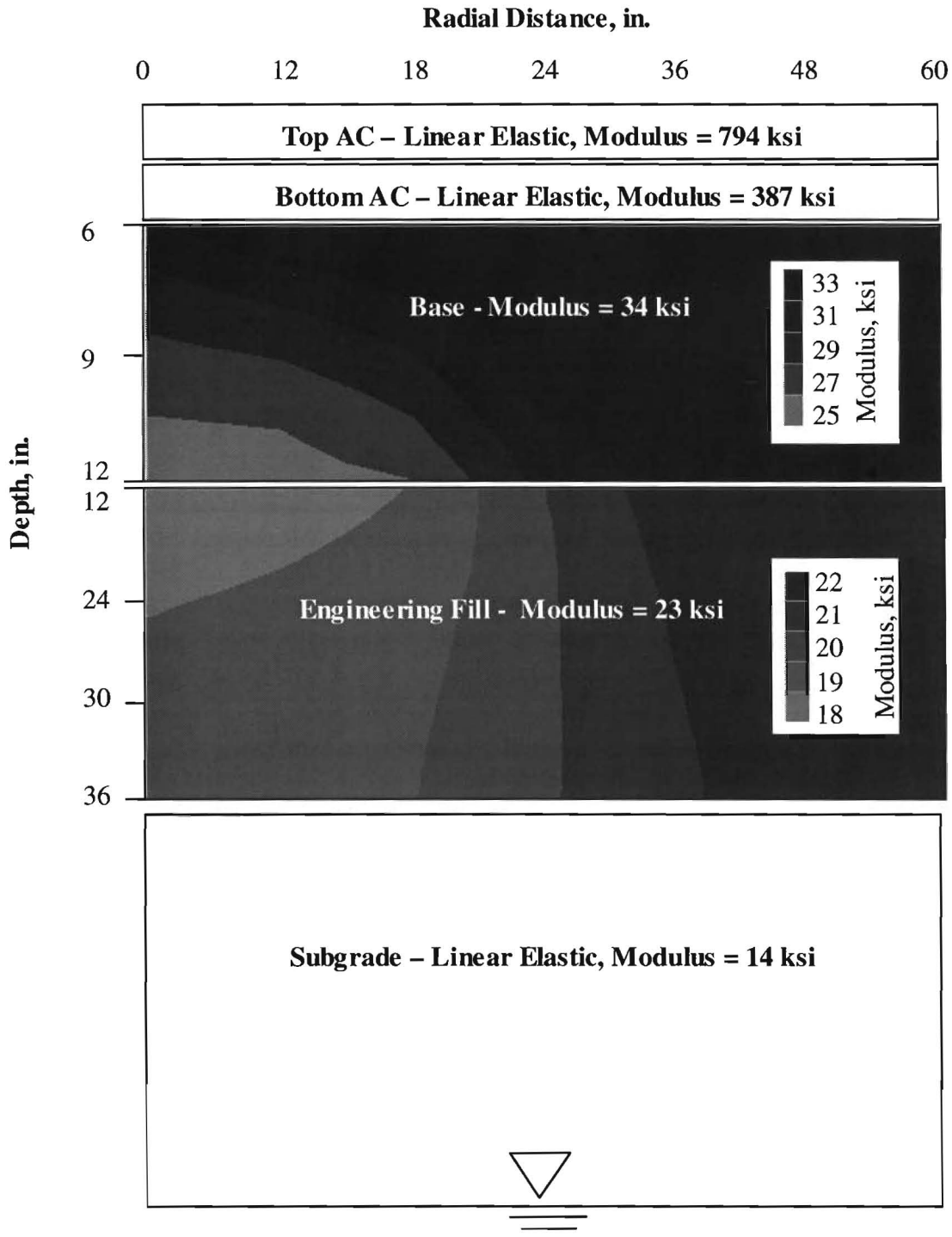

Figure 6.10 Variation in Moduli of the Base and Engineering Fill Under State of Stress Applied by a Standard Truck Load

As indicated before, one of the main goals from determining the design moduli is to estimate the critical strains. The critical strains and the remaining lives for all ten test points from the linear-elastic and the three equivalent linear approaches are summarized in Figure 6.11 and Tables 6.13 and 6.14. The linear-elastic model and the nonlinear model using the laboratory-derived parameters k_2 and k_3 are quite comparable. This trend should not be a surprise for this site. As discussed before, the nonlinear parameters k_3 are close to zero. The PI model results in much higher strains as compared with the linear elastic model. This occurs because the PI model provides much higher degree of nonlinear behavior. When the nonlinear parameters k_2 and k_3 were extracted from the literature, the results are somewhat close to the case when the parameters k_2 and k_3 were obtained from the laboratory. These three nonlinear cases clearly show the compromise between the accuracy of the results and the level of effort in testing the soil specimens. The strains from the FWD deflection analysis are not included because of the uncertainty in the backcalculated values.

Using the Asphalt Institute equations described in Chapter 2, the remaining lives of the pavement due to fatigue cracking and rutting criteria were calculated from the strains presented in Tables 6.13 and 6.14. The results are depicted in Figure 6.12 and Tables 6.13 and 6.14. The trends are quite similar to those of the strains. The remaining life due to fatigue cracking vary substantially depending on the model selected. The most conservative remaining lives are obtained from the PI model, with the least conservative being the linear elastic and the equivalent-linear model with nonlinear parameters k_2 and k_3 obtained from laboratory tests.

The remaining life due to rutting seems to be more or less independent of the model selected. This trend is logical since the rutting in the Asphalt Institute equation is related to the strain on top of the subgrade. Since the engineering fill or subgrade does not experience much load-induced nonlinearity, the compressive strains are similar, and as such the rutting remaining lives are similar.

BACKCALCULATION OF NONLINEAR PARAMETERS

The second process addressed in this case study is the determination of the nonlinear parameters k_2 and k_3 of the pavement material given the seismic modulus profile and the FWD deflection basin. The process is described in Chapter 5. The sensitivity analysis (Chapter 4) suggests that the FWD deflection basin is not sensitive to the parameters k_2 of the base and subgrade, therefore the backcalculation of these parameters is not pursued here. The same sensitivity analysis also indicated that for thick pavements, with materials that do not exhibit significant nonlinear behavior, the impact of the load-induced nonlinearity on the deflection basin is rather small. Furthermore, as indicated in Section 3, the determination of a reasonable pavement modulus from the measured deflection basin using a conventional backcalculation approach was rather difficult. With these three limitations, one should not have high expectations for obtaining robust and unique backcalculated nonlinear parameters at this site. Nevertheless, the backcalculation procedure was applied to the available data to estimate parameters k_3 of the base and the engineering fill.

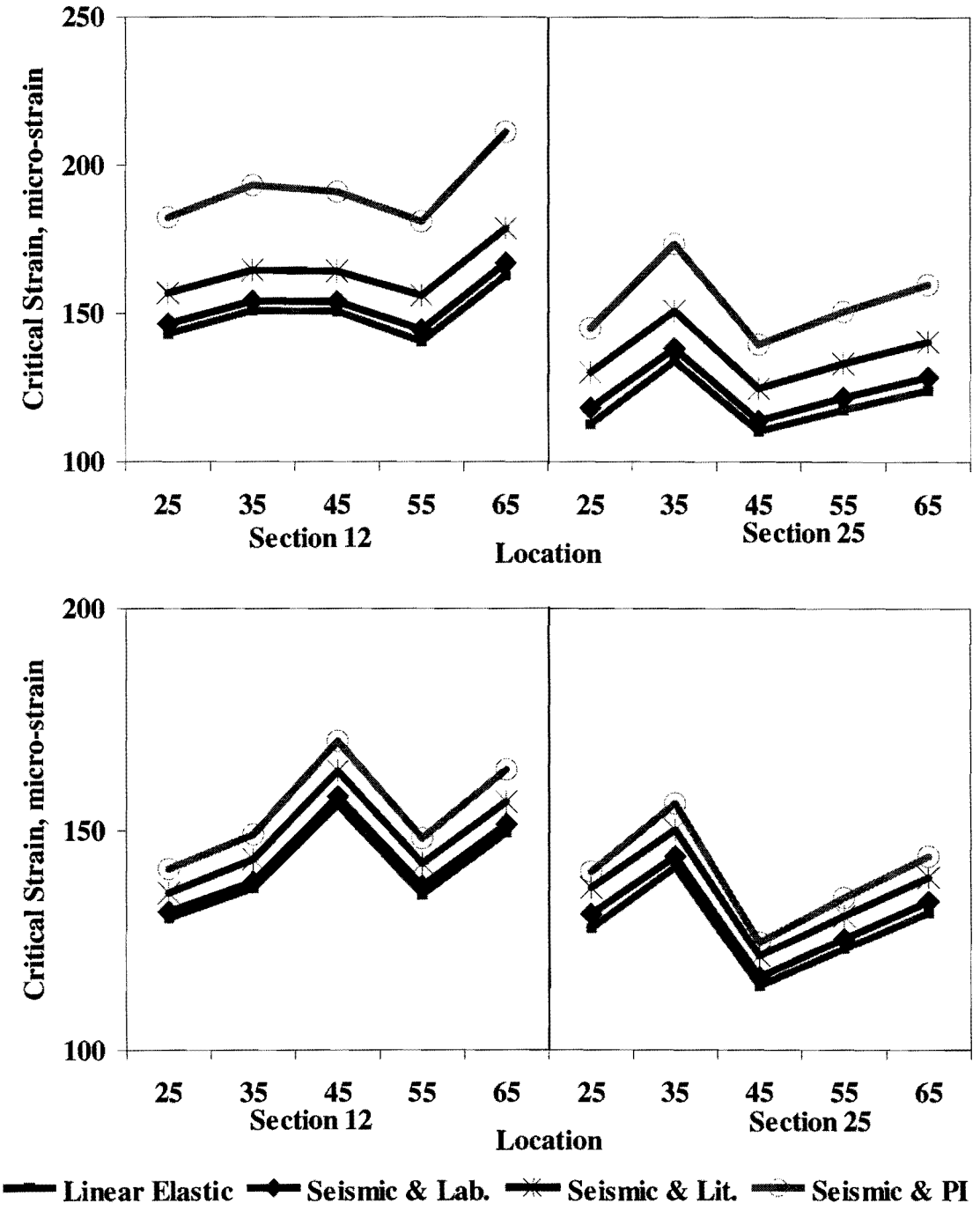

Figure 6.11 Variations in Critical Strains along Sections 12 and 25 from Seismic Moduli

Table 6.13 Estimated Critical Strains and Remaining Lives along Section 12 from Seismic Moduli

Model Used	Location	Critical Strain micro-strain		Remaining Life 10^6 ESALs	
		Tensile	Compressive	Fatigue Cracking	Rutting
Linear Elastic (BISAR)	25	143	130	4	338
	35	151	137	3	270
	45	151	156	4	152
	55	141	136	4	283
	65	163	150	3	182
PI	25	182	141	2	235
	35	193	149	2	185
	45	191	170	2	103
	55	181	148	2	190
	65	211	164	1	122
k_2 and k_3 from Laboratory	25	147	132	4	322
	35	154	139	3	258
	45	154	158	3	144
	55	144	138	4	266
	65	167	151	3	173
k_2 and k_3 from Literature	25	157	136	3	280
	35	165	144	3	219
	45	164	163	3	123
	55	156	143	3	226
	65	179	157	2	149

Table 6.14 Estimated Critical Strains and Remaining Lives along Section 25 from Seismic Moduli

Model Used	Location	Critical Strain micro-strain		Remaining Life 10^6 ESALs	
		Tensile	Compressive	Fatigue Cracking	Rutting
Linear Elastic (BISAR)	25	113	128	8	367
	35	134	142	5	232
	45	110	115	9	598
	55	118	123	7	435
	65	124	132	6	324
PI	25	145	141	3	240
	35	173	156	2	151
	45	140	125	4	411
	55	151	135	3	290
	65	160	144	3	215
k_2 and k_3 from Laboratory	25	118	131	7	328
	35	138	144	43	215
	45	114	117	8	555
	55	122	126	7	400
	65	129	134	6	298
k_2 and k_3 from Literature	25	130	137	5	270
	35	151	150	3	179
	45	125	122	6	461
	55	133	131	5	333
	65	141	139	4	250

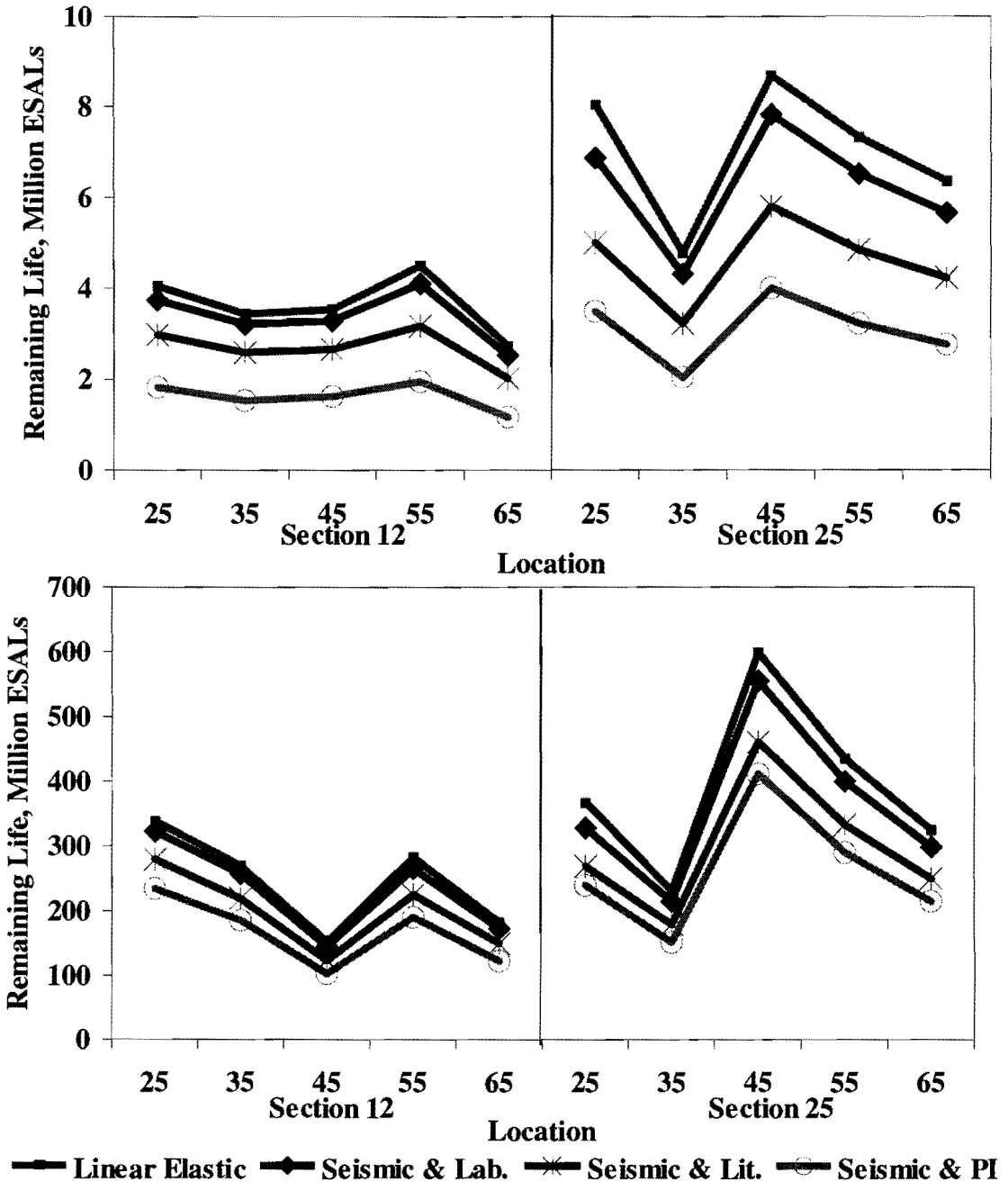

Figure 6.12 Variations in Remaining Life along Sections 12 and 25 from Seismic Moduli

The backcalculation process was based on the same pavement cross-section as used in equivalent linear analysis (see Figure 6.4a). The water table was considered at the depth of 144 in. (3.5 m). As indicated before, a constant value was assigned to the parameters k_2 of the base and engineering fill. Since in a practical field evaluation program the nonlinear parameters are unknown, the parameters k_2 suggested by the literature were used for the base and the engineering fill, first. The backcalculated parameters k_3 of the base and engineering fill are reported in Tables 6.15 along with the RMS errors after the termination of backcalculation. In all cases, the backcalculation process terminated because the maximum number of iterations (11 iterations) was reached. The backcalculated parameter k_3 of either the base or the engineering fill does not converge to a single or reasonable value. In most cases, the parameters k_3 are either equal to the upper (zero) or the lower (-0.5) feasible limits for those parameters. As such, the backcalculation process was considered unsuccessful.

To investigate whether improving the estimated value of parameters k_2 of the base and subgrade may improve the backcalculated k_3 parameters, the k_2 values from the literature were replaced with those derived from the laboratory tests. The backcalculated values of the k_3 of base and engineering fill are reported in Table 6.16 for this case. Once again, the backcalculation for each of the ten stations was terminated after 11 iterations (the maximum number allowed) with large RMS errors and impractical results. Even though not shown here, increasing the number of iterations to 20 did not result in more reasonable results. As anticipated, this case study demonstrates the impracticality of attempting to backcalculate nonlinear parameters of the pavement layers for thick structures with layers that do not exhibit substantial load-induced nonlinear behavior. These parameters should be obtained from laboratory testing. In the future, the process will be applied to thinner pavements to judge the overall feasibility of this backcalculation process.

In summary, the forward procedure, when the seismic moduli are combined with nonlinear parameters obtained from the laboratory tests, seems to be feasible. As judged with the estimated deflection basin and the correspondence of the values to the constructed layers, the forward procedure may yield more suitable design moduli. However, the backcalculation of the nonlinear parameters from the seismic moduli and the FWD deflection basin may not be feasible, especially for thicker pavements constructed with high-quality materials that do not exhibit nonlinear behavior.

Table 6.15 Backcalculated Parameters k_3 of Base and Engineering Fill When Parameters k_2 are Based on Literature Recommended Values

Section	Location	k_3 Base Backcalculated	k_3 of Engineering Fill Backcalculated	RMS Error
12	25	-0.28	0.00	8%
	35	-0.26	-0.19	8%
	45	-0.50	-0.27	27%
	55	0.00	0.00	8%
	65	-0.50	-0.20	36%
25	25	-0.25	0.00	19%
	35	-0.50	0.00	12%
	45	0.00	0.00	20%
	55	-0.13	-0.21	17%
	65	-0.18	0.00	9%

Table 6.16 Backcalculated Parameters k_3 of Base and Engineering Fill When Parameters k_2 Are Based on Laboratory Results

Section	Location	k_3 Base Backcalculated	k_3 of Engineering Fill Backcalculated	RMS Error
12	25	-0.25	-0.20	8%
	35	-0.50	-0.20	9%
	45	-0.50	0.00	28%
	55	0.00	-0.20	8%
	65	0.00	-0.50	38%
25	25	-0.28	-0.13	18%
	35	0.00	-0.50	13%
	45	-0.16	-0.31	20%
	55	-0.07	-0.50	17%
	65	-0.50	-0.50	9%

CHAPTER SEVEN
SUMMARY, CONCLUSIONS AND RECOMMENDATIONS

SUMMARY

Nondestructive testing techniques are widely used as tools for measuring the variation in moduli of pavement sections. The moduli of pavement materials obtained in this manner are used to determine the critical strains and, thus, to estimate the remaining lives of pavement systems.

TxDOT uses two nondestructive testing devices, the Falling Weight Deflectometer (FWD) and the Seismic Pavement Analyzer (SPA). The FWD applies an impulse load to the pavement, and seven sensors measure the surface deflections of the pavement. The moduli of pavement layers are obtained from these deflections using a backcalculation program. Since the load applied by the FWD to the pavement is similar to that exerted by traffic, the FWD moduli are used in pavement design and analysis without adjusting them for the nonlinear behavior of the materials. The operating principle of the SPA is based on generating and detecting stress waves in a layered medium. Seismic moduli of different layers can be obtained through an inversion process from the SPA. Seismic moduli are similar to the linear elastic ones since they correspond to very small external loads. It is essential to have a constitutive model that considers nonlinear behavior of pavement materials so that design moduli under the state of stress applied by a truck can be obtained form the seismic moduli. In this study, a constitutive model that relates the nonlinear modulus of a pavement material with its state of stress was used. The seismic moduli can be input into this model to calculate the nonlinear moduli under any load configuration. Using a computation algorithm, deflections of the pavement surface at locations of FWD sensors are calculated. An optimization process is then applied to the FWD deflection and calculated deflection to estimate the nonlinear parameters in the constitutive model used in this study.

The algorithm used to determine the nonlinear moduli of the pavement profile is based on an equivalent linear model. An equivalent linear model is a model that in an approximate fashion can consider the load-induced nonlinear behavior based on the static linear elastic layered theory. The algorithm used to optimize the deflection basins measured by FWD and calculated using the seismic moduli of the pavement profile is based on the singular value decomposition method.

Four typical pavement sections, ranging from interstate highways to city streets, were considered. A sensitivity study of the pavement response to variations of the nonlinear parameters of the base and subgrade for each pavement type was conducted. The level of sensitivity of the pavement response, in terms of surface deflections, critical strains and remaining lives, for several different common types of base and subgrade was documented. Finally, the algorithm was applied to several synthetic and actual case studies.

CONCLUSIONS

Based on this study, two sets of conclusions can be drawn. From the sensitivity analysis the following information is apparent:

a. Deflections under the load and 12 in. (305 mm) and 24 in. (610 mm) from the load (first three sensors of FWD) can be sensitive to the variation of the nonlinear parameters of the base and subgrade. The remaining sensors are not sensitive to the variation of the nonlinear parameters.

b. Deflections under the load in primary and secondary roads in pavement sections with a thicker base layer (12 in., 300 mm) are very sensitive to the k_3 of the base with the exception of high quality base material. In that case, deflection under the load is very sensitive or sensitive to k_3 of the subgrade.

c. Deflections under the load in county and street roads for pavement sections having a thin base layer (6 in., 150 mm) are very sensitive to k_3 of the subgrade, with the exception of a sandy subgrade. When subgrade material is sandy, deflection under the load is very sensitive to k_3 of the base.

d. Fatigue cracking is very sensitive to k_3 of the base. When the base material is sandy, fatigue cracking is moderately sensitive to sometimes sensitive to the k_3 of the base and subgrade.

e. Rutting is very sensitive to k_3 of the subgrade. When the subgrade layer is thicker (12in., 300 mm) such as in primary and secondary roads, k_3 of the subgrade has an effect. The parameter k_2 of the subgrade will affect rutting when the material is classified as high quality. Rutting is moderately sensitive to k_2 of the subgrade when the pavement section has a thin layer of base (6 in., 152 mm), such as county and street roads; and sensitive when the pavement layer has a thick layer of base (12 in., 305 mm), like primary and secondary roads.

f. Generally, surface deflection bowl of a pavement is not very sensitive to the parameters k_2, where as critical strains and remaining lives are.

A careful study of the attributes of the backcalculation algorithm developed, the following conclusions can be drawn under ideal circumstances:

a. Backcalculation of the nonlinear parameters k_3 of the base and subgrade seems feasible for thinner pavements.

b. Backcalculation of the nonlinear parameter k_2 of the base and subgrade are not feasible, and does not lead to a unique set of answers. Therefore to obtain these parameters, laboratory testing is recommended.

c. For thicker pavements, the backcalculation of the nonlinear parameters k_2 and k_3 of the base and subgrade from FWD deflections should be avoided or done with extreme caution.

Based on the limited experience from the case study, the following observation can be made:

a. Equivalent linear models utilizing the seismic moduli and nonlinear parameters of base and subgrade derived from laboratory tests, especially when a rigid layer or water table is close to surface, may provide more realistic design moduli than those backcalculated from the FWD.

b. Two empirical ways for determining the nonlinear parameters of the base and subgrade are also proposed. Estimating the nonlinear parameters k_2 and k_3 from values published in the literature seem to yield more realistic results than the models that solely require the PI of the soil for predicting the nonlinear behavior.

c. The spatial variation in moduli of the base and subgrade due to load-induced nonlinear behavior can be readily mapped with the developed algorithm.

d. The backcalculation of the nonlinear parameters k_3 of the base and subgrade from the seismic moduli and FWD deflection basin, especially for high quality base and subgrade, do not seem to lead to accurate values. This occurs because of the insignificantly small impact that these parameters have on the FWD deflections.

RECOMMENDATIONS FOR FUTURE RESEARCH

The followings items are recommended to further improve the process:

a. The backcalculation process should be validated with more than one set of field data.

b. Better classification of base and subgrade material is required in order to initialize the nonlinear parameters more accurately. This will reduce the number of iterations in the backcalculation algorithm and may yield more accurate results.

c. The backcalculation process is time-consuming. Better optimization methods for backcalculation algorithm or faster convergence methods for equivalent linear algorithm need to be incorporated.

d. The viscoelasticity of the AC pavement and the variation in modulus with temperature are considered using approximate relationships. These relationships can be studied and improved.

e. The impact of bedrock or a shallow water table on the measured FWD deflection basin has to be carefully studied and incorporated into the algorithms.

REFERENCES

- Asphalt Institute (1982), "Research and Development of the Asphalt Institute's Thickness Design Manual (MS-1)", 9th ed., Research Report 82-2, Asphalt Institute.

- Anderson, D. G., and Woods, R. D. (1975), "Comparison of Field and Laboratory Shear Modulus," proceedings, In Situ Measurement of Soil Properties, ASCE, Vol I, Rayleigh, NC, pp. 218-232.

- Ang, A. H-S, and Tang, W. H. (1984a), Probability Concepts in Engineering Planning and Design, Vol. I – Basic Principles, Wiley and Sons Inc., New York.

- Ang, A. H-S, and Tang, W. H. (1984b), Probability Concepts in Engineering Planning and Design, Vol. II – Decision, Risk, and Reliability, Wiley and Sons Inc., New York.

- Aouad, M. F. (1993), "Evaluation of Flexible Pavements and Subgrades Using the Spectral-Analysis-of-Surface-Waves (SASW) Method," Ph.D. Dissertation, The University of Texas at Austin.

- Aouad, M. F., Stokoe, K. H., and Briggs, R. C. (1993), "Stiffness of Asphalt Concrete Surface Layer from Stress Wave Measurements," Transportation Research Record 1384, Washington, D.C., pp. 29-35.

- Baig, S. (1991), "Evaluation of Piezo-Ceramic Bender Elements for Measuring Low-amplitude Shear Modulus of Various Soils," MS Thesis, The University of Texas at El Paso, pp. 75-162.

- Barksdale, R. D (1972), "Repeated Load Test Evaluation of Base Course Materials," Research Project 7002, Final Report, Federal Highway Administration, Washington D.C.

- Barksdale, R. D., Alba, J., Khosla, P. N., Kim, R., Lambe, P. C. and Rahman, M. S. (1994), "Laboratory Determination of Resilient Modulus for Flexible Pavement Design," Interim Report Project 1-28, Federal Highway Administration, Washington, D.C.

- Boussinesq, J. (1885), Application des Potentiels a l'Etude de l'Equilibre et du Mouvement des Solids Elastiques, Gauthier-Villars, Paris.

- Brown, S. F. (1996), "Soil Mechanics in Pavement Engineering," Geotechnique, Vol 46., No. 3, pp. 383-426.

- Burmister, D. M. (1943), "The Theory of Stresses and Displacements in Layered Systems and Applications to the Design of Airport Runways," Highway Research Board, Vol. 23.

- Burmister, D. M. (1945), "The General Theory of Stresses and Displacements in Layered Soil Systems," Journal of Applied Physics, Vol. 16, pp. 84-94, 126-127, 296-302.

- Bush, A. J. (1980), "Development of the Nondestructive Testing for Light Aircraft Pavements," Phase I, Evaluation of NDT Device Report No. FAA-RD-80-9, Washington, D.C.

- Daniel, J. S. and Kim, Y. R. (1998), "Relationships Among Rate-Dependent Stiffnesses of Asphalt Concrete Using Laboratory and Field Test Methods," Transportation Research Record 1630, Washington D.C., pp. 3-9.

- De Jong, D. L., Peatz, M. G. F., and Korswagen, A. R. (1973), "Computer Program Bisar Layered Systems Under Normal and Tangential Loads," Konin Klijke Shell-Labaratorium, External Report AMSR.0006.73, Amsterdam.

- Dobry, R., and Gazetas, G. (1986), "Dynamic Response of Arbitrary Shaped Foundations," Journal of Geotechnical Engineering, ASCE, Vol. 112, No. 2, New York, NY, pp. 109-35.

- Ellstien, A. and Ishibashi, I. (1992) "Effect of Soil Plasticity on Cyclic Response," Journal of Geotechnical Engineering, Vol. 118, No. 5, pp. 829-832.

- Feliberti, M. and Nazarian, S. (1993), "Methodology for Resilient Modulus Testing of Cohesionless Subgrades," Transportation Research Record 1406, Washington D.C., pp 108-115.

- Foster, C. R., and Ahlvin, R. G. (1954), "Stresses and Deflections Induced by a Uniform Circular Load," Proceedings, Highway Research Board, Vol. 33, pp. 467-470.

- Golub, G.H., and Reinsch, C., (1970), "Singular Value Decomposition and Least Squares Solutions," Numerische Mathematik, Vol. 4, No. 1, pp. 17-34.

- Hardin, B. O. and Drnevich, V. P. (1972), "Shear Modulus and Damping in Soils: Design Equations and Curves," Journal of Soil Mechanics and Foundations Division, ASCE, Vol. 98, No. SM7, New York, NY, pp. 667-692.

- Hicks, R. G., and Monismith, C. L. (1971), "Factors Influencing the Resilient Response of Granular Materials," Highway Research Record 345, Washington, D.C., pp. 15-31.

- Hoffman, M. S., and Thompson, M. R. (1982), "Comparative Study of Selected Nondestructive Testing Devices," Transportation Research Record 852, Washington D.C., pp. 32-41.

- Huang, Y. H. (1994), Pavement Analysis and Design, Prentice Hall, Inc., Englewood Cliffs, NJ, 805p.

- Ishibashi, I. and Zhang, X. (1993), "Unified Dynamic Shear Moduli and damping Ratios of Sand and Clay," Soils and Foundations, Vol. 33,No. 1, pp. 182-191.

- Ke, L., Nazarian, S., Abdallah, I., and Yuan, D., (2000), "A Sensitivity Study of Parameters Involved in Design with Seismic Moduli," Research Report 1780-2, Center for Highway Materials Research, the University of Texas at El Paso.

- Kim, Y. R. and Lee, Y. C. (1995), "Interrelationships among Stiffnesses of Asphalt Aggregate Mixtures," Journal of Association of Asphalt Paving Technologists, Vol. 64, pp. 575-609.

- Kramer, S. L. (1996), Geotechnical Earthquake Engineering, Prentice Hall, Inc., Upper Saddle River, California.

- Li, Y. and Nazarian, S. (1994), "Evaluation of Aging of Hot-Mix Asphalt Using Wave Propagation Techniques," Proceedings, Engineering Properties of Asphalt Mixtures And the Relationship to Their Performance, ASTM STP 1265, Philadelphia, PA, pp.166-179.

- Lytton, R. L., Roberts, R. L., and Stoffels, S. (1985), "Determination of Asphaltic Concrete Pavement Structural Properties by Nondestructive Testing," NCHRP Report No. 10-27, Texas A & M University, College Station, Texas.

- Lytton, R. L., and Michalak, C. H. (1979), "Flexible Pavement Deflection Evaluation Using Elastic Moduli and Field Measurements," Research Report 207-7F, Texas Transportation Institute, Texas A & M University, College Station, Texas.

- Lytton, R. L. (1989), "Backcalculation of Pavement Layer Properties," Proceedings, Nondestructive Testing of Pavements and Backcalculation of Moduli, ASTM, STP 1026, Philadelphia, pp.7-38.

- May, R.W. and Witczak, M.W. (1981), "Effective Granular Modulus to Model Pavement Responses," Transportation Research Record 810, Washington D.C., pp. 1-9.

- Michalak, C.H. and Scullion, T. (1995), "MODULUS 5.0: User's Manual," Texas Transportation Institute, Research Report 1987-1, College Station, TX.

- Mikhail, M.Y., Seeds, S.B., Alavi, S.H., and Ott, W.C. (1999), "Evaluation of Laboratory and Backcalculated Resilient Moduli from the WesTrack Experiment," Transportation Research Record 1687, Washington D.C., pp. 55-65.

- Nazarian, S. and Desai, M. R. (1993), "Automated Surface Wave Method: Field Testing," Journal of Geotechnical Engineering Division, ASCE, Vol. 119, No. GT7, New York, NY, pp. 1094-1111.

- Nazarian, S., Yuan D. and Baker M. R. (1995), "Rapid Determination of Pavement Moduli with Spectral-Analysis-of-Surface-Waves Method," Research Report 1243-1F, Center for Geotechnical and Highway Materials Research, The University of Texas at El Paso, El Paso, TX, 76 p.

- Nazarian, S., Pezo R. and Picornell, M. R. (1996), "Application of Resilient Modulus Tests to Texas Base Material," Research Report 0-1336, Center for Highway Materials Research, The University of Texas at El Paso, El Paso, TX, 86 p.

- Nazarian, S., Abdallah, I., Yuan, D., and Ke, L. (1998a), "Design Modulus Values Using Seismic Data Collection," Research Report 1780-1, Center for Highway Materials Research, the University of Texas at El Paso.

- Nazarian, S., Yuan D. and Tandon, V. (1998b), "Specifications for Tools Used in Structural Field Testing of Flexible Pavement Layers," Research Report 1735-1, Center for Highway Materials Research, The University of Texas at El Paso, El Paso, TX, 67 p.

- Odemark, N. (1949), Investigation as to the Elastic Properties of Soil Design of Pavements According to the Theory of Elasticity, Staten Valginstitut, Stockholm, Sweden.

- Pezo, R. F., Kim, D. S., Stokoe II, K. H., and Hudson, W. R. (1991), "A Reliable Resilient Modulus Testing System," Transportation Research Record 1307, Washington D.C., pp. 90-98.

- Rada, G.R., Witczak, M.W., and Rabinow, S.D. (1988), "Comparison of AASHTO Structural Evaluation Techniques Using Nondestructive Deflection Testing," Transportation Research Record 1207, Washington D.C., pp. 134-144.

- Richardson, M.H., and Formenti, D. L. (1982), "Parameter Estimation from Frequency Response Measurements Using Rational Fraction Polynomials." Proceedings, First International Model Analysis Conference, Society for Experimental Mechanics, Orlando, FL, pp. 167-181.

- Rojas, J. (1999), "Quality Management of Asphalt Concrete Layers Using Wave Propagation Techniques," MS Thesis, The University of Texas at El Paso, 54 p.

- Sansalone, M., and Carino, N. J. (1986), "Impact-Echo: A Method for Flaw Detection in Concrete Using Transient Stress Waves," Report NBSIR 86-3452, National Bureau of Standards, Gaithersburg, MD.

- Santh, B.L. (1994), "Resilient Modulus of Subgrade Soils: Comparison of Two Constitutive Equations," Transportation Research Record 1462, Washington D.C., pp. 79-90.

- Seeds, S., Alavi, S., Ott, W., Mikhail, M., and Mactitus, J. (2000), "Evaluation of Laboratory Determined and Nondestructive Test Based Resilient Modulus Values from WesTrack Experiment," ASTM, STP 1375,West Conshohocken, PA, pp. 72-94.

- Shook, J.F. and Kallas, B.F. (1969), "Factors Influencing Dynamic Modulus of Asphalt Concrete," Association of Asphalt Paving Technologists, Vol. 38, pp. 140-178.

- Siddharthan, R., Norries, G. M., and Epps, J. A. (1991), "Use of FWD Data for Pavement Material Characterization and Performance," Journal of Transportation Engineering, ASCE, Vol. 117, No. 6, New York, NY, pp. 660-678.

- Sivaneswaran, N., Pierce, L. M., and Mahoney, J. P., 1999, EVERCALC 5.0, Washington State Department of Transportation.

- Sousa, J. B. and Monismith, C. L. (1988), "Dynamic Response of Paving Materials," Transportation Research Record 1136, TRB, Washington, D.C., pp. 57-68.

- Uddin, W., Meyer, A. H., and Hudson, W. R. (1983), "Rigid Bottom Considerations for Nondestructive Evaluation of Pavement," Transportation Research Record 1007, Washington, D.C.

- Uddin, W., and McCullough, B. F. (1989), "In Situ Material Properties from Dynamic Deflection Equipment," Nondestructive Testing of Pavements and Backcalculation of Moduli, ASTM, STP 1026, Philadelphia.

- Ullidtz, P. (1987), Pavement Analysis, Elsevier, Amsterdam.

- Ullidtz, P., and Peattie, K. R. (1980), "Pavement Analysis by Programmable Calculators," Journal of Transportation Engineering, ASCE, Vol. 106, No. TE5, New York, NY, pp. 581-598.

- Uzan, J., (1985), "Characterization of Granular Materials," Transportation Research Record 1022, Washington, D.C., pp. 52-59.

- Uzan, J., R. L. Lytton, and Germann, F. P. (1989), "General Procedure for Backcalculating Layer Moduli," STP 1026, ASTM, Philadelphia, PA, pp. 217-228.

- Uzan, J., and Lytton, R. L. (1990), "Analysis of Pressure Distribution Under Falling Weight Deflectometer Loading," Journal of Transportation Engineering, ASCE, Vol. 116, No. 2, New York, NY, pp. 246-251.

- Uzan, J. (1994), "Advanced Backcalculation Techniques," ASTM, STP 1198, Philadelphia, PA, pp. 3-37.

- Van Cauwelaert, F. J., Alexander, D. R., White, T. D., and Baker, W. R. (1989). "Multilayer Elastic Program for Backcalculating Layer Moduli in Pavement Evaluation," ASTM, STP 1026, Philadelphia, PA, pp.171-188.

- Von Quintus H. L. and Killingsworth, B. M. (1998), "Comparison of Laboratory and In-Situ Determined Elastic Layer Moduli," presented in 77th Annual TRB Meeting, Washington, D.C.

- Yuan, D. and Nazarian, S. (1993), "Automated Surface Wave Testing: Inversion Technique," Journal of Geotechnical Engineering, ASCE, Vol. 119, No. GT7, New York, NY, pp. 1112-1126.

- Westergaard, H. M. (1926), "Stresses in Concrete Pavements Computed by Theoretical Analysis," Public Roads, Vol. 7, pp. 25-35.

- Willis, M. E. and Toksoz, M. N. (1983), "Automatic P and S Velocity Determination from Full Wave Form Digital Acoustic Logs," Geophysics, Vol. 48, No. 12, pp. 1631-44.

- Witczak, M.H., and Uzan, J. (1988), "The Universal Airport Design System, Report I of IV: Granular Material Characterization," Department of Civil Engineering, University of Maryland, College Park, MD.

APPENDIX A
SEISMIC PAVEMENT ANALYZER

The Seismic Pavement Analyzer (SPA) is a trailer-mounted nondestructive testing device, as shown in Figure A.1. Its operating principle is based on generating and detecting stress waves in a layered medium. Several seismic testing techniques are combined. A detailed discussion on the background of the device can be found in Nazarian et al. (1995).

The SPA lowers several transducers and sources to the pavement. Surface deformations are recorded digitally. A large pneumatic hammer, which generates low frequency vibrations, and a small pneumatic hammer, which generates high frequency vibrations, induce the deformations.

The SPA is similar in size to the FWD. However, the SPA uses more transducers with higher frequencies and more sophisticated interpretation techniques. The measurement is rapid. A complete testing cycle at one point takes less than one minute (lowering sources and receivers, making measurements, and withdrawing the equipment).

The SPA collects three categories of data; raw data, processed data and interpreted data. Raw data are the waveforms generated by hammer impacts and collected by the transducers. The processed data are pavement layer properties derived from the raw data through established theoretical models. Interpreted data are diagnoses of pavement distress precursors from data processed through models.

Pavement properties estimated by the SPA include: Young's modulus, shear modulus, thickness, and temperature at the top pavement layer; Young's modulus and thickness of the base layer; and Young's modulus of the subgrade Five methods are used in the SPA tests. In the Impulse Response (IR) tests, the low frequency source and geophone G1 are used (see Figure A.1). With this method, the modulus of the subgrade and the damping ratio of the system are extracted from the flexibility spectrum measured in the field (Nazarian and Desai, 1993). The pavement is modeled as a single-degree- of-freedom (SDOF) system. To determine the model parameters, a curve is fitted to the flexibility spectrum. The shear modulus of the subgrade, G, is calculated

a) Schematic of the SPA

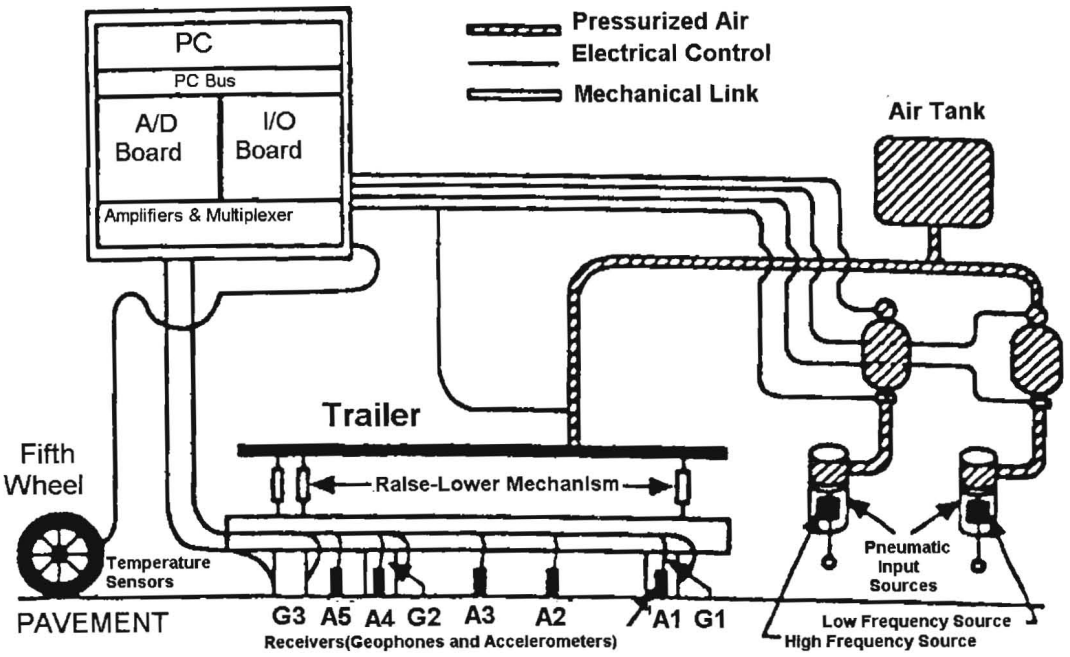

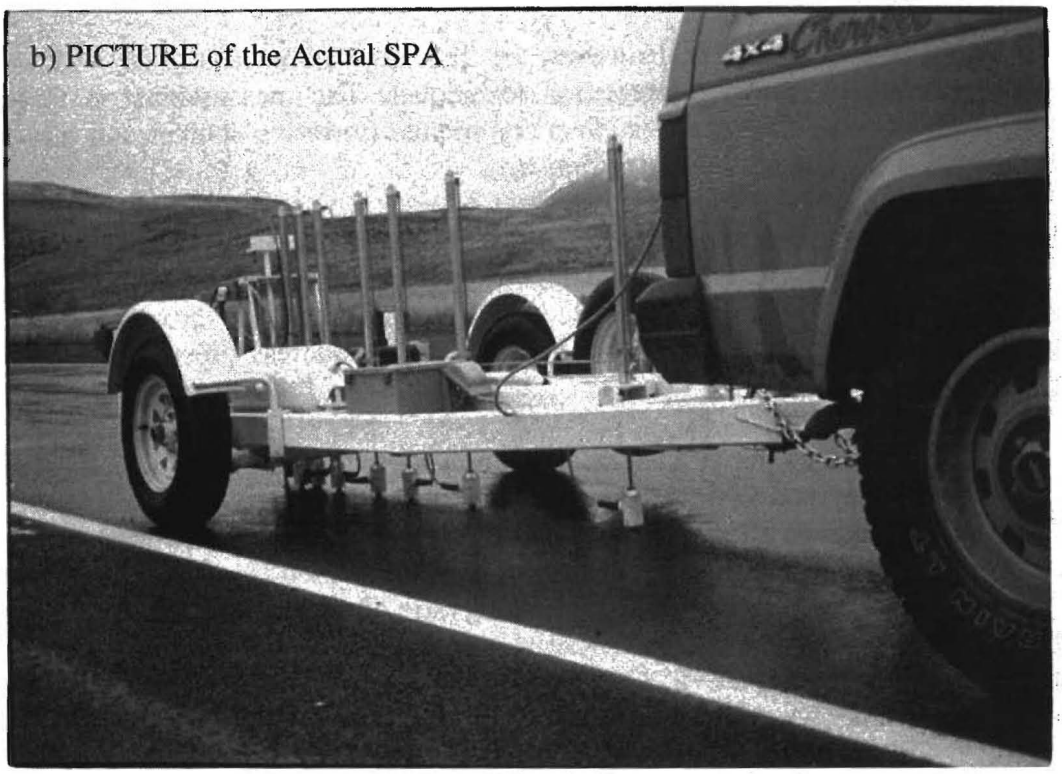

Figure A.1 Seismic Pavement Analyzer

from (Dobry and Gazetas, 1986);

$$G = \frac{(1-\nu)}{2LA_0 I_s S_z} \tag{A.1}$$

in which ν is the Poisson's ratio of subgrade, L is the length of slab, and A_0 is the state of the flexibility of the slab. Dobry and Gazetas (1986) developed the shape factor S_z. The value of S_z is equal to 0.80 for a long flexible pavement. Parameter I_s, is a function of the length and width of the slab, as well as the coordinates of the impact point relative to one corner. The damping ratio is a qualitative indicator of the slab's resistance to movement. For example, if a slab contains an edge void, it would demonstrate a damping ratio of approximately 10 to 40 percent.

The Spectral Analysis of Surface Waves (SASW) method is a seismic method that can determine modulus profiles of pavement sections by considering the dispersive nature of surface waves. All accelerometers and geophones are active in the SASW tests. The procedure includes collecting data, determining the experimental dispersion curve, and obtaining the stiffness profile.

In date collection, the transfer function and the coherence function between pairs of receivers are determined. Thus, the phase information of the cross power spectra and the coherence functions are used to determine a representative dispersion curve in an automated fashion (Nazarian and Desai, 1993). Finally, the elastic modulus of different layers can be determined from the dispersion curve using an automated inversion process (Yuan and Nazarian, 1993).

The Ultrasonic Surface Wave (USW) method is similar to the SASW method. The difference is that, in the USW method; the properties of the top pavement layer can be easily and directly determined without a complex inversion algorithm. The high-frequency source and accelerometers A2 and A3 are utilized in this method.

Up to a wavelength approximately equal to the thickness of the uppermost layer, the velocity of propagation is independent of wavelength. Therefore, if high-frequency waves are generated and if it is assumed that the properties of the uppermost layer are uniform, the shear modulus of the top layer, g, can be determined by

$$G = \rho[(1.13-0.16\nu)V_{ph}]^2 \tag{A.2}$$

where V_{ph} is the phase velocity of surface waves, ρ is the mass density and ν is Poisson's ratio. The shear modulus can be readily converted to Young's modulus, E, using

$$E = 2G(1+\nu) \tag{A.3}$$

The thickness of the surface layer can be estimated by determining the wavelength above which the surface velocity is constant.

The setup to measure the compressional wave velocity of the upper layer of the pavement is the same as the SASW tests. Once the compressional wave velocity of a material is known, its

Young's modulus can be determined. Miller and Pursey (1995) found that when the surface of a medium is impacted most of the energy is propagated as Rayleigh waves. A small portion of the generated stress wave energy propagates with shear and compressional waves. Compressional waves arrive first on seismic records because they travel faster than any other type of seismic waves. An automated technique has been developed to determine the compressional wave velocity by measuring the times of first arrival of compressional waves (Willis and Toksoz, 1983).

The impact-echo method is employed to locate defects, voids, cracks, and zones of deterioration within concrete. The high-frequency source and accelerometer A1 and, possibly, A2 are used. Once the compressional wave velocity of concrete, V_p, is measured, the depth to reflector, T, can be determined from (Sansalone and Carino, 1986):

$$T = {}^{V_p}\!/_{(2f)} \tag{A.4}$$

where f is the resonant frequency obtained by transforming the deformation record into the frequency domain.

APPENDIX B
RELATIONSHIP BETWEEN SEISMIC AND DESIGN MODULUS

Figure B.1a shows stresses for an infinitesimal material element during seismic tests. Only a very small external load is applied to generate various waves. Therefore, only stresses generated by geostatic pressure should be considered. Assuming n layers of material above the element shown in Figure B.1a, each with a unit weight of γ_i and a thickness of h_i, the vertical stress, σ_v is:

$$\sigma_v = \sum_{i=1}^{n} \gamma_i h_i \tag{B.1}$$

The horizontal stress, σ_h is related to σ_v by the coefficient of lateral earth pressure at rest, k_0:

$$\sigma_h = k_k \sigma_v \tag{B.2}$$

As shown in Figure B.1a, additional stresses, σ_x, σ_y, σ_z, are induced under the application of an external load. A multi-layer elastic program can conveniently compute these additional stresses. The constitutive model described in Equation B.4 includes the influence of deviator stress and confining pressure. Deviatoric stress and confining pressure are formulated in terms of vertical and horizontal stresses. Figure B.1b shows the transformed state of stress, which includes the initial confining pressure $\sigma_{c\text{-init}}$, and the initial deviatoric stress, $\sigma_{d\text{-init}}$. The initial confining pressure is the arithmetic mean value of the three original principal stresses. Since the two horizontal stresses can be considered equal:

$$\sigma_{c-init} = \frac{1+2k_0}{3}\sigma_v \tag{B.3}$$

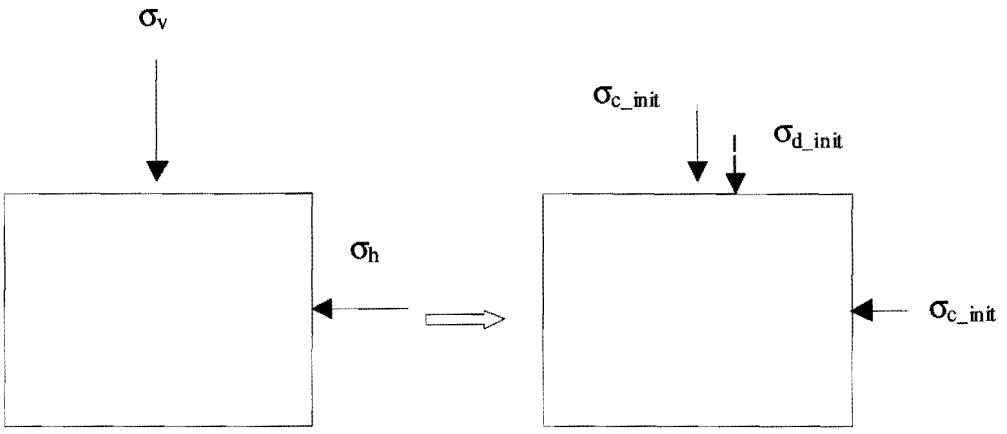

(a) Actual state of stress (b) Transformed state of stress

Figure B.1 State of the Stress under Seismic Load

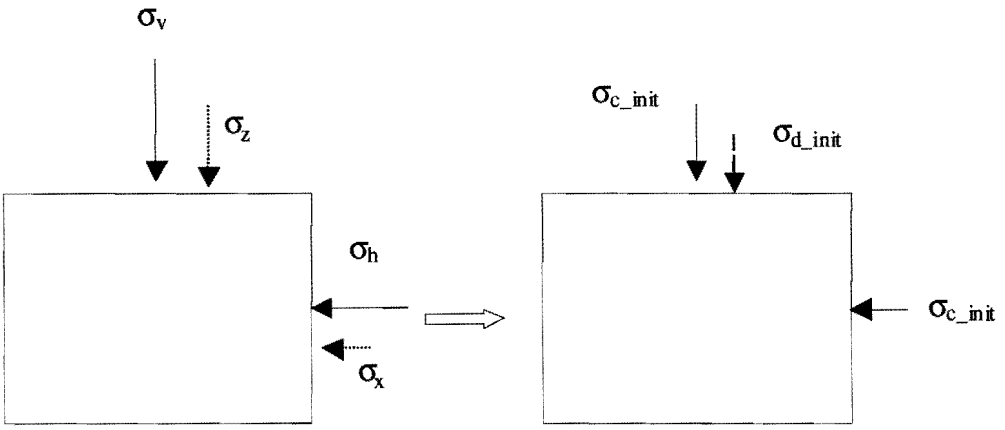

(a) Actual state of stress (b) Transformed state of stress

Figure B.2 State of the Stress under Traffic Load

The initial deviatoric stress, which is the difference between σ_v and $\sigma_{c\text{-init}}$, can be written as:

$$\sigma_{d-init} = \frac{2-2k_0}{3}\sigma_v \tag{B.4}$$

Figure B.1b shows the transformed state of the stress under load, such as those applied by an FWD or imposed by traffic. The state of stress consists of an ultimate confining pressure, $\sigma_{c\text{-ult}}$, and an ultimate deviatoric stress, $\sigma_{d\text{-ult}}$. The ultimate pressure contains two components, $\sigma_{c\text{-init}}$ and $\Delta\sigma_c$, the mean value of the three principal stresses σ_x, σ_y, and σ_z:

$$\Delta\sigma_c = \frac{\sigma_x + \sigma_y + \sigma_z}{3} \tag{B.5}$$

The ultimate confining pressure is

$$\sigma_{c-ult} = \sigma_{c-init} + \Delta\sigma_c \tag{B.6}$$

or

$$\sigma_{c-ult} = \frac{1+2k_0}{3} + \frac{\sigma_x + \sigma_y + \sigma_z}{3} \tag{B.7}$$

The ultimate deviatoric stress also includes two parts, $\sigma_{d\text{-init}}$ and $\Delta\sigma_d$, the difference between σ_z and $\Delta\sigma_c$:

$$\Delta\sigma_d = \sigma_z - \Delta\sigma_c \tag{B.8}$$

or

$$\Delta\sigma_d = \frac{2\sigma_z - \sigma_x - \sigma_y}{3} \tag{B.9}$$

Thus the ultimate deviatoric stress is:

$$\sigma_{d-ult} = \sigma_{d-init} + \Delta\sigma_d \tag{B.10}$$

$$\sigma_{d-ult} = \frac{2-2k_0}{3}\sigma_v + \frac{2\sigma_z - \sigma_x - \sigma_y}{3} \tag{B.11}$$

To obtain the seismic modulus, E_{seis}, very small external loads are applied; therefore, the corresponding confining pressure and deviatoric stress are $\sigma_{c\text{-init}}$ and $\sigma_{d\text{-init}}$. Thus, Equation 3.1

can be changed to

$$E_{seis} = k_1 \sigma_{c-init}^{k_2} \sigma_{d-init}^{k_3} \tag{B.12}$$

Thus the parameter k_1 is

$$k_1 = \frac{E_{seis}}{\sigma_{c-init}^{k_2} \sigma_{d-init}^{k_3}} \tag{B.13}$$

In FWD tests or under actual truckloads, the modulus can become nonlinear depending on the amplitude of confining pressure $\sigma_{c\text{-}ult}$ and deviatoric stress of $\sigma_{d\text{-}ult}$. Thus, Equation B.5 is changed to:

$$E = k_1 \sigma_{c-ult}^{k_2} \sigma_{d-ult}^{k_3} \tag{B.14}$$

Substituting Equation B.18 into the above equation:

$$E = E_{seis} \left(\frac{\sigma_{c-ult}}{\sigma_{c-init}} \right)^{k_2} \left(\frac{\sigma_{d-ult}}{\sigma_{d-init}} \right)^{k_3} \tag{B.15}$$

Eliminating parameter k_1 in Equation B.5 may reduce some of the uncertainties associated with laboratory tests used for determining k_1.

APPENDIX C
SENSITIVITY ANALYSIS FIGURE

(By request, please contact:

The Center for Highway Materials Research
The University of Texas at El Paso
Civil Engineering E-201
500 West University Ave.
El Paso, TX 79968-0516
Phone: (915) 747-6925
Email: chmr@utep.edu